HYBRID MAGNON MODES

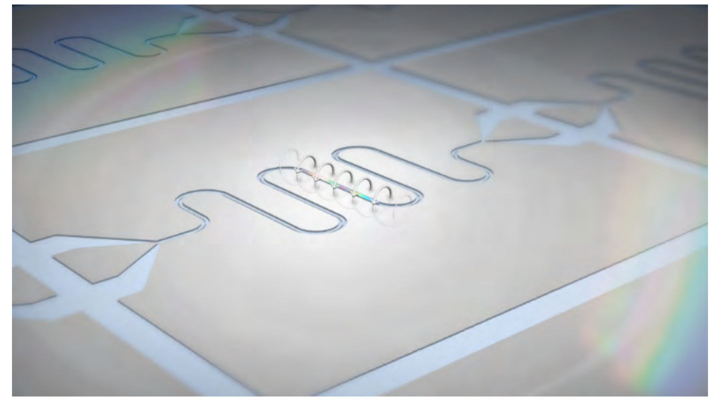

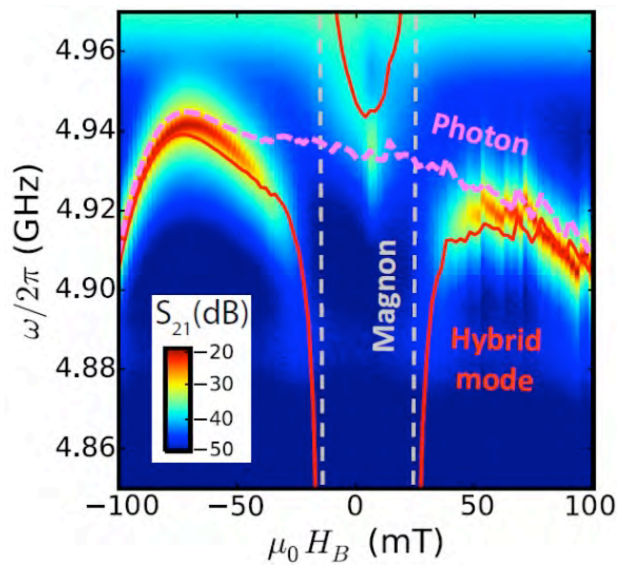

Axel Hoffmann
Department of Materials Science and Engineering
University of Illinois at Urbana-Champaign

SPICE-SPIN+X, August 26, 2020

MAGNETIC MATCHMAKING: HYBRID MAGNON MODES

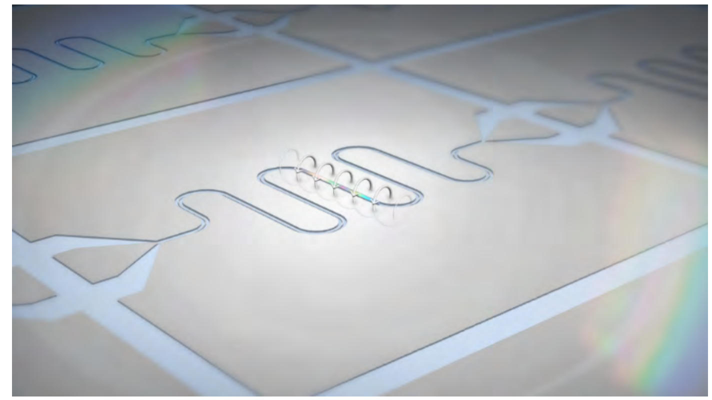

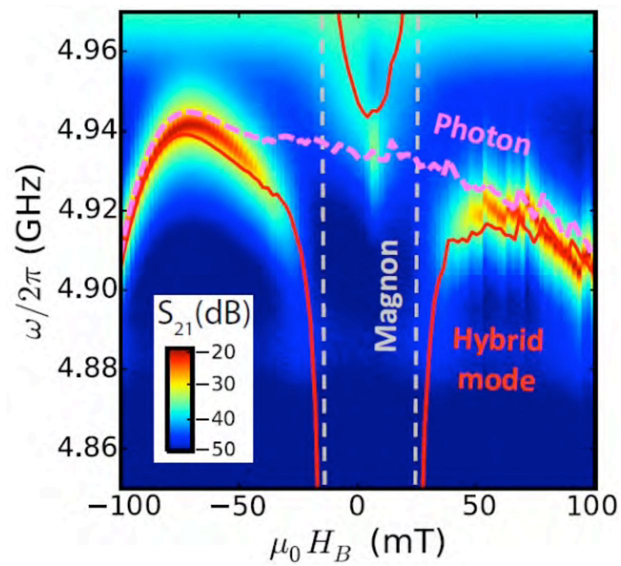

Axel Hoffmann

Department of Materials Science and Engineering

University of Illinois at Urbana-Champaign

SPICE-SPIN+X, August 26, 2020

MAGNETIC MATCHMAKING: HYBRID MAGNON MODES

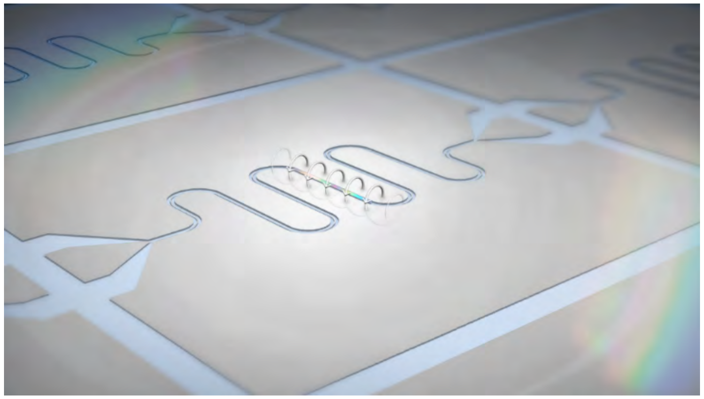

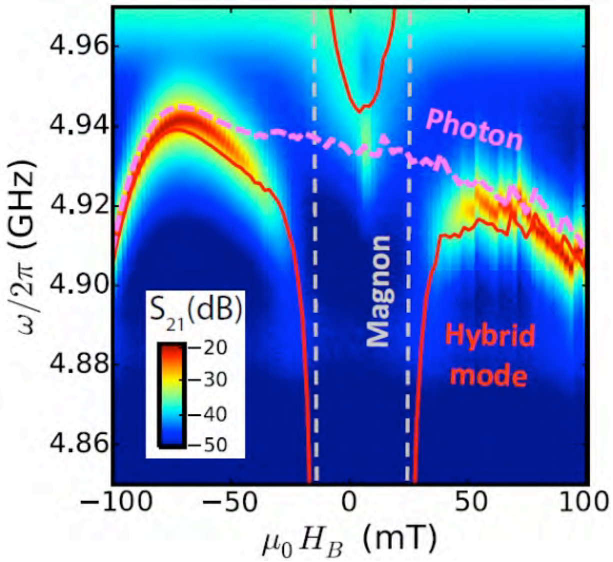

Axel Hoffmann
Department of Materials Science and Engineering
University of Illinois at Urbana-Champaign

SPICE-SPIN+X = XICE

OUTLINE

- Introduction
- On-chip magnon-photon coupling with superconducting resonator
- Magnon-magnon coupling in magnetic bilayer thin film
- Manipulating phonon transport with magnons
- Conclusions

OUTLINE

- **Introduction**
- **On-chip magnon-photon coupling with superconducting resonator**
- **Magnon-magnon coupling in magnetic bilayer thin film**
- **Manipulating phonon transport with magnons**
- **Conclusions**

COMPUTING OF YESTERDAY

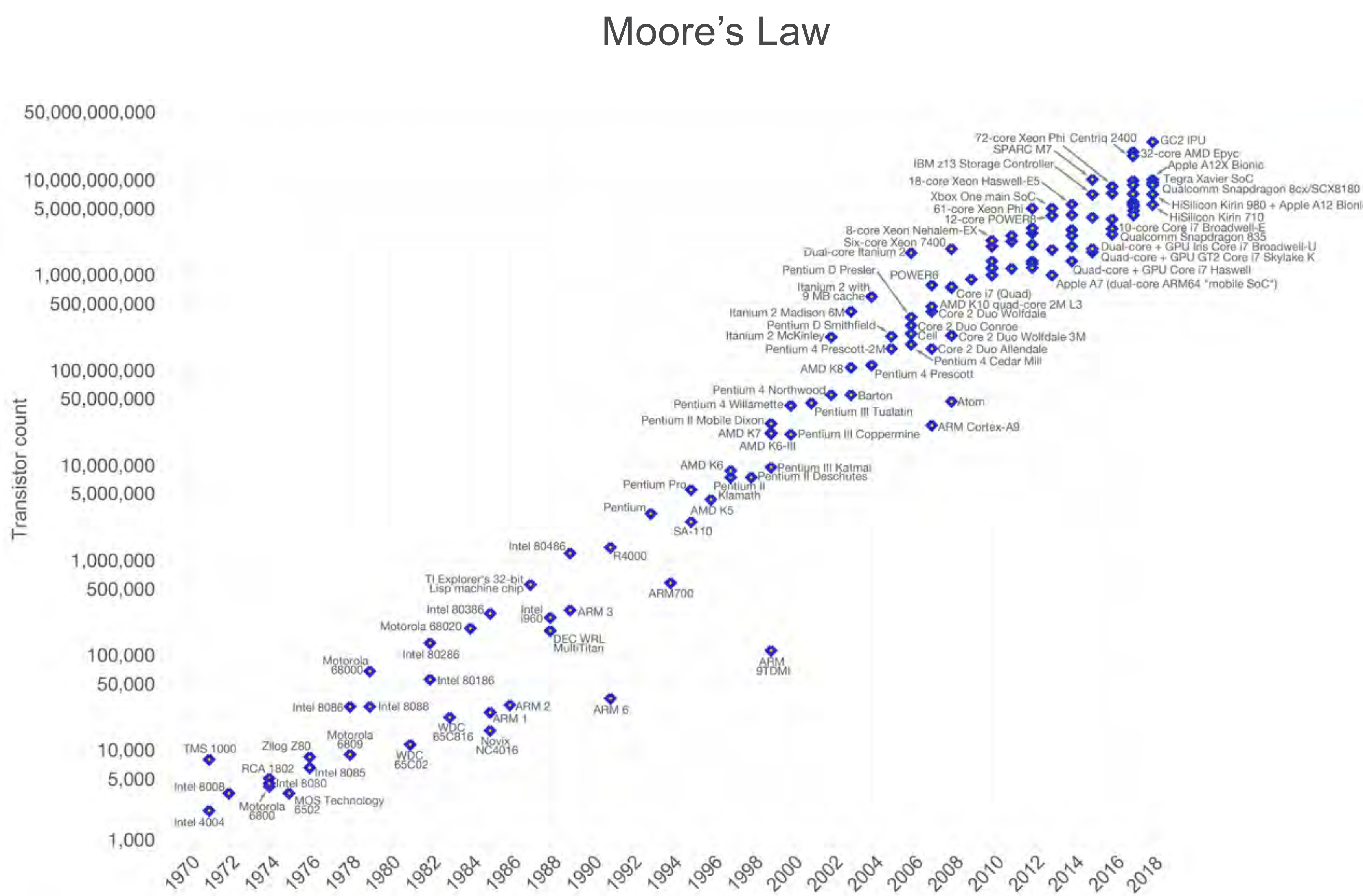

COMPUTING OF YESTERDAY

Moore’s Law

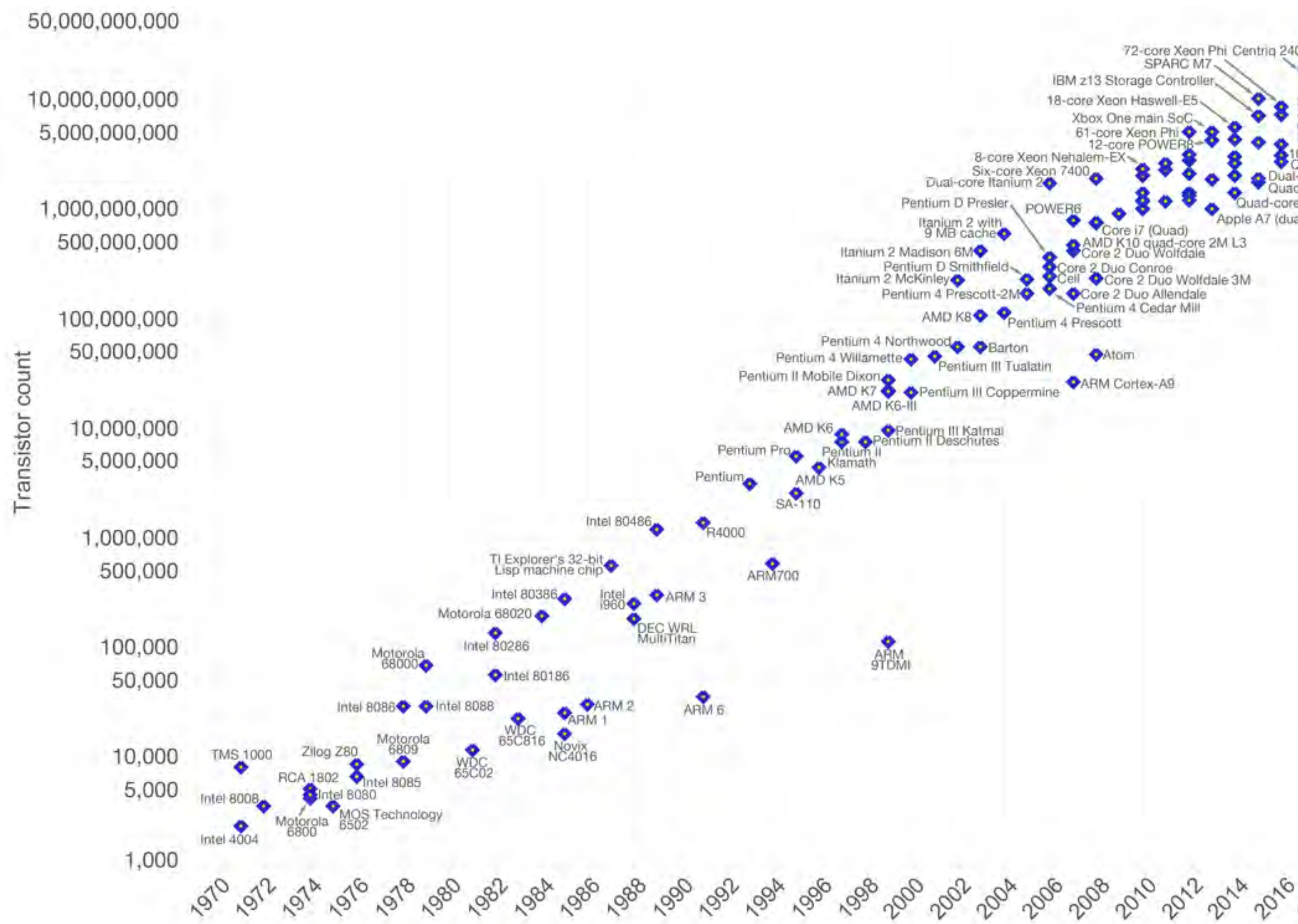

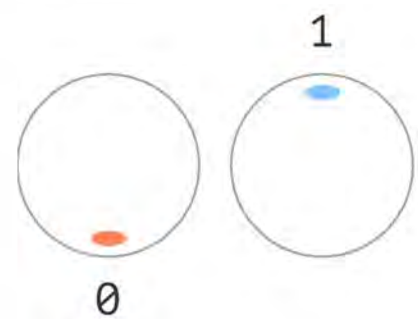

COMPUTING OF YESTERDAY

Moore's Law

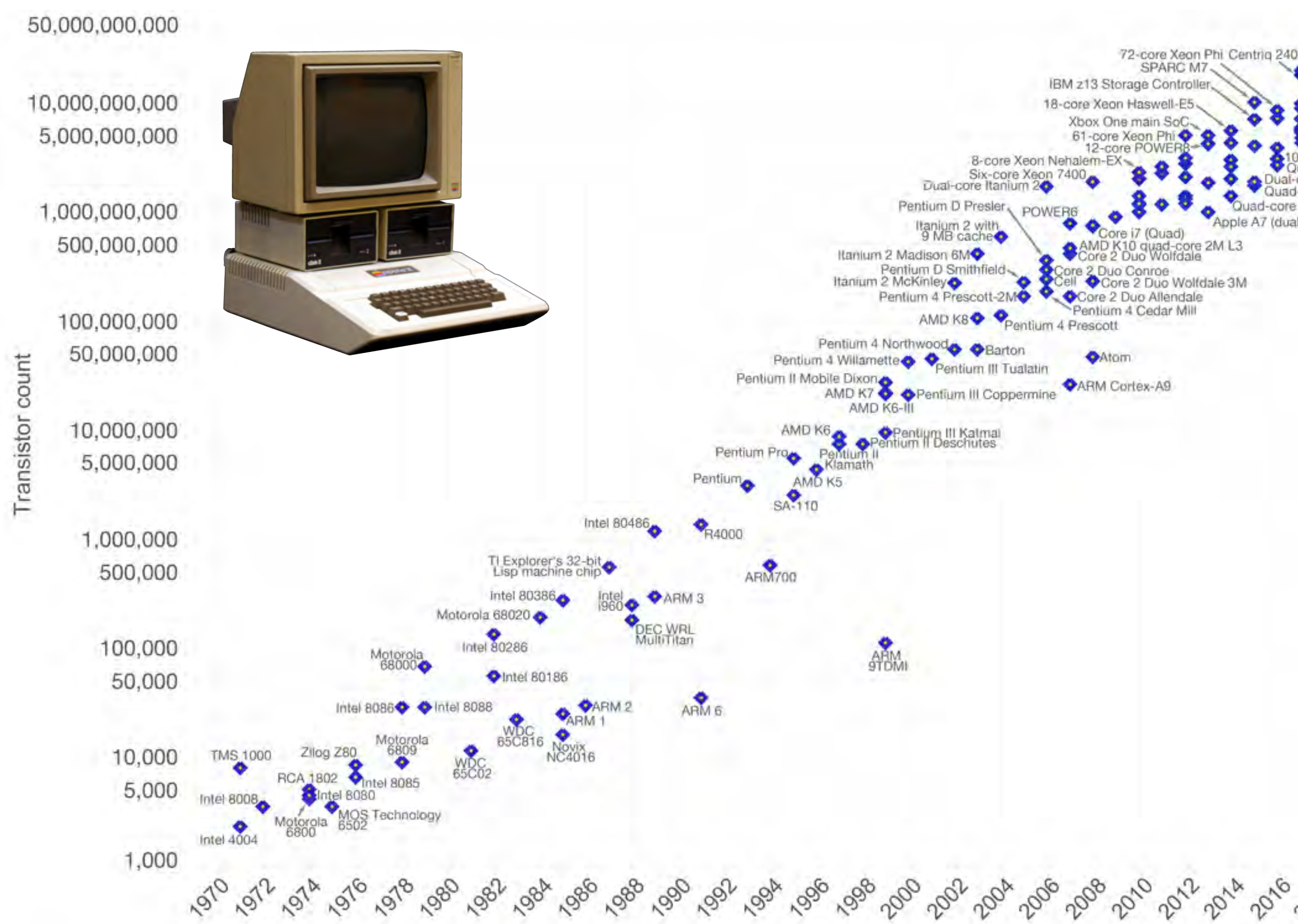

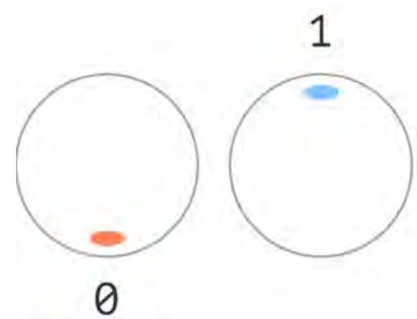

COMPUTING OF YESTERDAY

Moore's Law

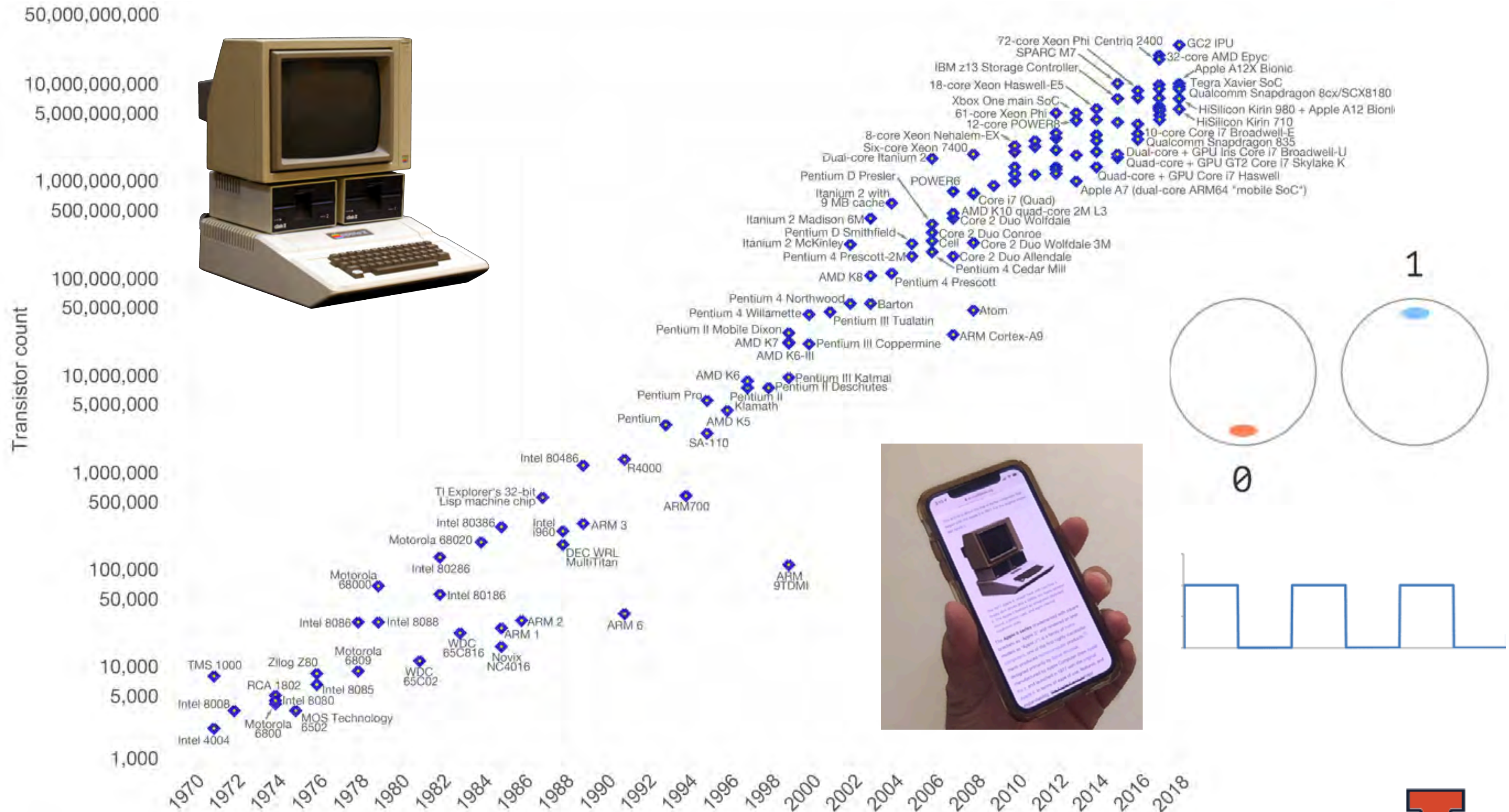

COMPUTING OF TODAY

COMPUTING OF TODAY

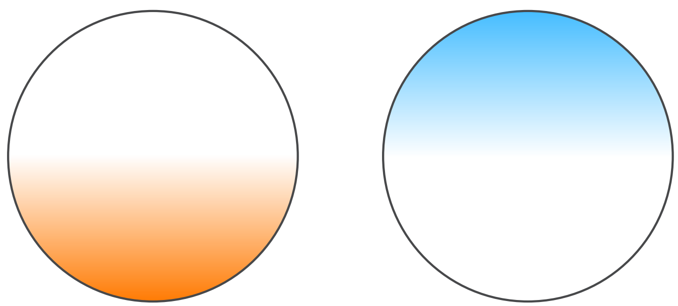

“0” “1”

COMPUTING OF TOMORROW (MAYBE)

Quantum computing

Qubits

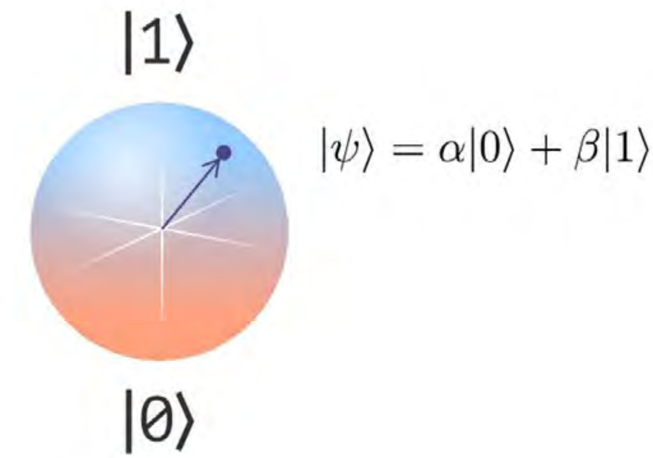

COHERENT INFORMATION PROCESSING

Qubit 1

Qubit 2

COHERENT INFORMATION PROCESSING

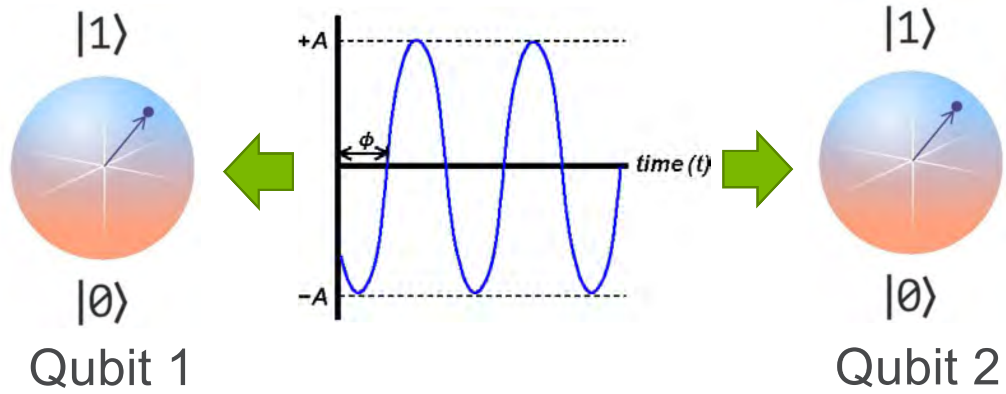

$$y = A\sin(\omega t + \varphi)$$

Amplitude Phase

COHERENT INFORMATION PROCESSING

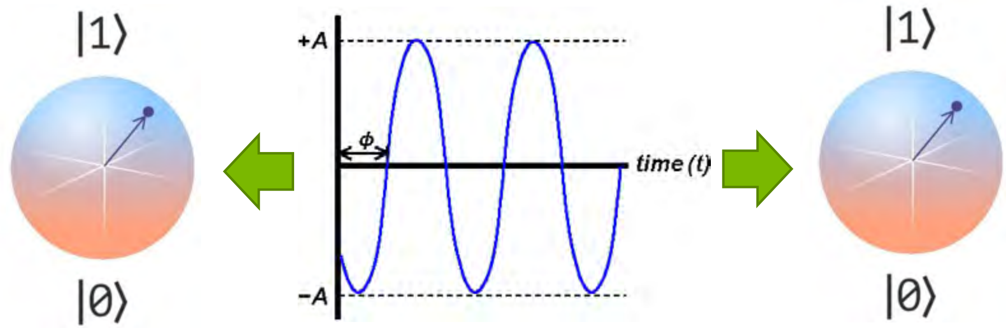

Qubit 1

Qubit 2

$$y = A\sin(\omega t + \varphi)$$

Amplitude Phase

Two-level system

$$|\psi\rangle = \alpha|0\rangle + \beta|1\rangle$$

Qubit

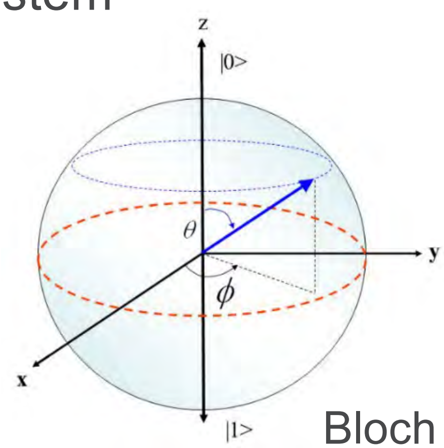

Bloch sphere

COHERENT INFORMATION PROCESSING

Quantum hybrid systems

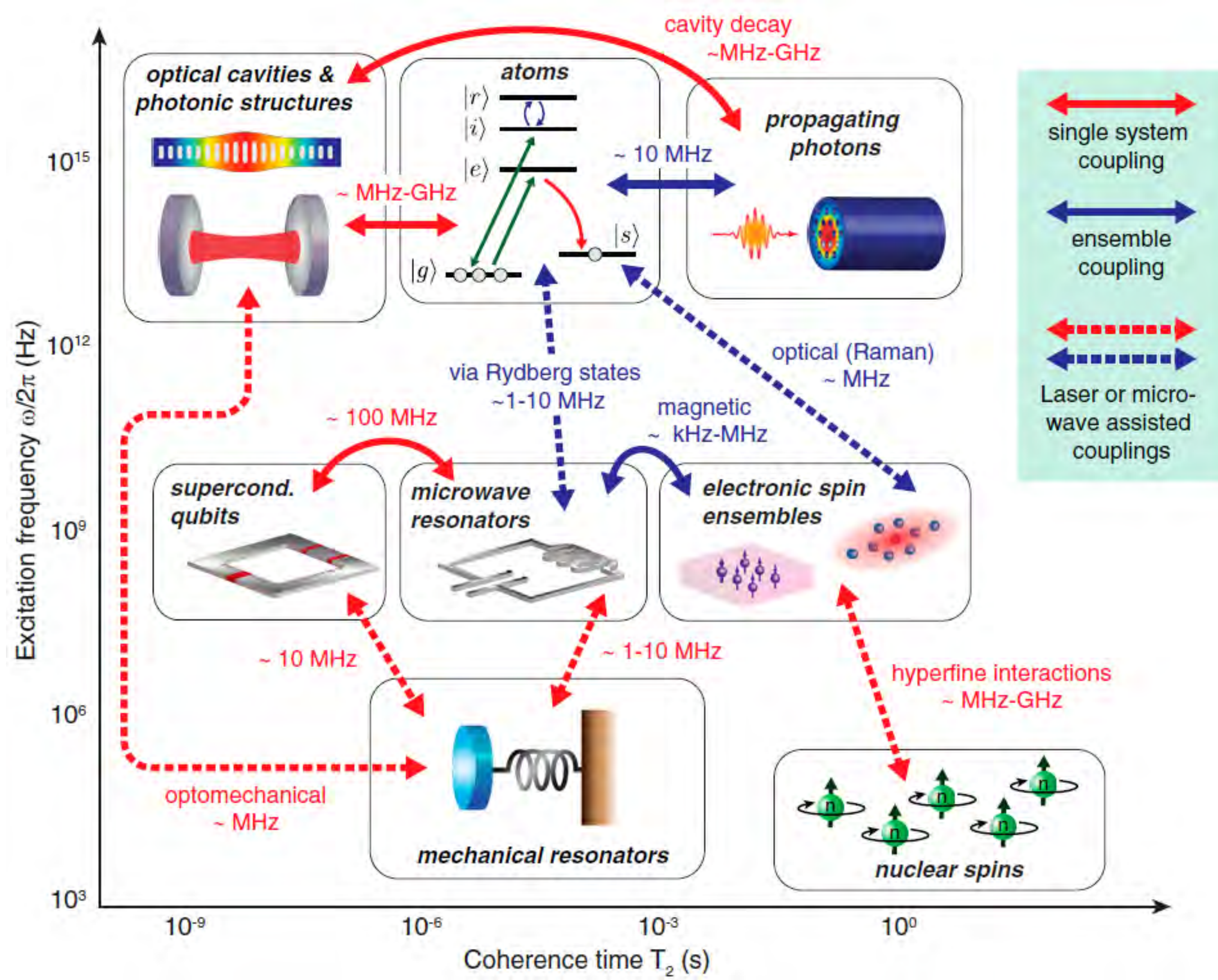

Kurizki, et al. PNAS 112, 3866 (2015)

COHERENT INFORMATION PROCESSING

Quantum hybrid systems

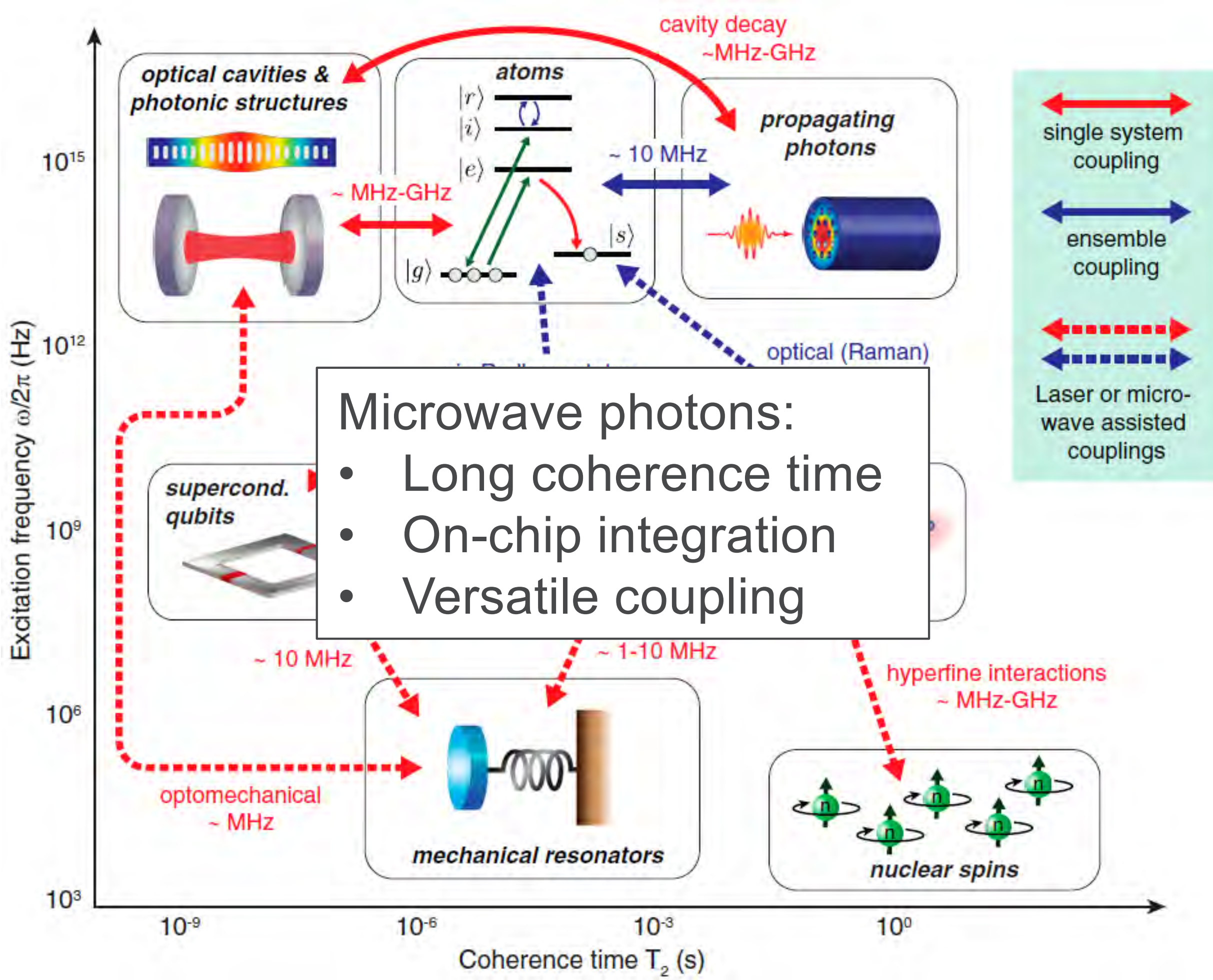

Microwave photons:

- Long coherence time
- On-chip integration
- Versatile coupling

Kurizki, et al. PNAS 112, 3866 (2015)

HYBRID SYSTEM AND STRONG COUPLING

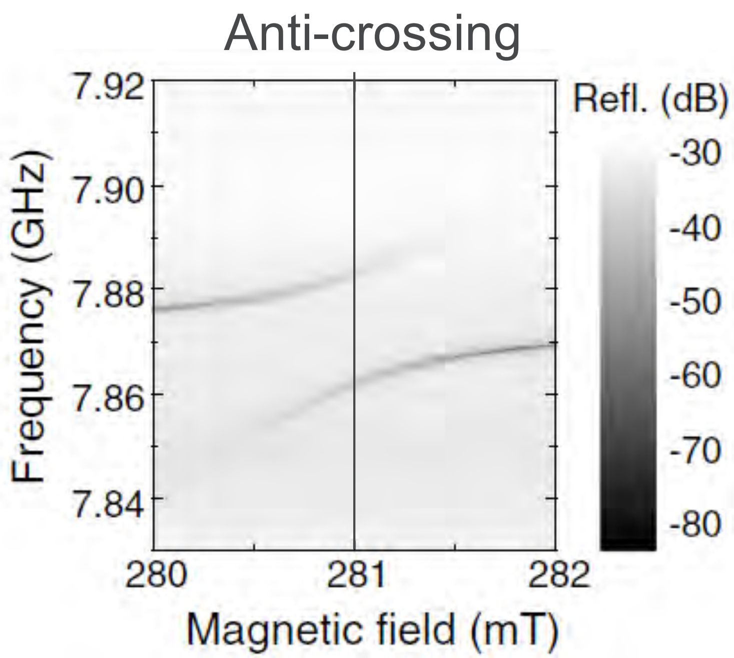

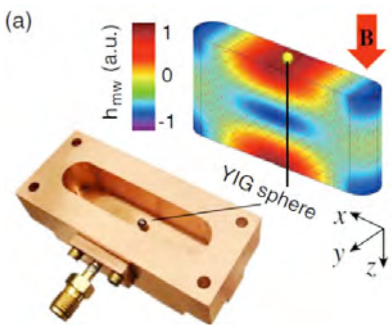

X. Zhang et al. PRL 113, 156401 (2014)

HYBRID SYSTEM AND STRONG COUPLING

Anti-crossing

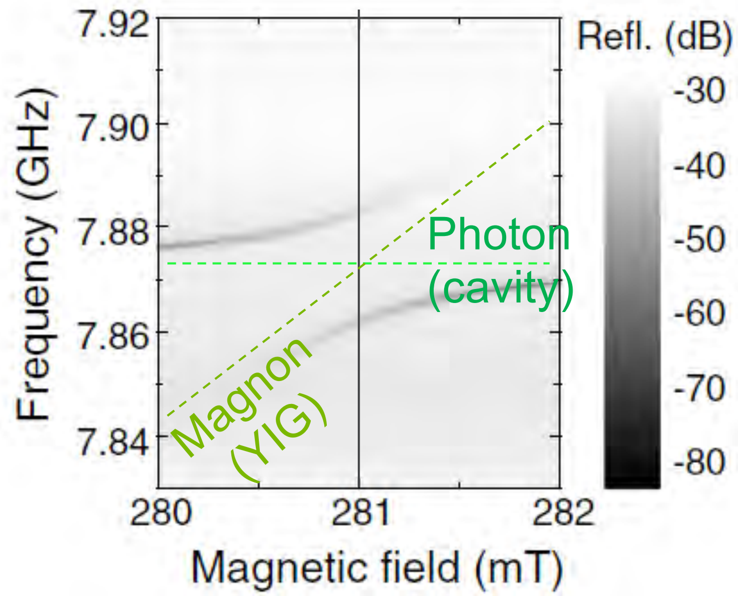

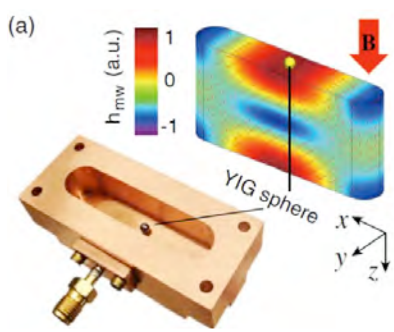

Coupling:
dipolar interaction

$$E = \mu_0 \vec{M} \cdot \vec{h}_{rf}$$

X. Zhang et al. PRL 113, 156401 (2014)

HYBRID SYSTEM AND STRONG COUPLING

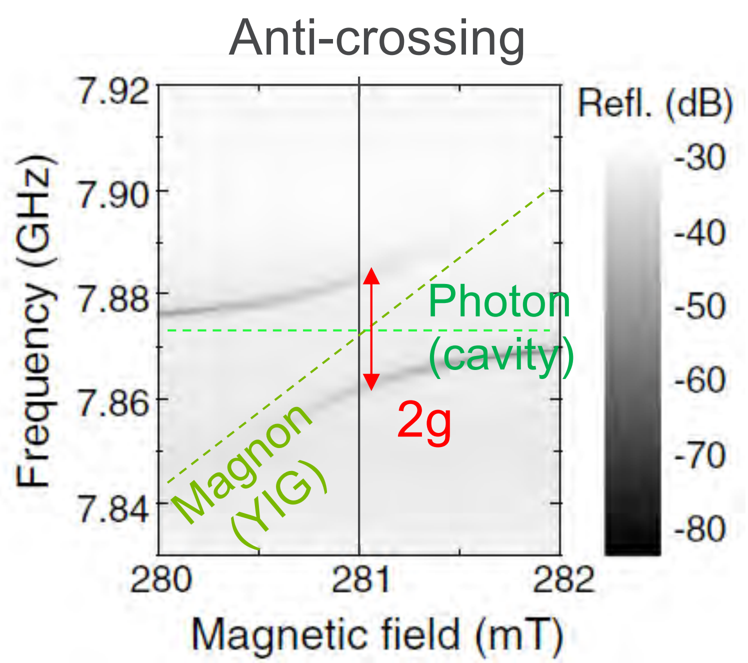

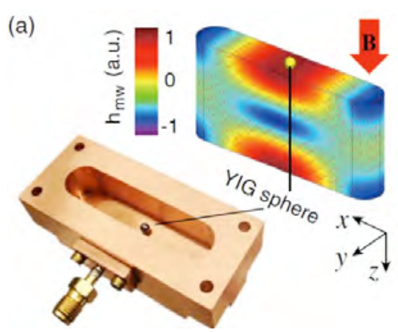

Coupling:
dipolar interaction

$$E = \mu_0 \vec{M} \cdot \vec{h}_{rf}$$

X. Zhang et al. PRL 113, 156401 (2014)

HYBRID SYSTEM AND STRONG COUPLING

Anti-crossing

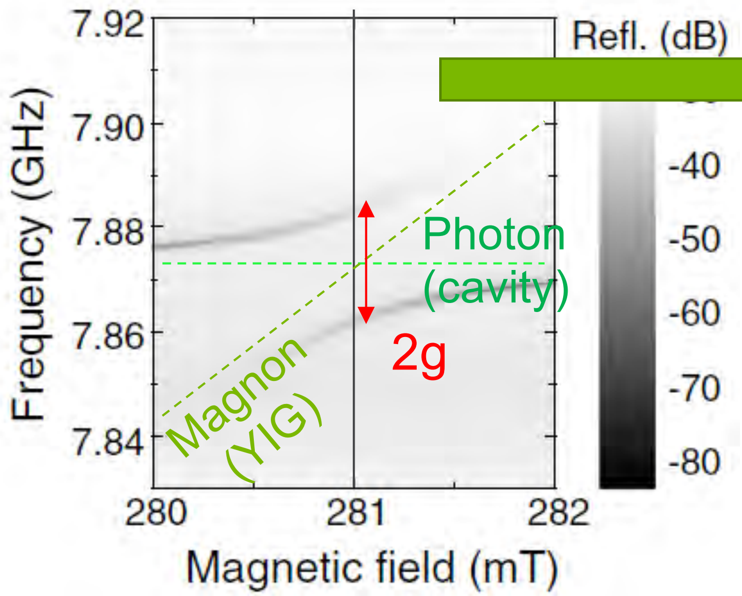

Rabi oscillation

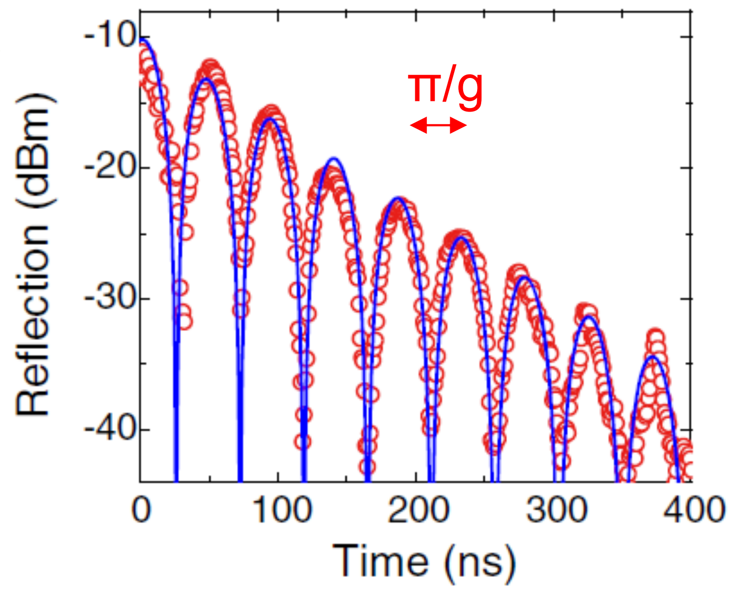

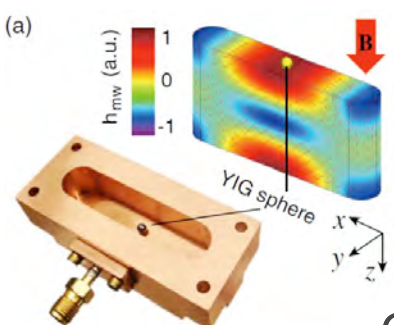

Coupling:
dipolar interaction

$$E = \mu_0 \vec{M} \cdot \vec{h}_{rf}$$

Cooperativity: $C = g^2/\kappa_m\kappa_p$

Strong coupling: $C > 1$, $g > \kappa_m, \kappa_p$

photon

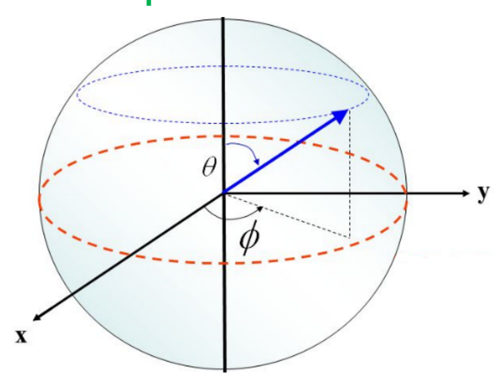

magnon

X. Zhang et al. PRL 113, 156401 (2014)

HYBRID SYSTEM AND STRONG COUPLING

Anti-crossing

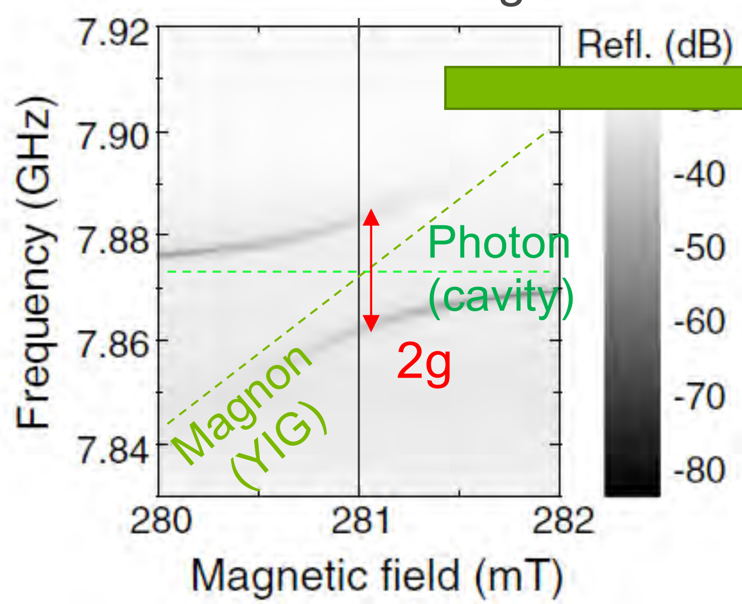

Rabi oscillation

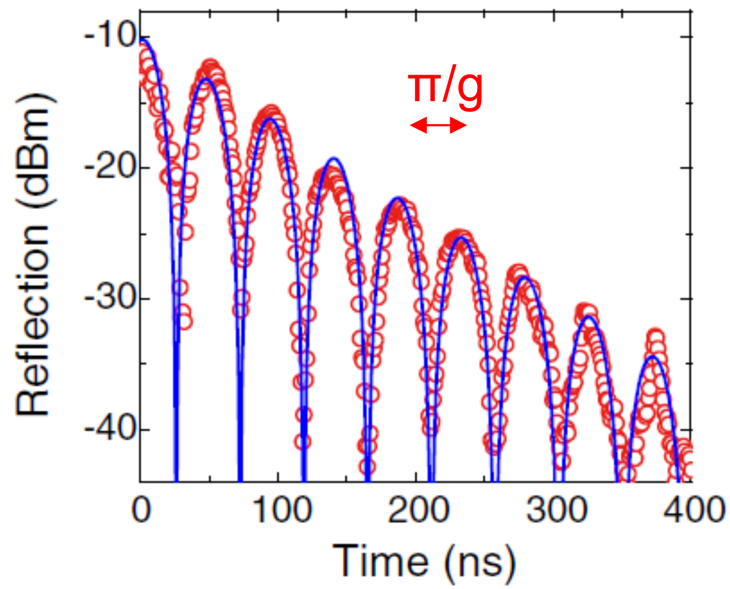

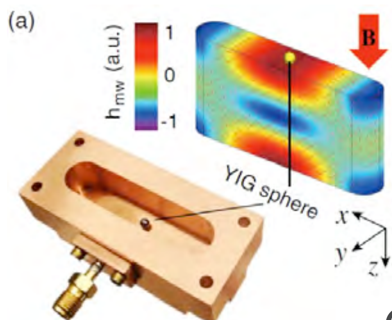

Coupling:
dipolar interaction

$$E = \mu_0 \vec{M} \cdot \vec{h}_{rf}$$

Cooperativity: $C = g^2/\kappa_m\kappa_p$

Strong coupling: $C > 1$, $g > \kappa_m, \kappa_p$

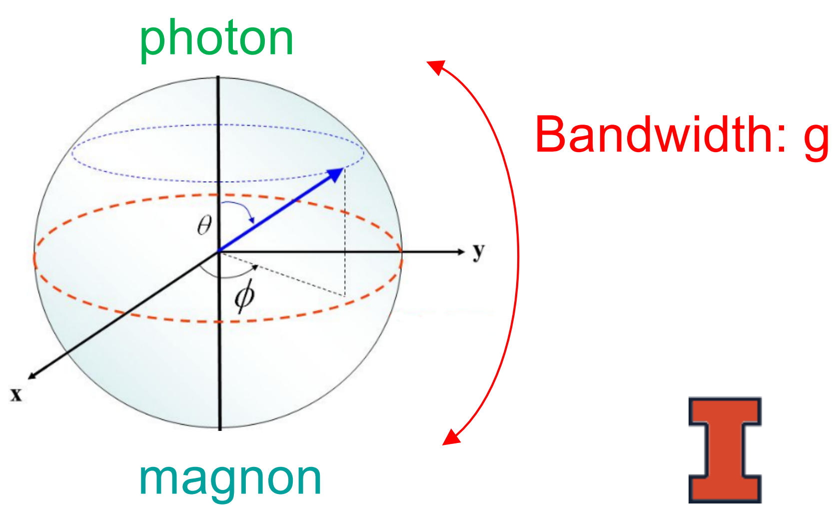

X. Zhang et al. PRL 113, 156401 (2014)

MAGNONS

Uniform mode (k=0)

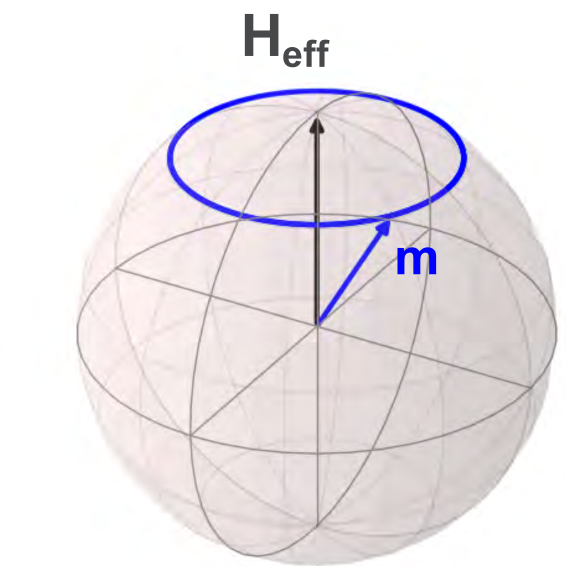

MAGNONS

Uniform mode (k=0)

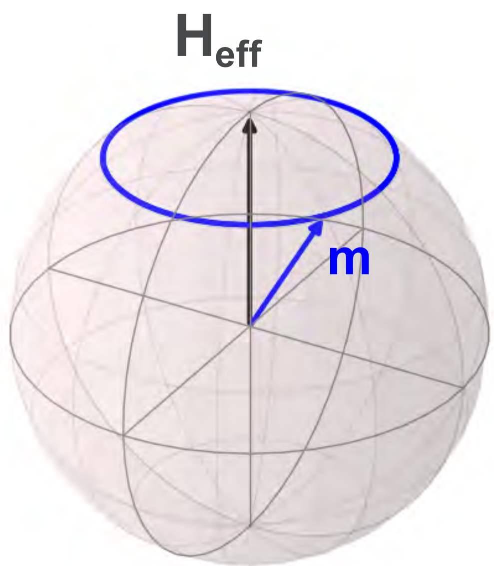

Landau-Lifshitz-Gilbert equation:

$$\frac{d\mathbf{m}}{dt} = -\gamma \mathbf{m} \times \mathbf{H_{eff}} + \alpha \mathbf{m} \times \frac{d\mathbf{m}}{dt}$$

MAGNONS

Uniform mode (k=0)

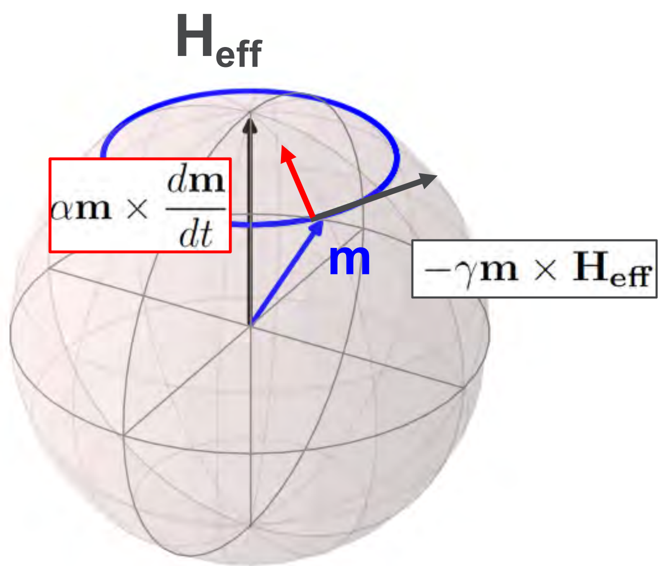

Landau-Lifshitz-Gilbert equation:

$$\frac{d\mathbf{m}}{dt} = \boxed{-\gamma\mathbf{m} \times \mathbf{H}_{\mathrm{eff}}} + \boxed{\alpha\mathbf{m} \times \frac{d\mathbf{m}}{dt}}$$

MAGNONS

Uniform mode (k=0)

$\omega = \gamma H_{eff}$ (in GHz)

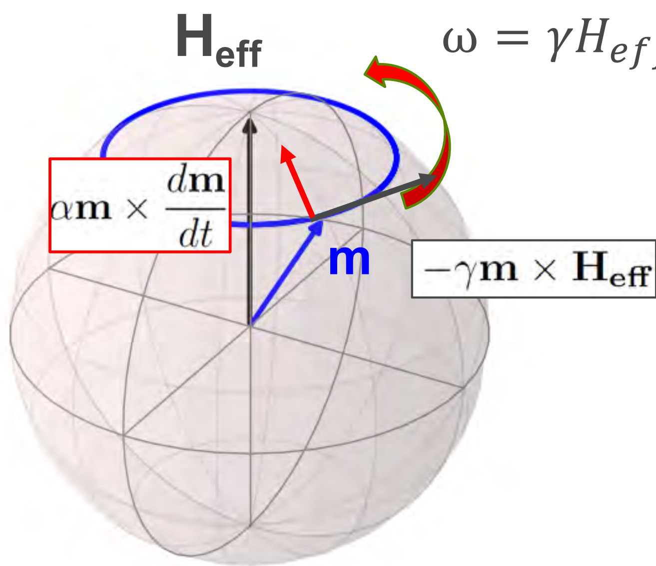

Landau-Lifshitz-Gilbert equation:

$$\frac{d\mathbf{m}}{dt} = \boxed{-\gamma\mathbf{m} \times \mathbf{H}_{\mathrm{eff}}} + \boxed{\alpha\mathbf{m} \times \frac{d\mathbf{m}}{dt}}$$

Gyromagnetic ratio: $\gamma/2\pi \sim 28$ GHz/Tesla

Gilbert damping: $\alpha \sim 10^{-3}$

(Q factor~1/α)

MAGNONS

Spin wave (k>0)

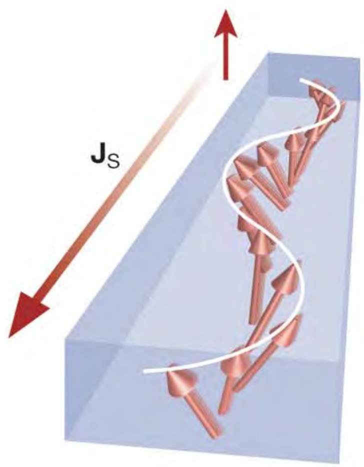

MAGNONS

Spin wave (k>0)

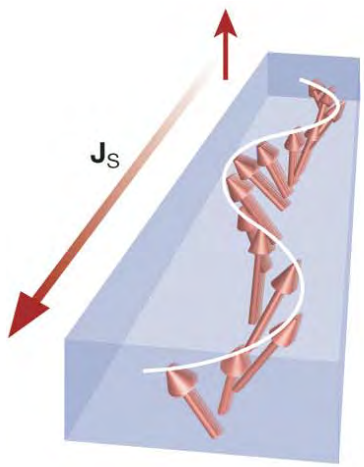

Magnon dispersion:

$$\omega = \gamma H_{eff} + Dk^2$$

D: Exchange constant
(magnon: Dk^2 ~ 3 GHz for λ~100 nm)

MAGNONS

Spin wave (k>0)

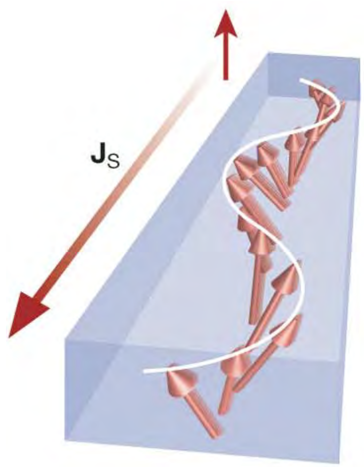

Magnon dispersion:

$$\omega = \gamma H_{eff} + Dk^2$$

D: Exchange constant
(magnon: Dk^2 ~ 3 GHz for λ~100 nm)

(Photon/phonon dispersion:)

$$\omega = ck$$

(photon: ω ~ 3 GHz for λ~100 mm)
(phonon: ω ~ 3 GHz for λ~1 μm)

MAGNONS

Spin wave (k>0)

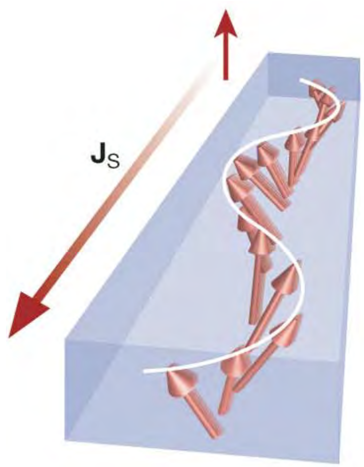

Small + more flexible

Magnon dispersion:

$$\omega = \gamma H_{eff} + Dk^2$$

D: Exchange constant
(magnon: Dk^2 ~ 3 GHz for λ~100 nm)

(Photon/phonon dispersion:)

$$\omega = ck$$

(photon: ω ~ 3 GHz for λ~100 mm)
(phonon: ω ~ 3 GHz for λ~1 μm)

MAGNONS FOR COHERENT INFORMATION PROCESSING

Advantage of Magnons for coherent information processing:

- *Strong Coupling (sub-GHz)*

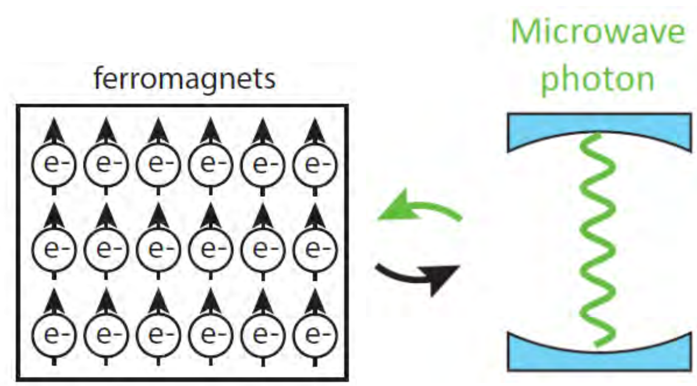

Coupling strength: $g = g_0\sqrt{N}$

Y. Li et al. arXiv:2006.16158

MAGNONS FOR COHERENT INFORMATION PROCESSING

Advantage of Magnons for coherent information processing:

- *Strong Coupling (sub-GHz)*
- *Quantum Transduction*

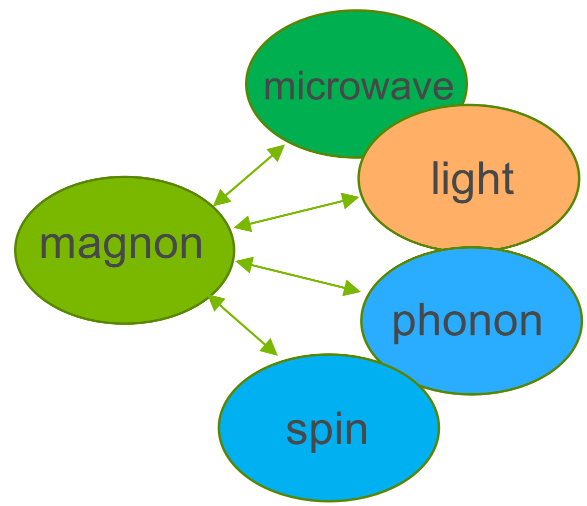

Y. Li et al. arXiv:2006.16158

MAGNONS FOR COHERENT INFORMATION PROCESSING

Advantage of Magnons for coherent information processing:

- *Strong Coupling (sub-GHz)*
- *Quantum Transduction*
- *Wave Propagation*

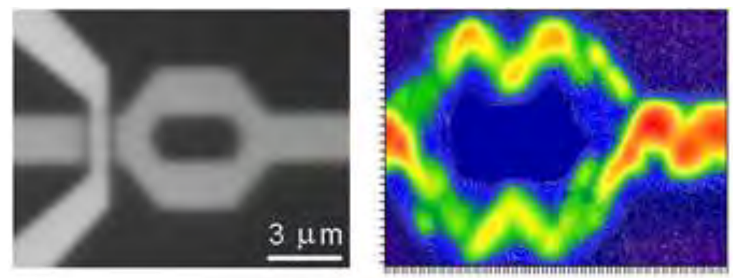

Magnonic logic

Y. Li et al. arXiv:2006.16158

Picture courtesy of Sergei Urazdhin

MAGNONS FOR COHERENT INFORMATION PROCESSING

Advantage of Magnons for coherent information processing:

- *Strong Coupling (sub-GHz)*
- *Quantum Transduction*
- *Wave Propagation*
- *On-chip Integration*

Microwave quantum circuits

Y. Li et al. arXiv:2006.16158

MAGNONS FOR COHERENT INFORMATION PROCESSING

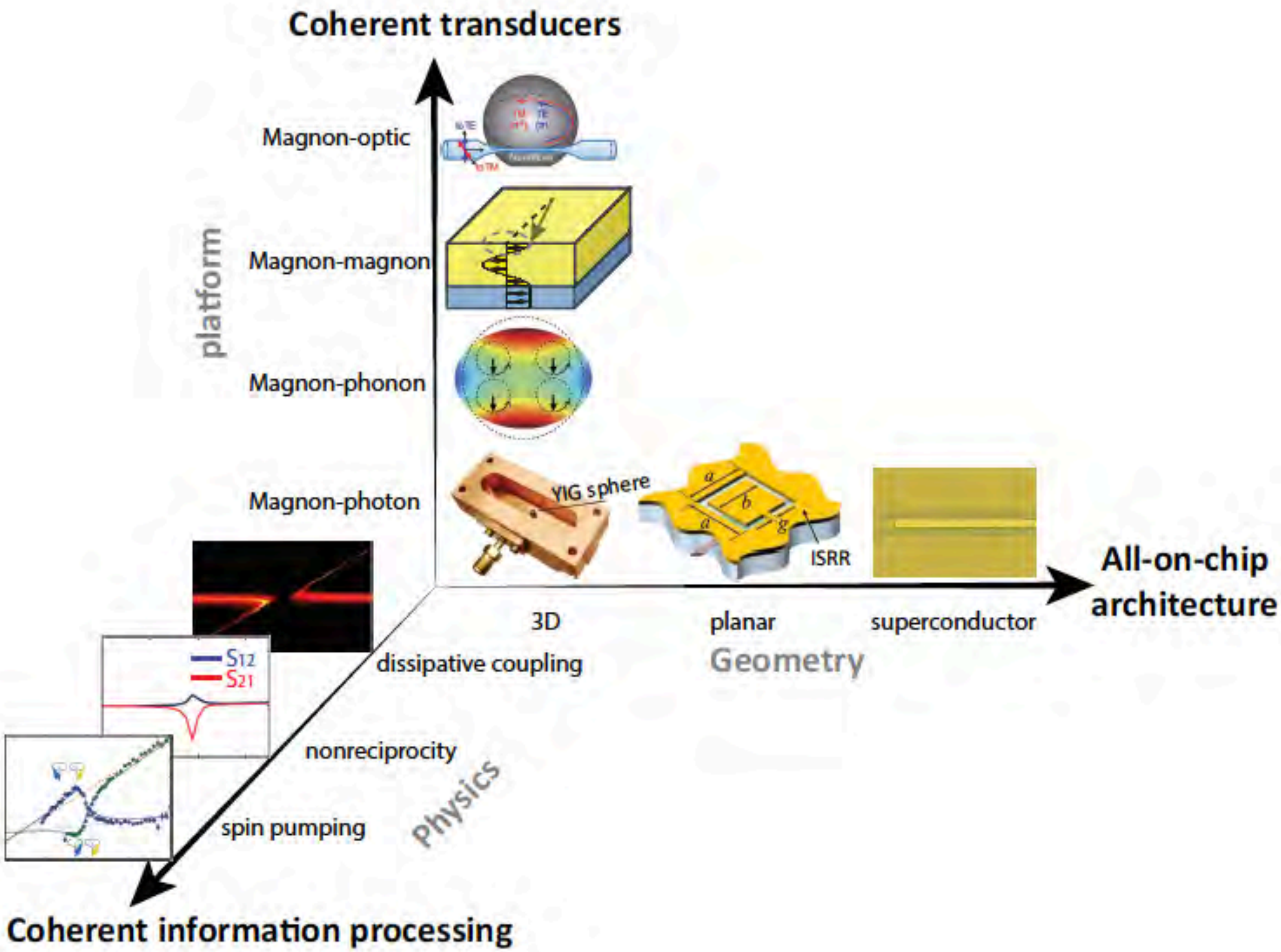

Y. Li et al. arXiv:2006.16158

QUANTUM MAGNONICS

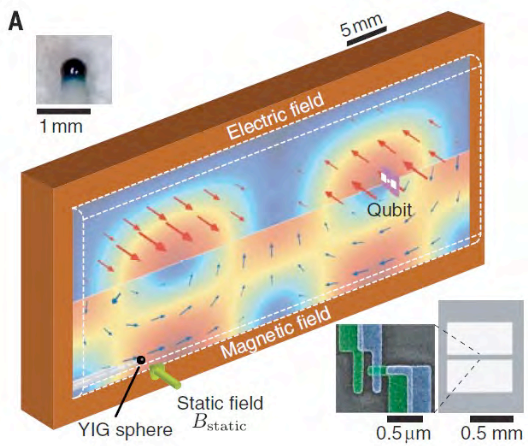

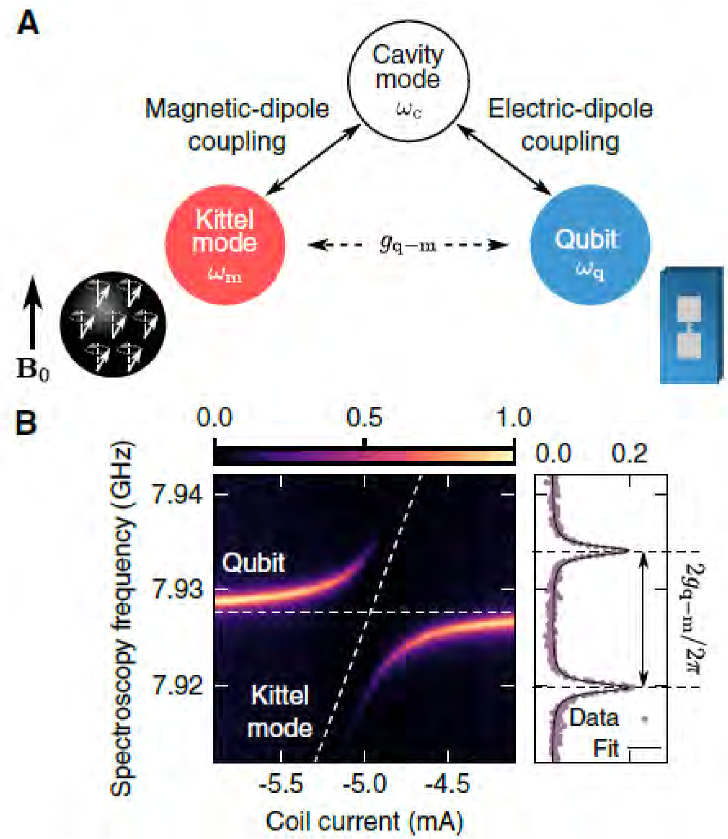

Y. Tabuchi et al. Science 349, 405 (2015)
D. Lachance-Quirion, et al. Science 367, 425 (2020)

QUANTUM MAGNONICS

Goal of quantum magnonics:
microwave quantum circuits

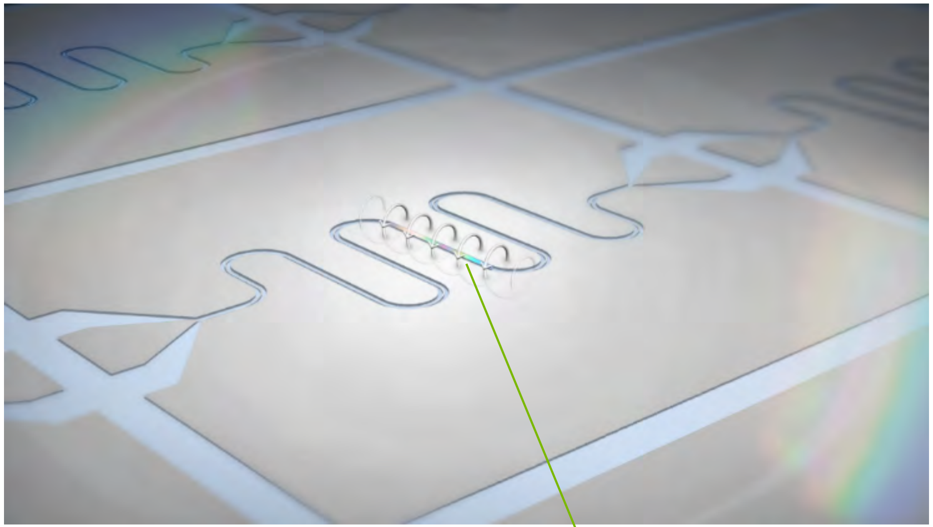

Magnonic
devices

OUTLINE

- Introduction
- **On-chip magnon-photon coupling with superconducting resonator**
- Magnon-magnon coupling in magnetic bilayer thin film
- Manipulating phonon transport with magnons
- Conclusions

MAGNON-PHOTON HYBRID SYSTEM

Most previous demonstrations:
Bulk FM (YIG) or 3D cavity

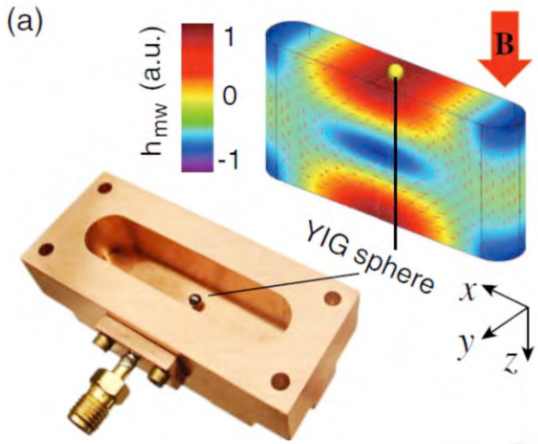

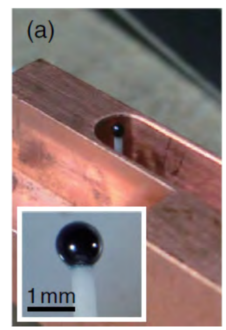

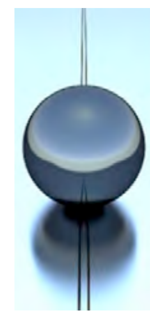

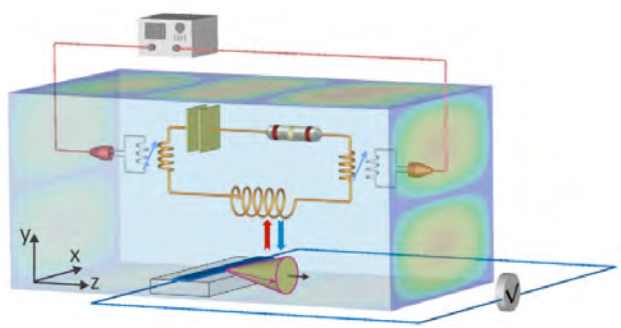

Tabuchi et al. PRL 113, 083603 (2014)
Bai et al. PRL 114, 227201 (2015)
Morris et al. Sci. Rep. 7, 11511 (2017)

ON-CHIP MAGNON-PHOTON HYBRID SYSTEM

Coplanar superconducting resonator

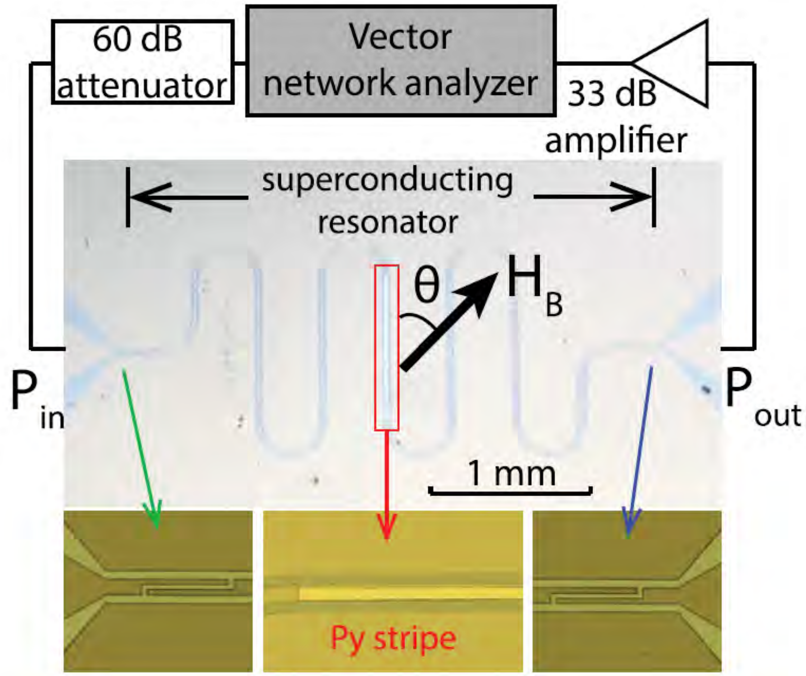

Yi Li, et al. PRL 123, 107701 (2019)

ON-CHIP MAGNON-PHOTON HYBRID SYSTEM

Coplanar superconducting resonator

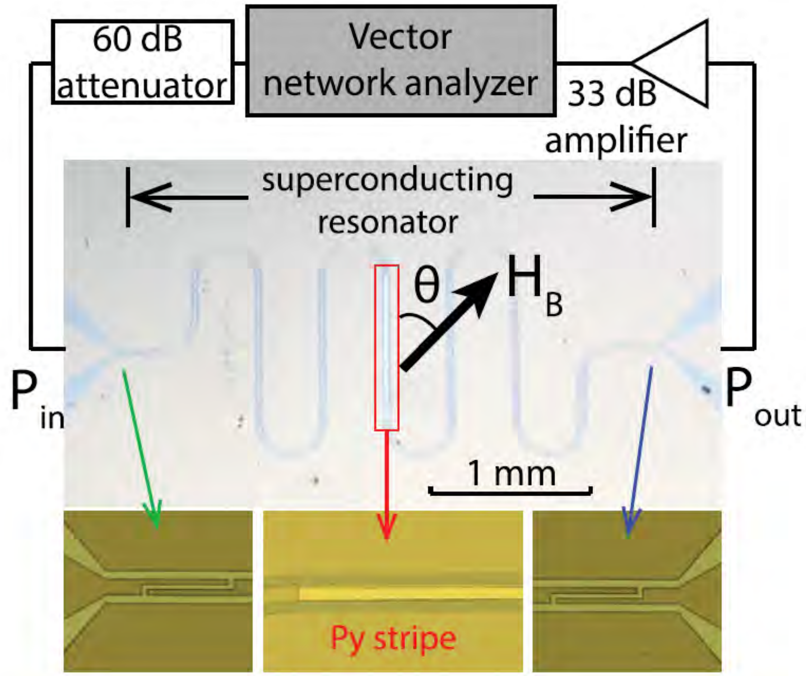

Photon system:
NbN coplanar superconducting resonator

Magnon system:
$Ni_{80}Fe_{20}$ device (permalloy, Py)

- High T_c (14 K)
- Large magnetization ($\mu_0 M_s$ = 1 T)

Yi Li, et al. PRL 123, 107701 (2019)

SUPERCONDUCTING CIRCUIT

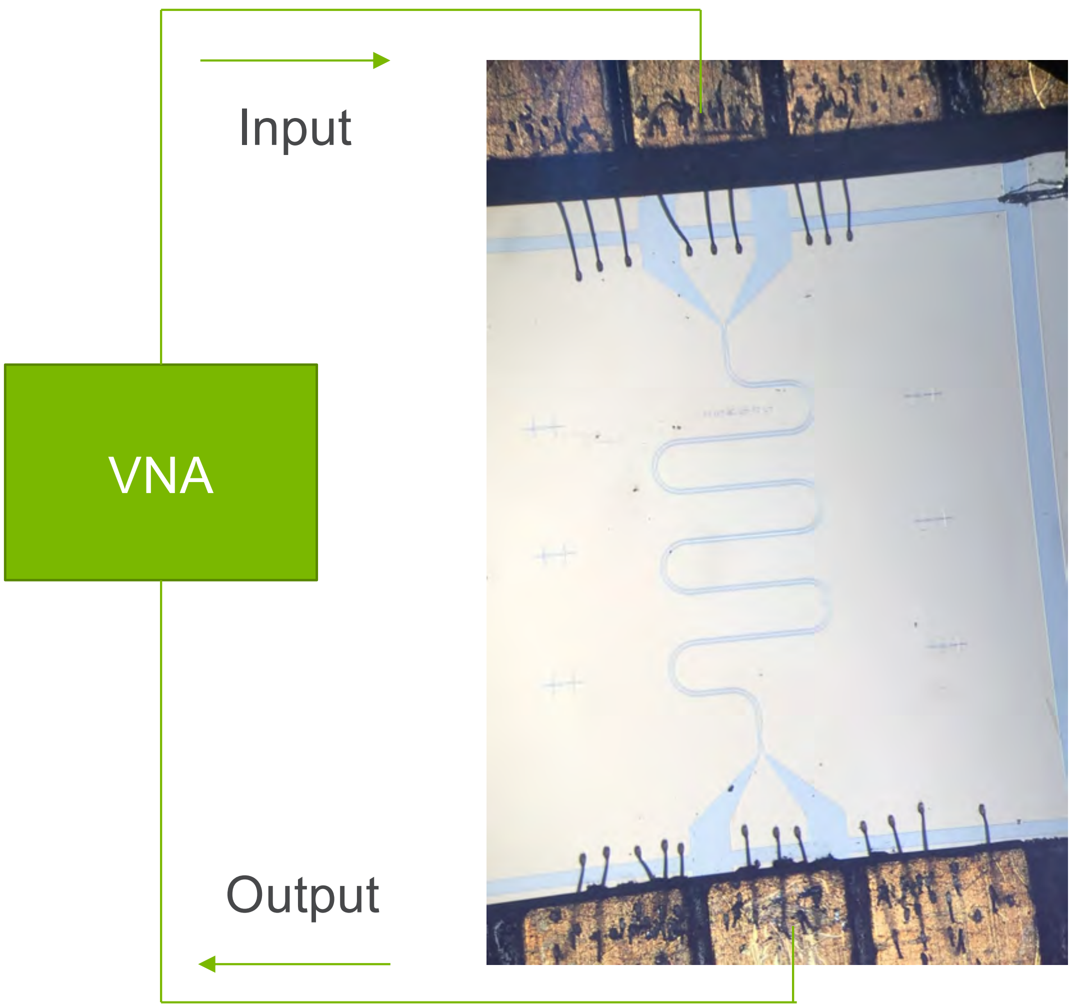

Yi Li, et al. PRL 123, 107701 (2019)

SUPERCONDUCTING CIRCUIT

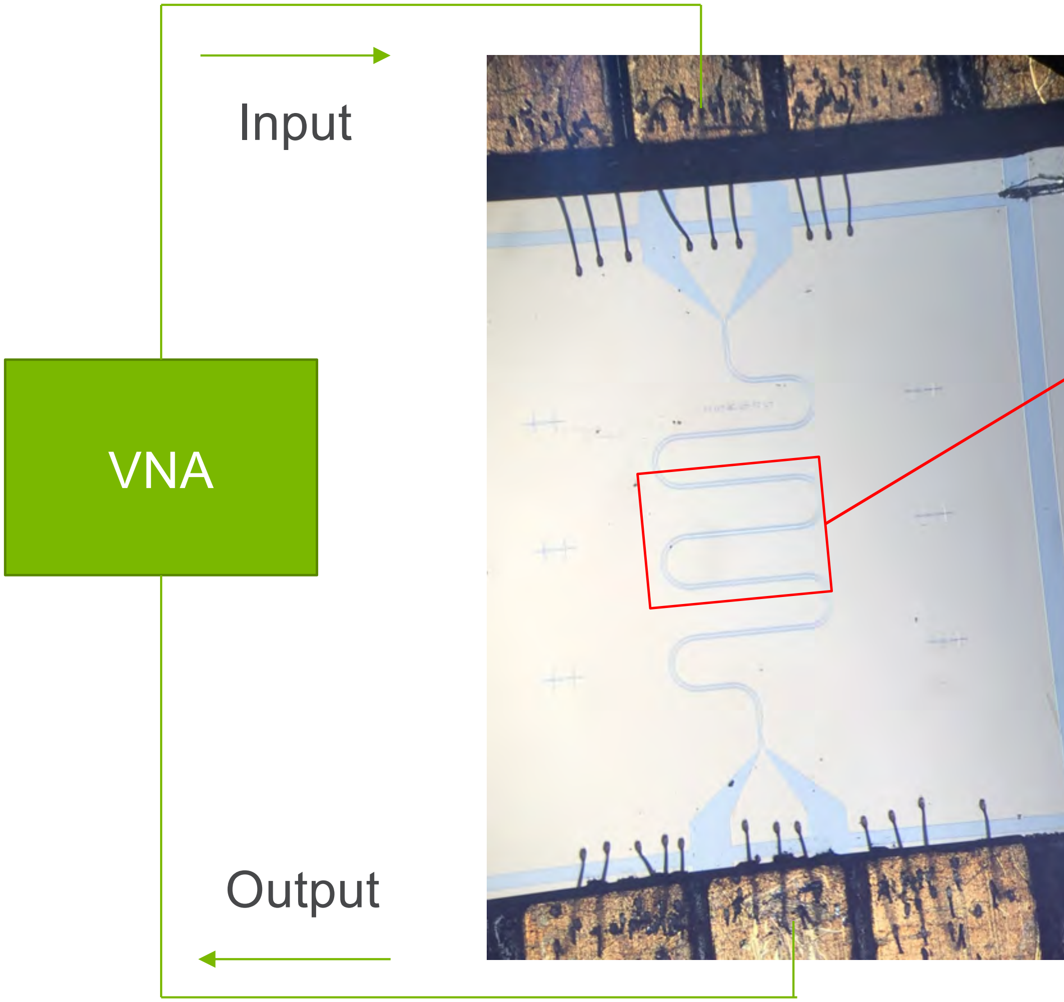

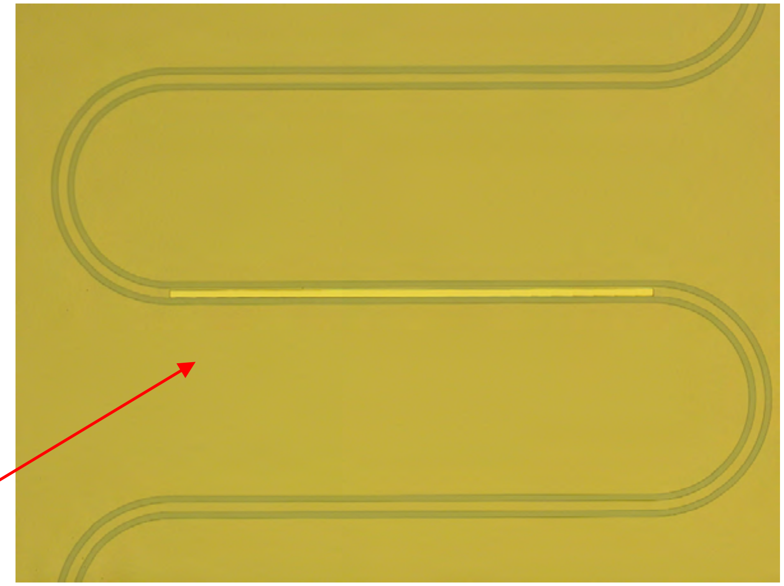

Yi Li, et al. PRL 123, 107701 (2019)

SUPERCONDUCTING CIRCUIT

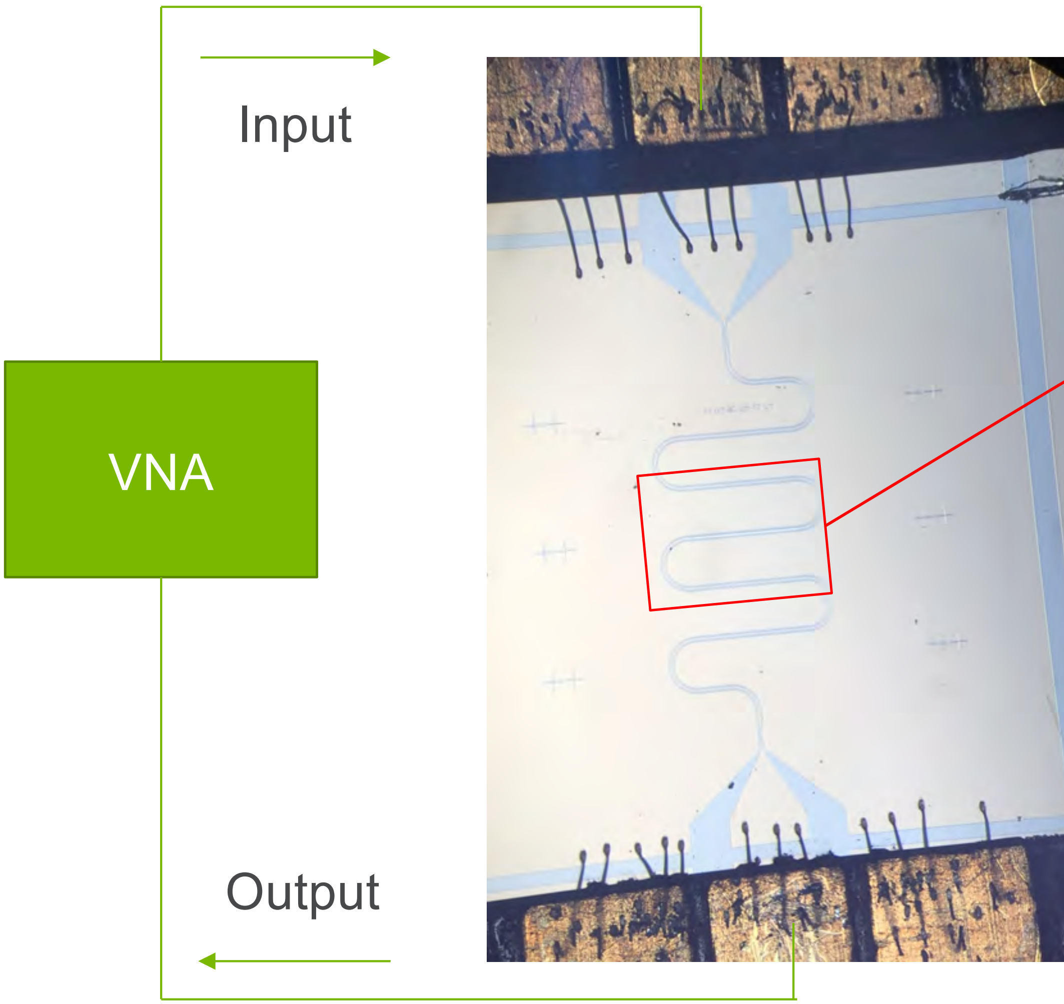

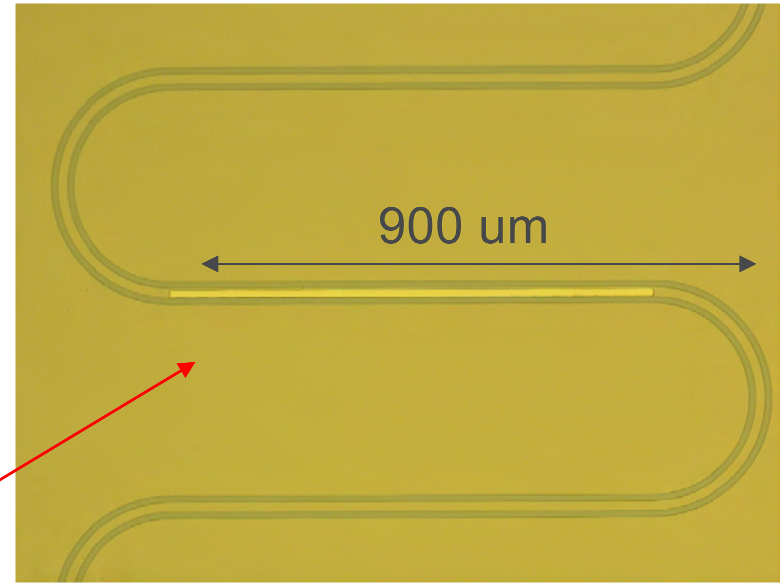

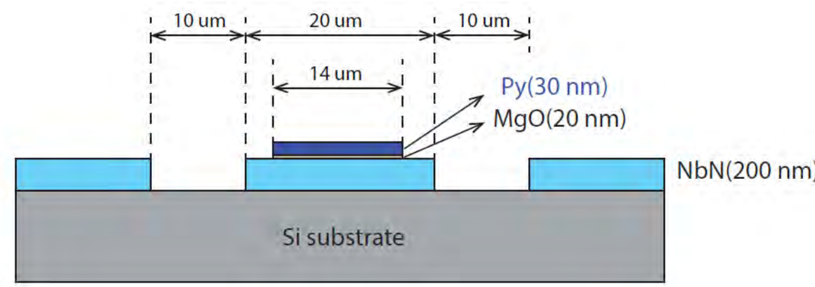

Yi Li, et al. PRL 123, 107701 (2019)

PHOTON SYSTEM:
UNLOADED NbN SUPERCONDUCTING RESONATOR

Zero-field cooling

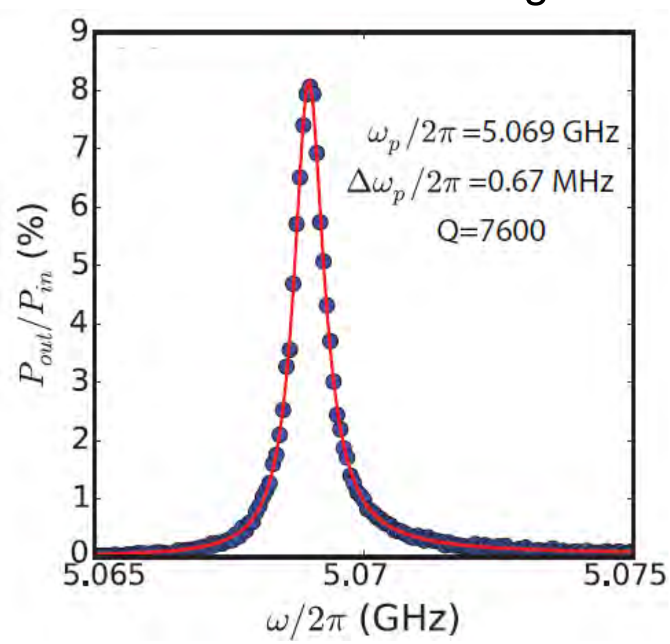

T = 1.4 K

P_{in} = -55 dBm

(0 dBm = 1 mWatt)
(-55 dBm = 4 nWatt)

Yi Li, et al. PRL 123, 107701 (2019)

PHOTON SYSTEM:
UNLOADED NbN SUPERCONDUCTING RESONATOR

Zero-field cooling

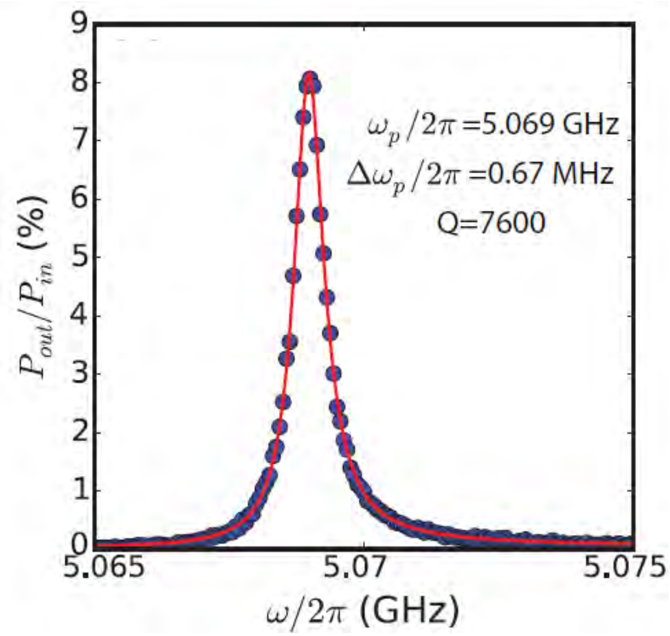

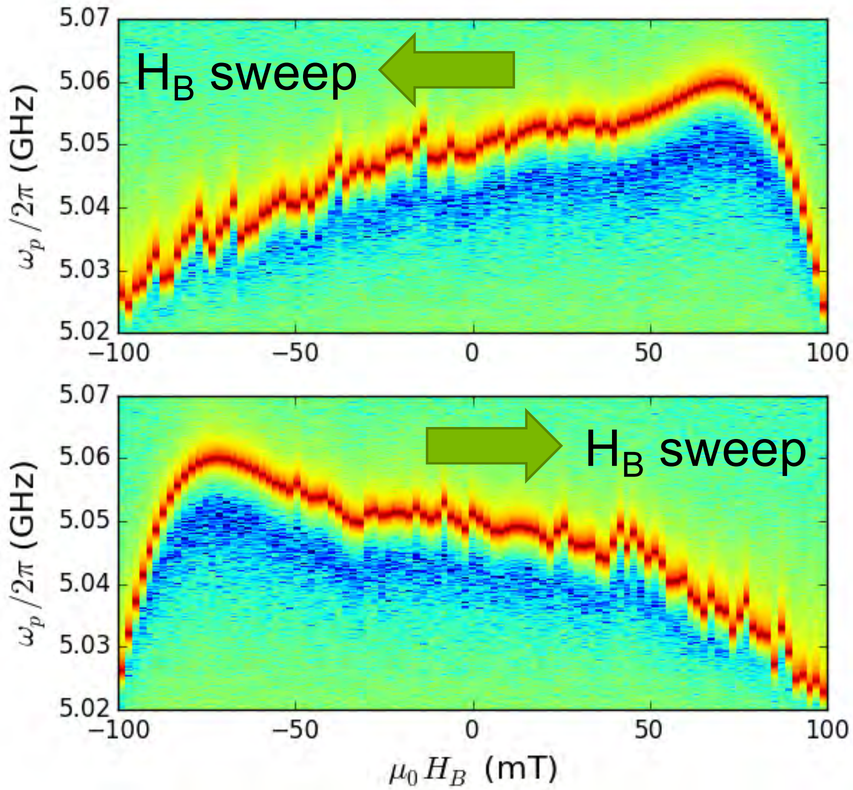

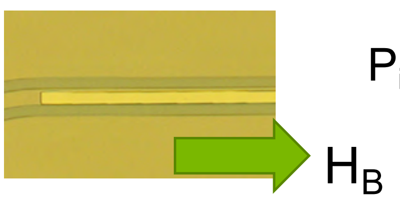

T = 1.4 K

P_{in} = -55 dBm

(0 dBm = 1 mWatt)
(-55 dBm = 4 nWatt)

Yi Li, et al. PRL 123, 107701 (2019)

PHOTON SYSTEM:
UNLOADED NbN SUPERCONDUCTING RESONATOR

Zero-field cooling

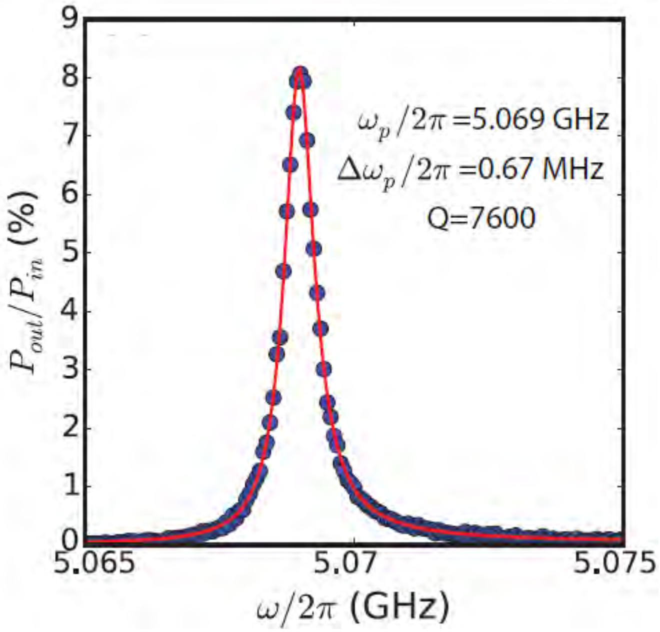

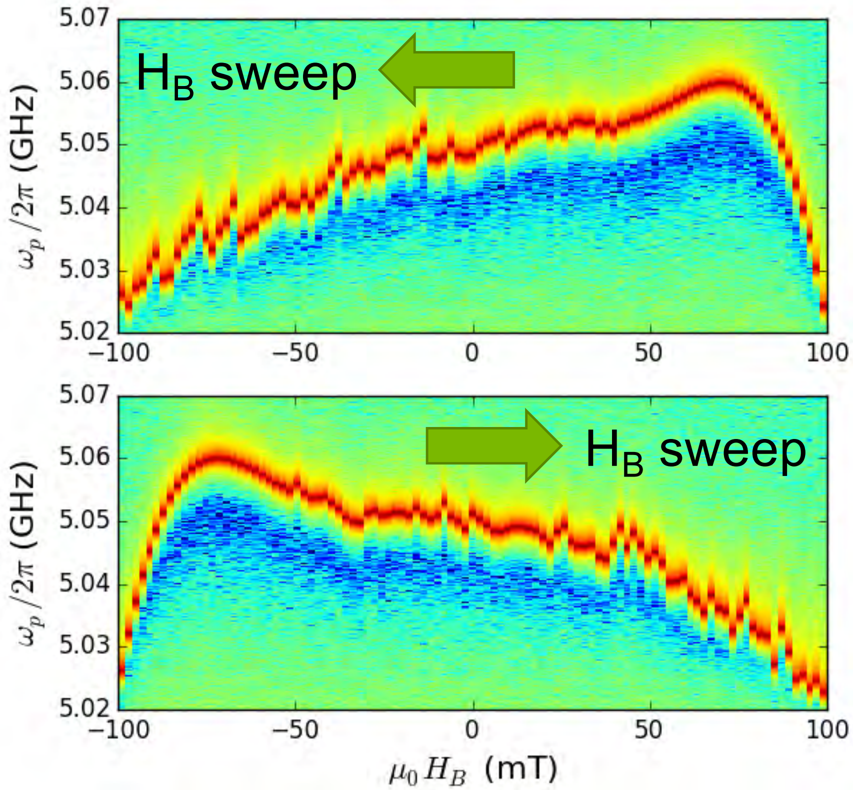

T = 1.4 K

P_{in} = -55 dBm

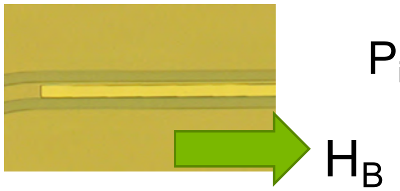

(0 dBm = 1 mWatt)
(-55 dBm = 4 nWatt)

Yi Li, et al. PRL 123, 107701 (2019)

Superconducting vortex

$$\frac{\omega}{2\pi} = \frac{1}{\sqrt{LC}}$$

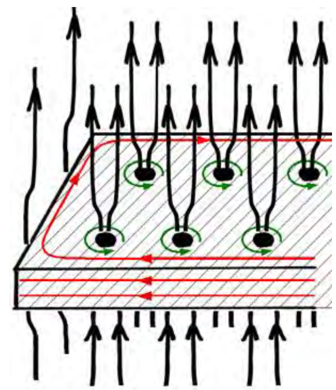

MAGNONS SYSTEM: $Ni_{80}Fe_{20}$ (Py) STRIPE

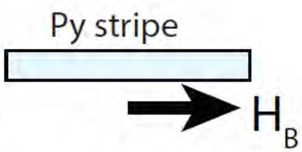

$$\frac{\omega}{\gamma} = \sqrt{H_B(H_B+M_s)}$$

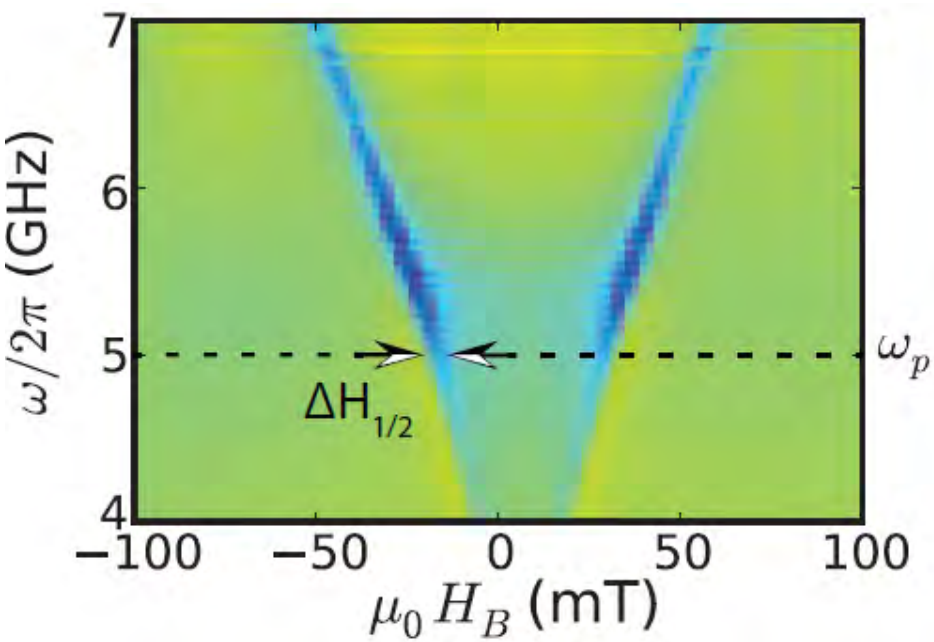

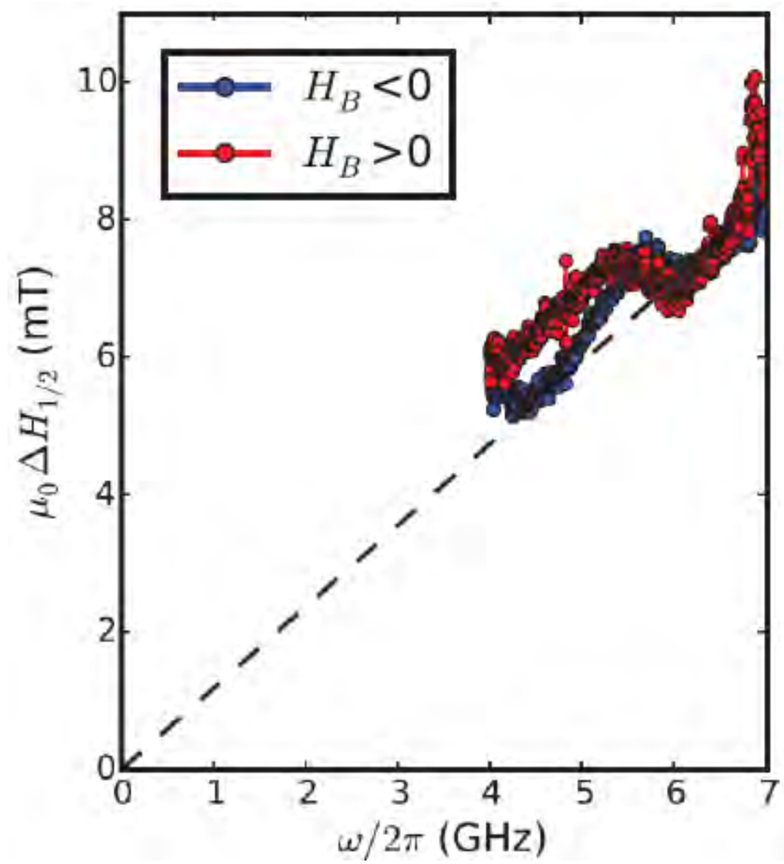

T=1.4 K

P_{in} = 0 dBm

Magnon relaxation rate (5 GHz):

$\kappa_m/2\pi$ = 0.168 GHz

$$\mu_0 \Delta H_{1/2} = \frac{2\alpha\omega}{\gamma}$$

Damping: α = 0.016

Yi Li, et al. PRL 123, 107701 (2019)

MAGNON-PHOTON HYBRID SYSTEM

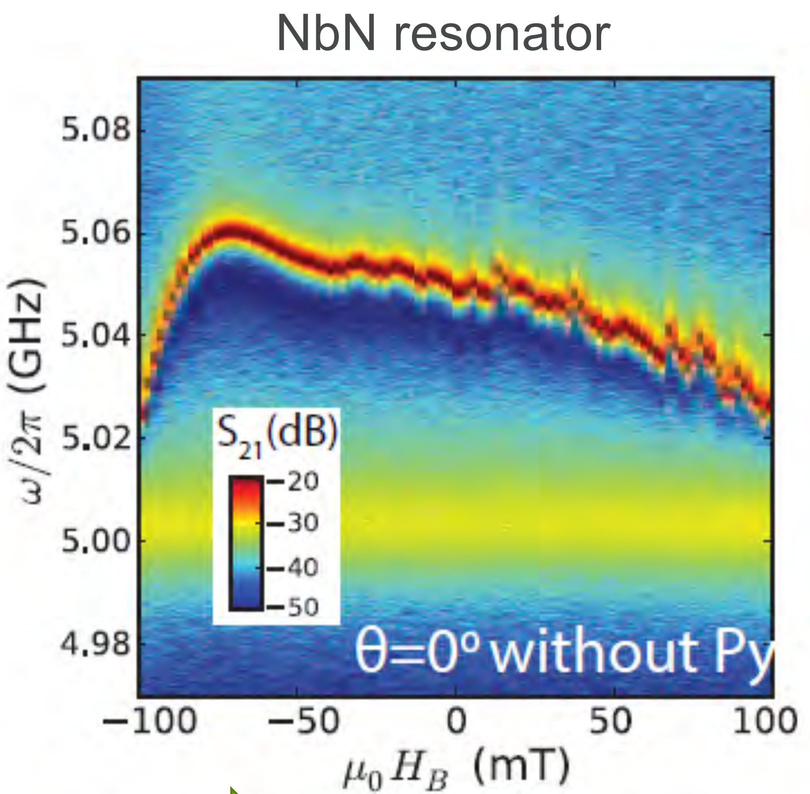

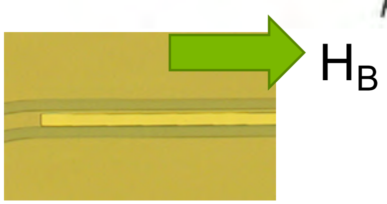

T=1.4 K

P_{in}=-55 dBm

Yi Li, et al.
PRL 123, 107701 (2019)

MAGNON-PHOTON HYBRID SYSTEM

NbN resonator

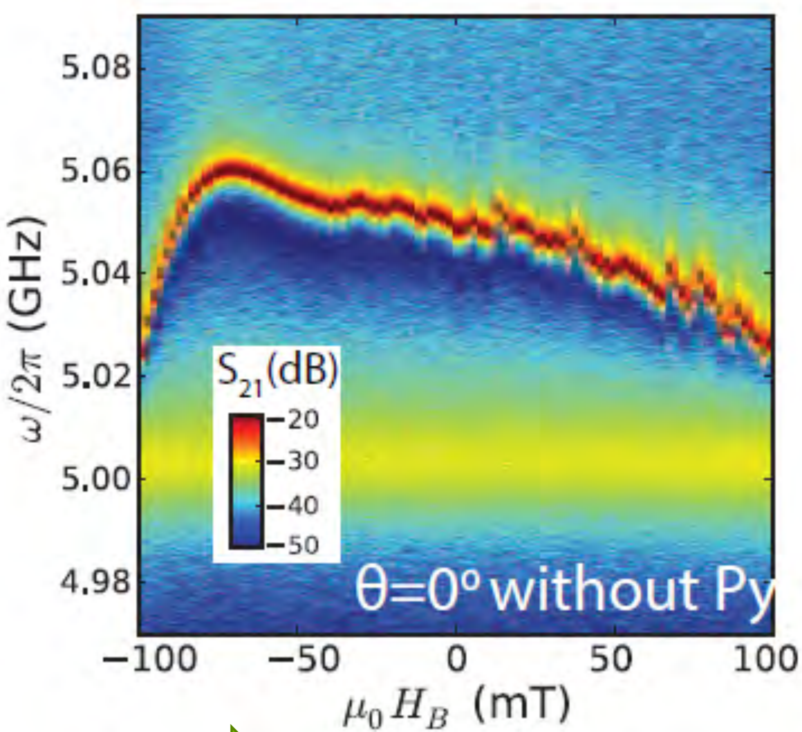

NbN resonator + Py device

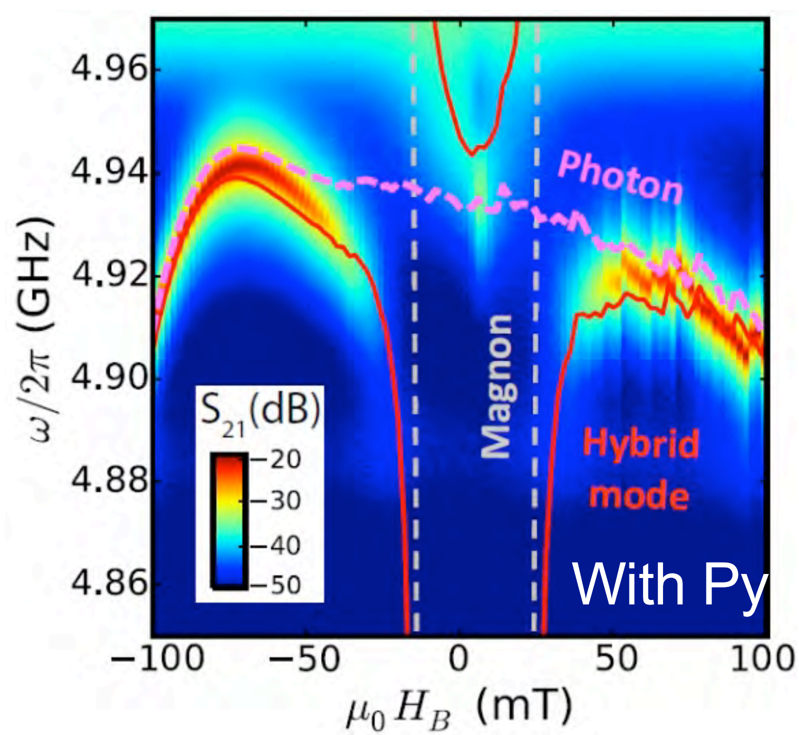

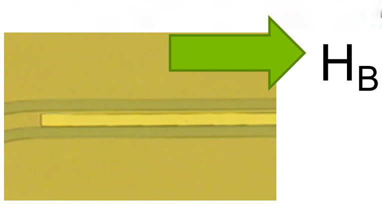

T=1.4 K

P_{in}=-55 dBm

Yi Li, et al.
PRL 123, 107701 (2019)

MAGNON-PHOTON HYBRID SYSTEM

Photon damping rate: $\kappa_p/2\pi$=2.0 MHz

Q=2500

NbN resonator

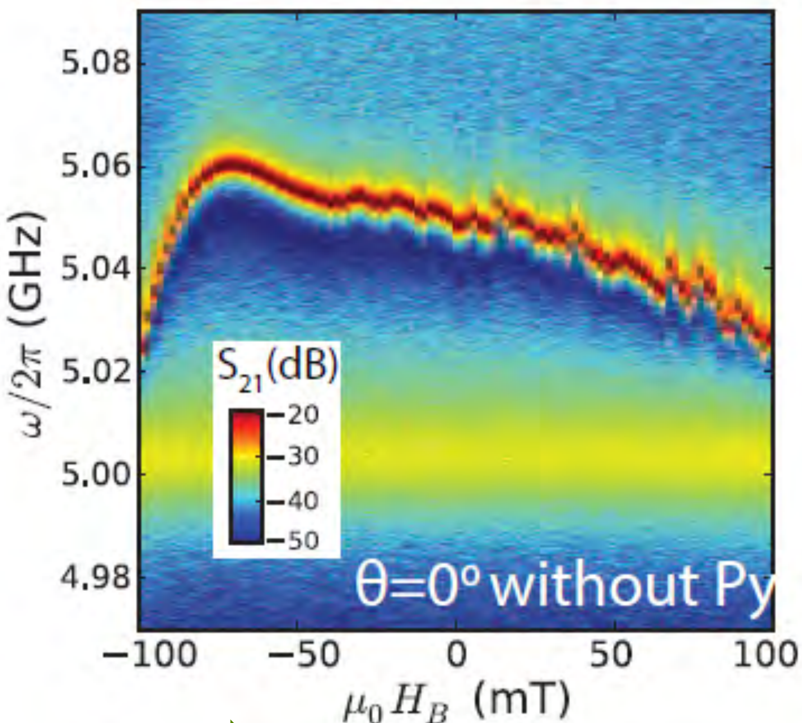

NbN resonator + Py device

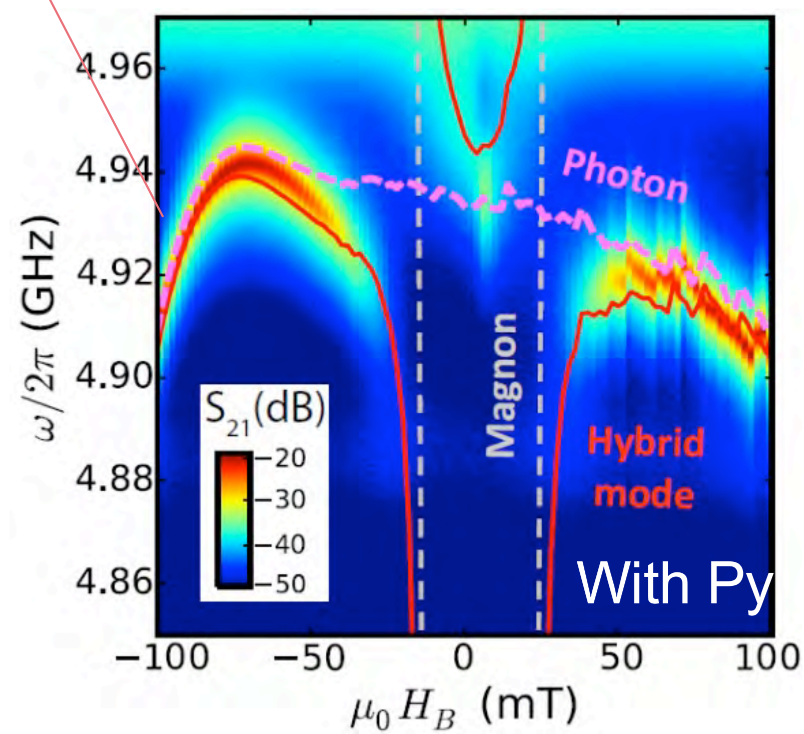

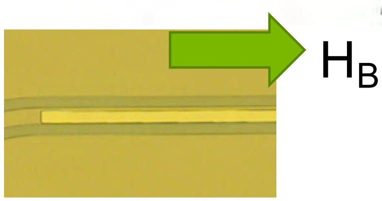

T=1.4 K

P_{in}=-55 dBm

Yi Li, et al.
PRL 123, 107701 (2019)

MAGNON-PHOTON HYBRID SYSTEM

Photon damping rate: $\kappa_p/2\pi$=2.0 MHz

Q=2500

NbN resonator

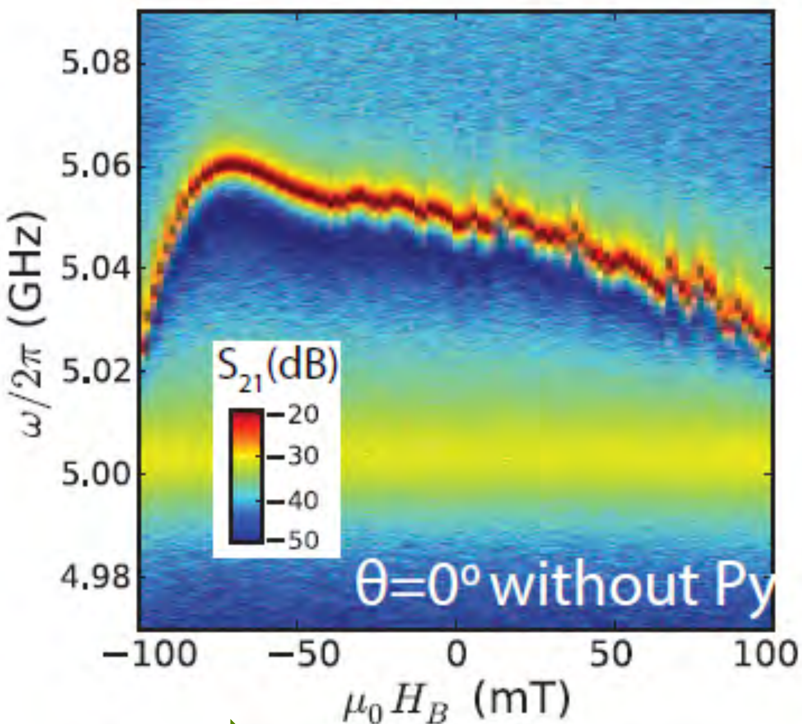

NbN resonator + Py device

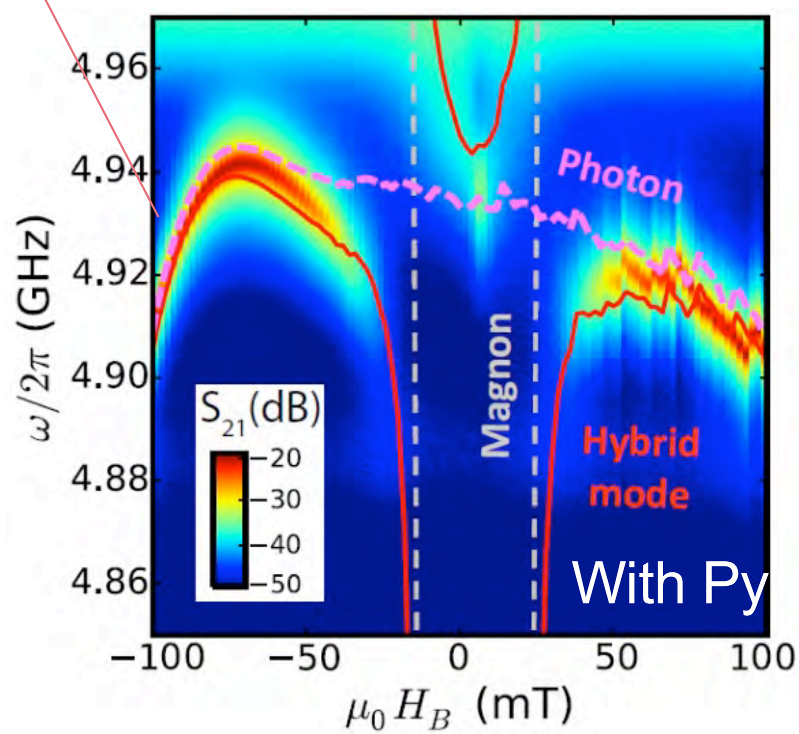

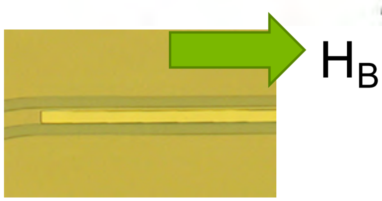

Coupling energy: $E = \mu_0 \vec{M} \cdot \vec{h}_{rf}$

magnon

$$H = \begin{pmatrix} E_1 & W \\ W & E_2 \end{pmatrix}$$

photon

T=1.4 K

P_{in}=-55 dBm

Yi Li, et al.
PRL 123, 107701 (2019)

MAGNON-PHOTON HYBRID SYSTEM: ANALYSIS

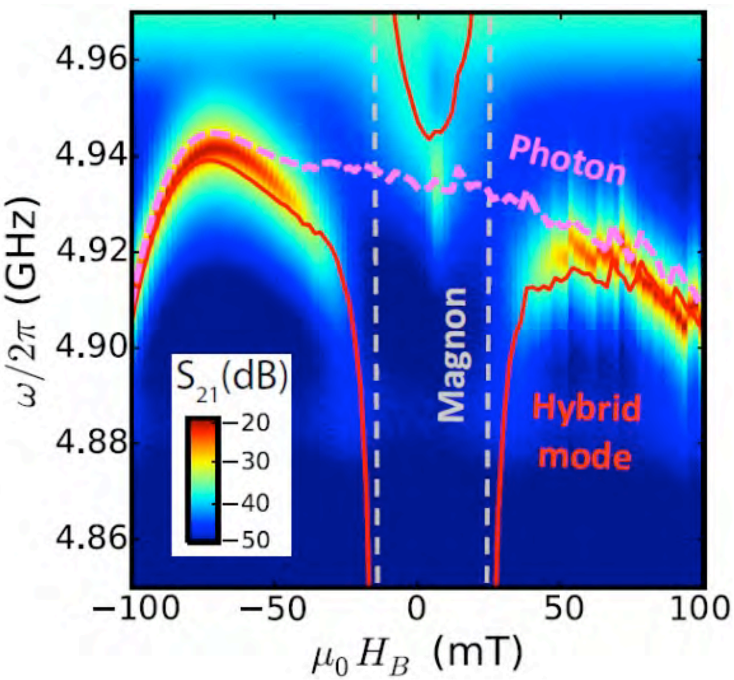

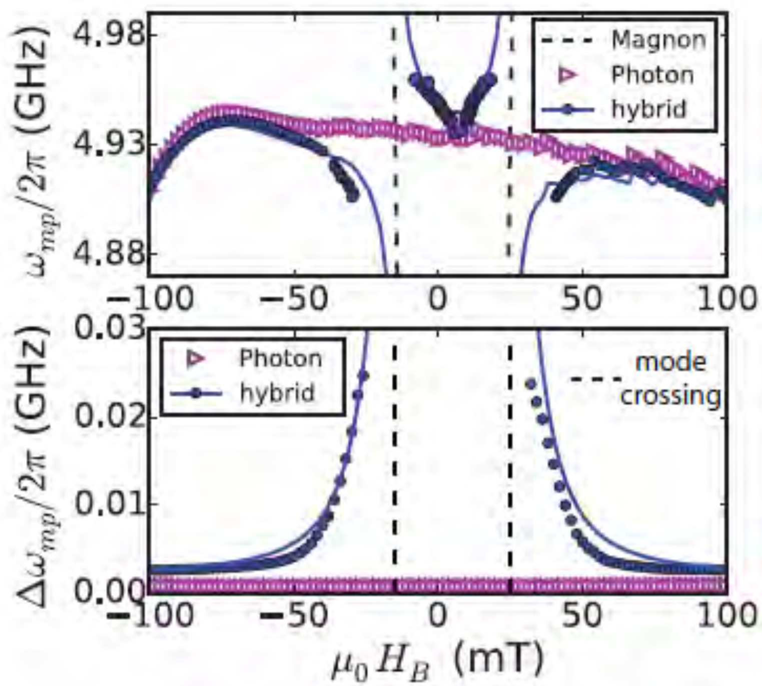

Yi Li, et al. PRL 123, 107701 (2019)

MAGNON-PHOTON HYBRID SYSTEM: ANALYSIS

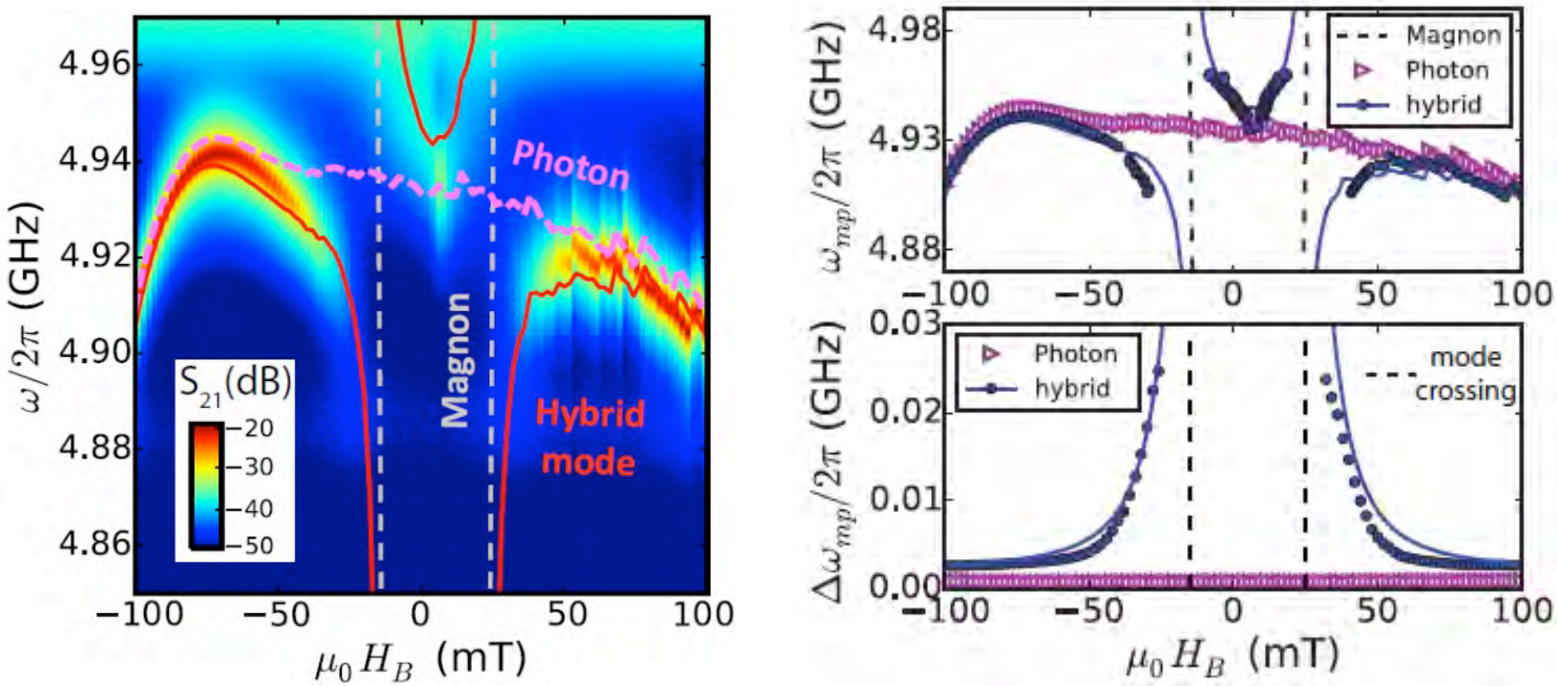

Hybrid system:

$$\frac{P_{out}}{P_{in}} = \frac{\kappa_R}{i(\omega_p - \omega) + \kappa_p + \frac{g^2}{i(\omega_m - \omega) + \kappa_m}}$$

Yi Li, et al. PRL 123, 107701 (2019)

MAGNON-PHOTON HYBRID SYSTEM: ANALYSIS

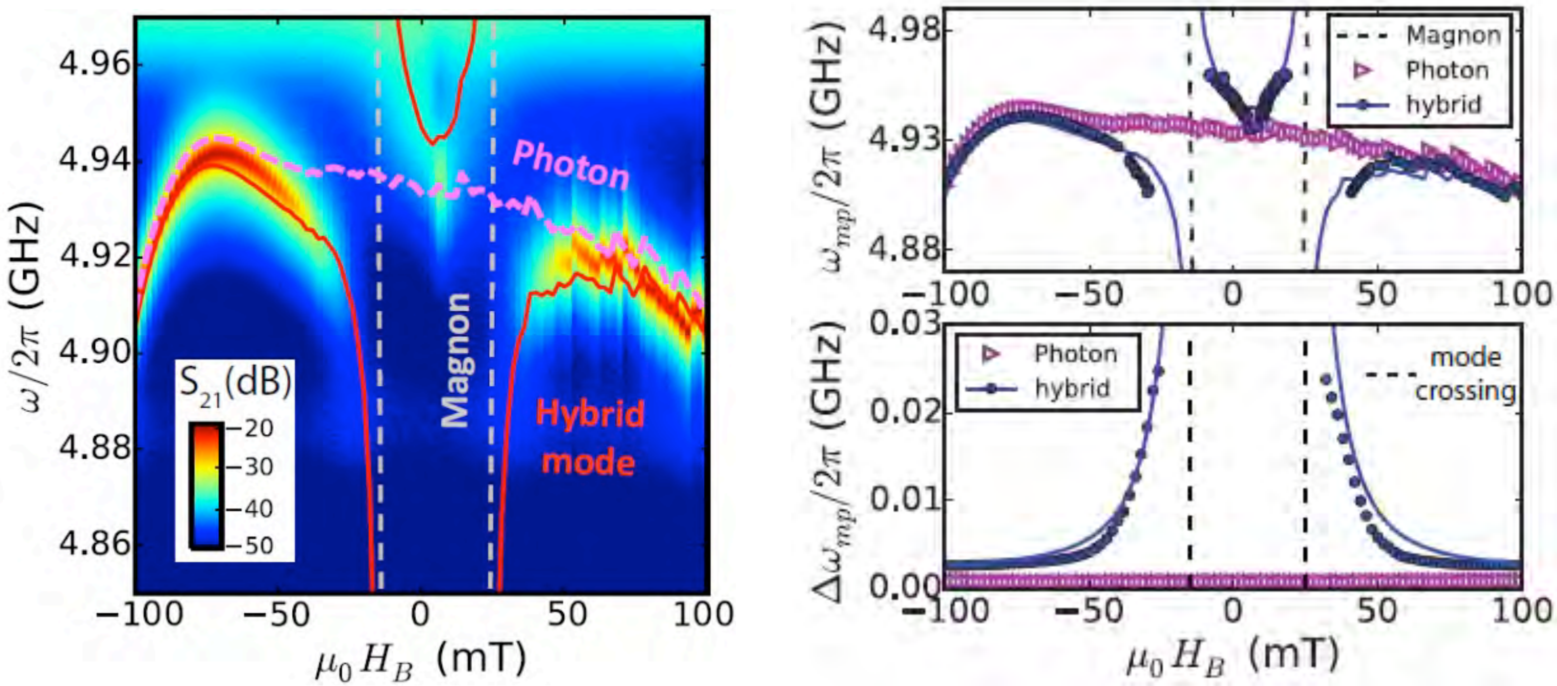

Hybrid system:

$$\frac{P_{out}}{P_{in}} = \frac{\kappa_R}{i(\omega_p - \omega) + \kappa_p + \frac{g^2}{i(\omega_m - \omega) + \kappa_m}}$$

Fitting result:
$g/2\pi = 0.152$ GHz
$C = g^2/\kappa_m\kappa_p = 68$

Yi Li, et al. PRL 123, 107701 (2019)

MAGNON-PHOTON HYBRID SYSTEM: ANALYSIS

Hybrid system:

$$\frac{P_{out}}{P_{in}} = \frac{\kappa_R}{i(\omega_p - \omega) + \kappa_p + \frac{g^2}{i(\omega_m - \omega) + \kappa_m}}$$

Fitting result:
$g/2\pi = 0.152$ GHz
$C = g^2/\kappa_m\kappa_p = 68$

3D cavity

Superconducting resonator

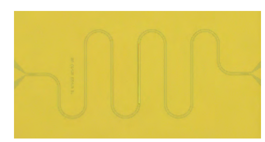

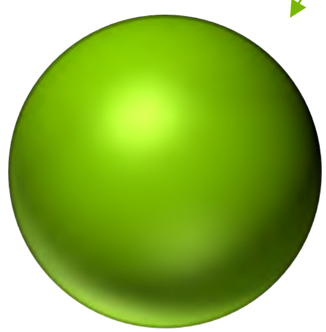

Py stripe
(900 μm x 14 μm x 30 nm)

YIG sphere
(d=1mm)

Yi Li, et al. PRL 123, 107701 (2019)

MAGNON-PHOTON HYBRID SYSTEM: ANALYSIS

Hybrid system:

$$\frac{P_{out}}{P_{in}} = \frac{\kappa_R}{i(\omega_p - \omega) + \kappa_p + \frac{g^2}{i(\omega_m - \omega) + \kappa_m}}$$

Coupling per Bohr magneton
$g_0 = g/N$

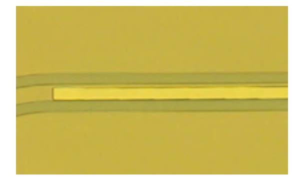

$g_0/2\pi$ = 26.7 Hz

(This work)

Fitting result:
$g/2\pi$ = 0.152 GHz
$C = g^2/\kappa_m \kappa_p = 68$

3D cavity

Superconducting resonator

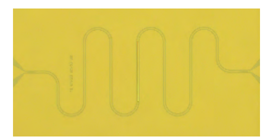

YIG sphere
(d=1mm)

Py stripe
(900 μm x 14 μm x 30 nm)

Yi Li, et al. PRL 123, 107701 (2019)

MAGNON-PHOTON HYBRID SYSTEM: ANALYSIS

Hybrid system:

$$\frac{P_{out}}{P_{in}} = \frac{\kappa_R}{i(\omega_p - \omega) + \kappa_p + \frac{g^2}{i(\omega_m - \omega) + \kappa_m}}$$

Coupling per Bohr magneton
$g_0 = g/N$

Fitting result:
$g/2\pi = 0.152$ GHz
$C = g^2/\kappa_m \kappa_p = 68$

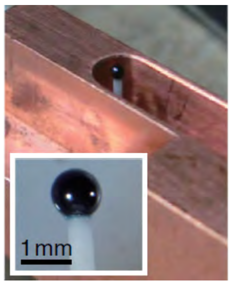

$g_0/2\pi = 0.038$ Hz

Tabuchi, et al. PRL 113, 083603 (2013)

3D cavity

YIG sphere
(d=1mm)

Superconducting resonator

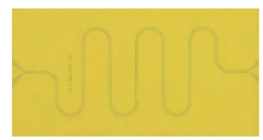

Py stripe
(900 μm x 14 μm x 30 nm)

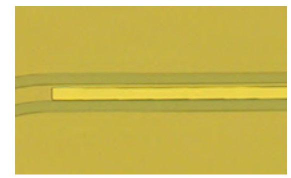

$\boldsymbol{g_0/2\pi = 26.7}$ **Hz**

(This work)

Yi Li, et al. PRL 123, 107701 (2019)

MAGNON-PHOTON HYBRID SYSTEM: ANALYSIS

Hybrid system:

$$\frac{P_{out}}{P_{in}} = \frac{\kappa_R}{i(\omega_p - \omega) + \kappa_p + \frac{g^2}{i(\omega_m - \omega) + \kappa_m}}$$

Coupling per Bohr magneton
$g_0 = g/N$

Fitting result:
$g/2\pi = 0.152$ GHz
$C = g^2/\kappa_m\kappa_p = 68$

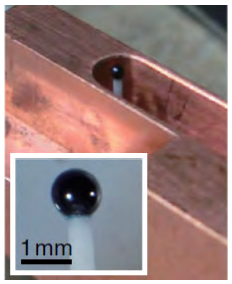

$g_0/2\pi = 0.038$ Hz

Tabuchi, et al. PRL 113, 083603 (2013)

3D cavity

Superconducting resonator

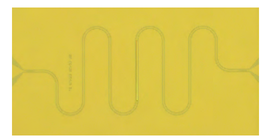

YIG sphere
(d=1mm)

Py stripe
(900 μm x 14 μm x 30 nm)

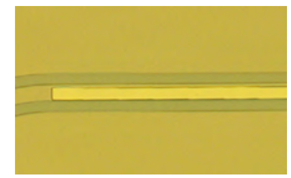

$g_0/2\pi = 26.7$ Hz

(This work)

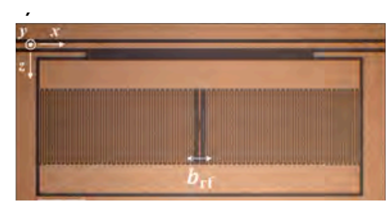

$g_0/2\pi = 263$ Hz

Hou, et al. PRL 123, 107701 (2019)

Yi Li, et al. PRL 123, 107701 (2019)

TUNE COUPLING EFFICIENCY

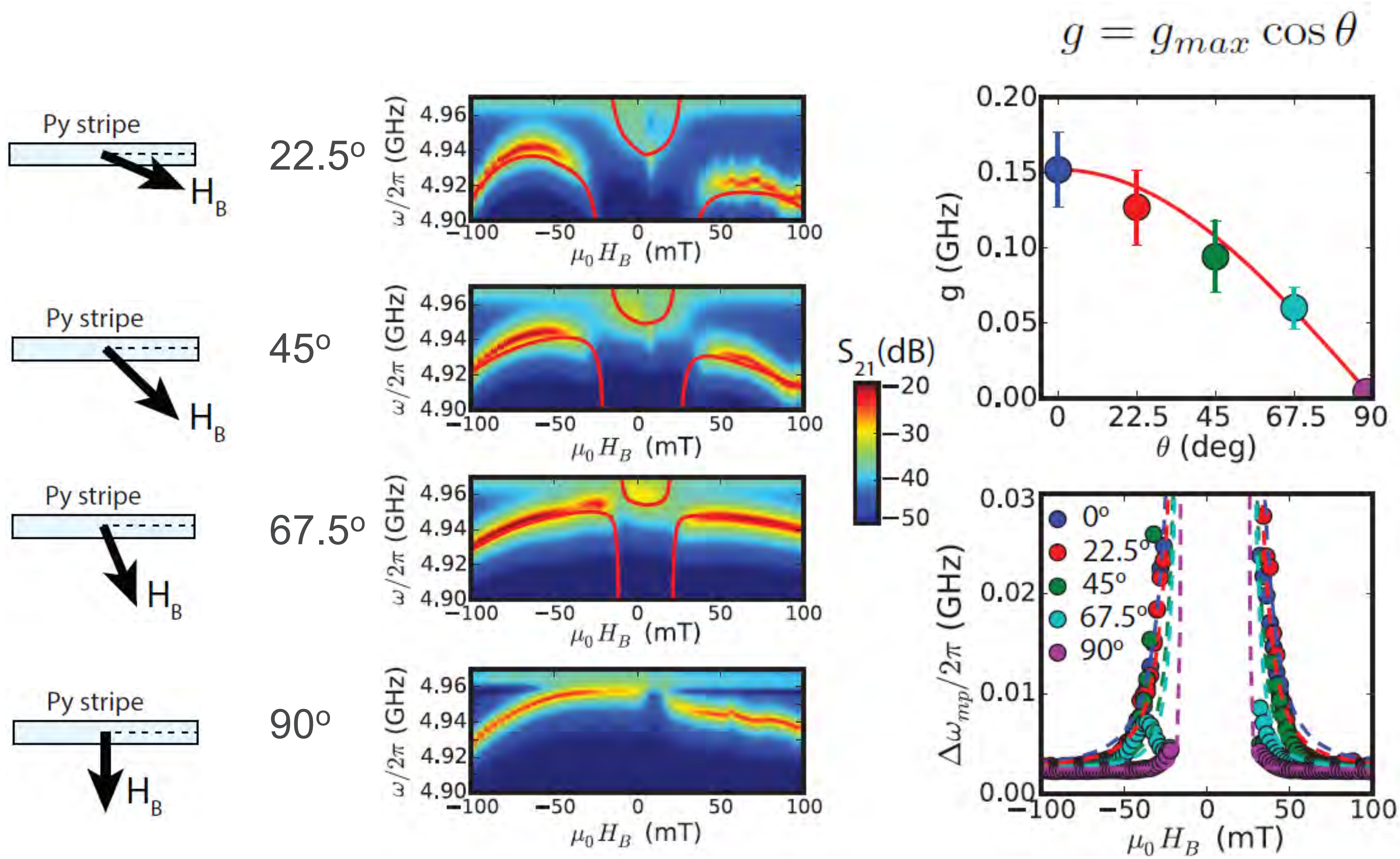

Yi Li, et al. PRL 123, 107701 (2019)

TUNE COUPLING EFFICIENCY

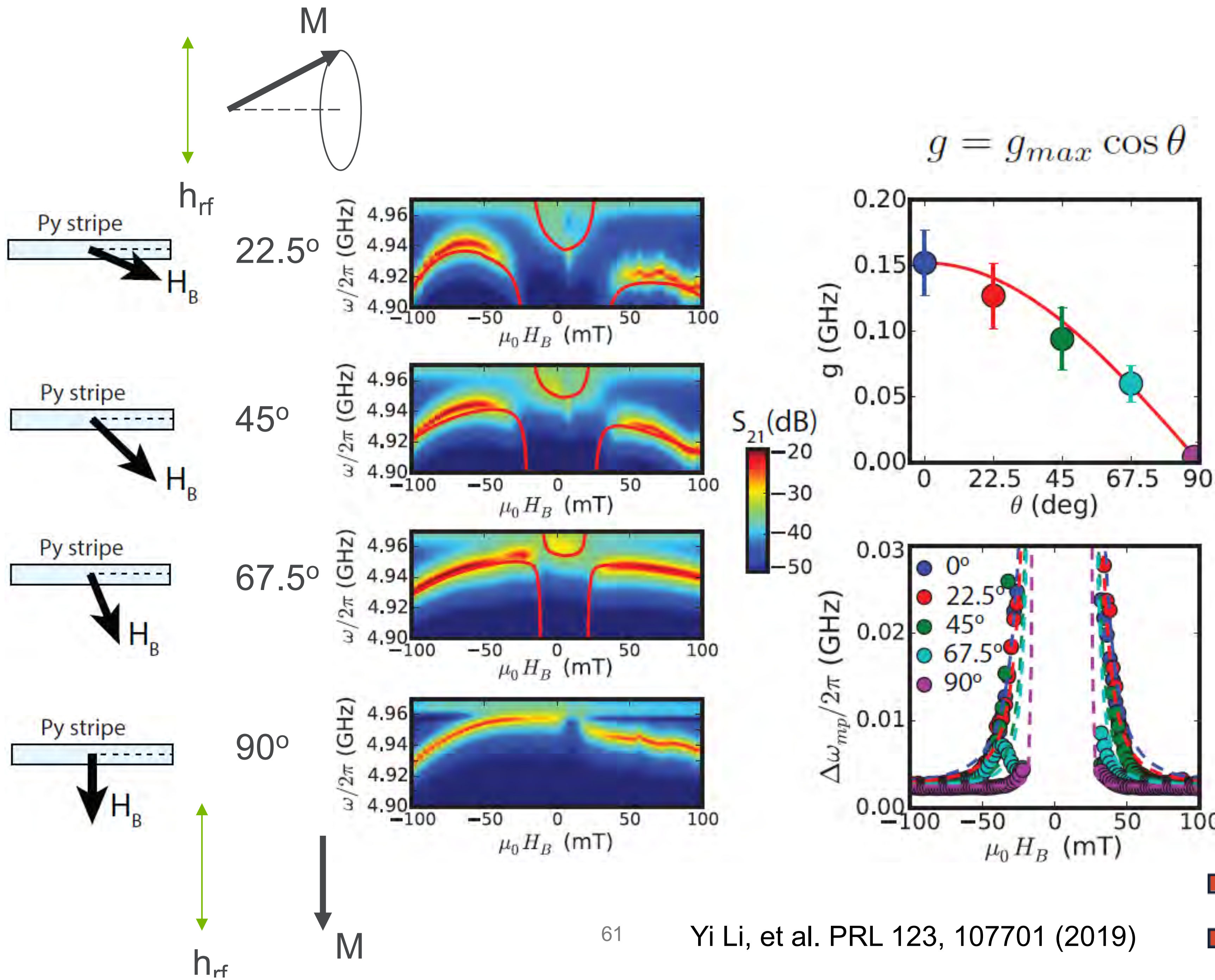

Yi Li, et al. PRL 123, 107701 (2019)

NUMBER OF SPINS

$$\sqrt{V/V_0} = \sqrt{5/3}$$

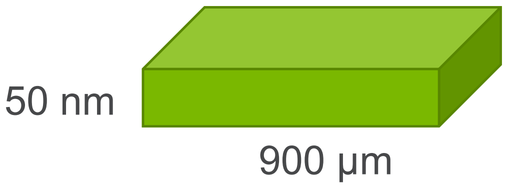

$$\sqrt{V/V_0} = 1$$

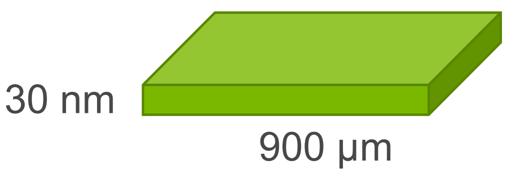

$$\sqrt{V/V_0} = \sqrt{1/3}$$

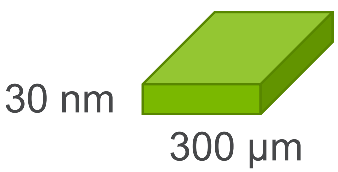

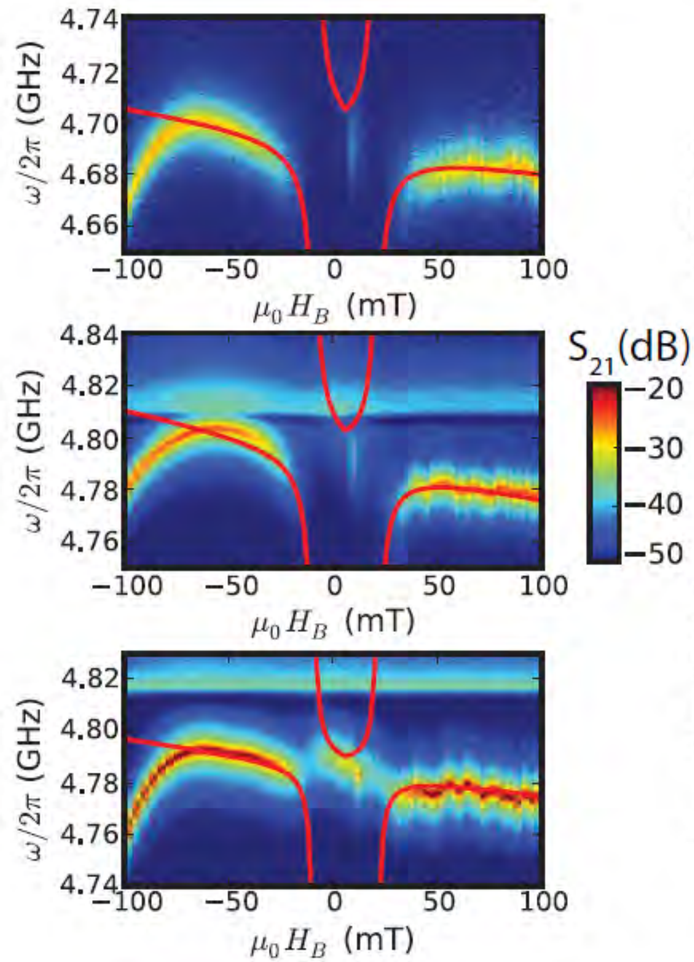

$$g = g_0\sqrt{N}$$

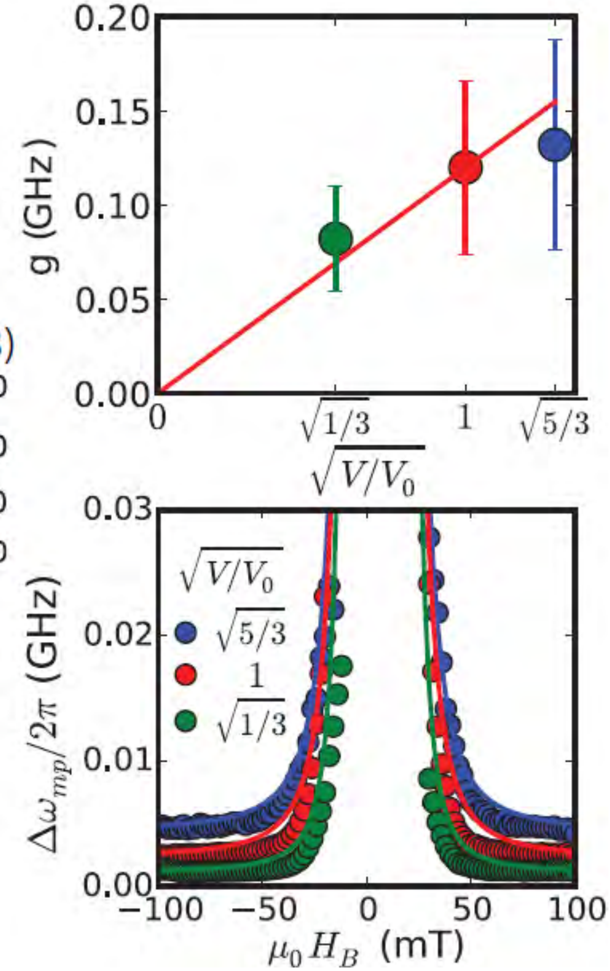

Yi Li, et al. PRL 123, 107701 (2019)

NONLINEARITY FROM SUPERCONDUCTING VORTICES

$\mu_0 H_B$=100 mT

Critical power:
P_c = -5 dBm

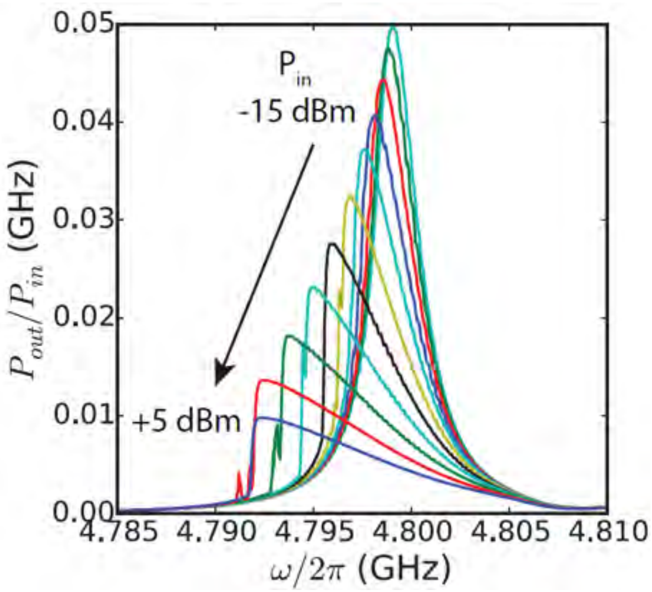

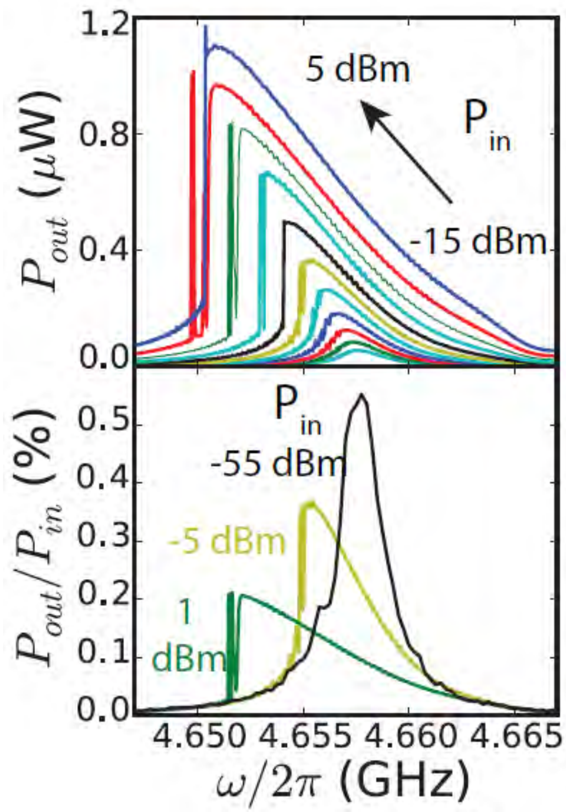

Yi Li, et al. PRL 123, 107701 (2019)

NONLINEARITY FROM SUPERCONDUCTING VORTICES

$\mu_0 H_B$=100 mT

Critical power:
P_c = -5 dBm

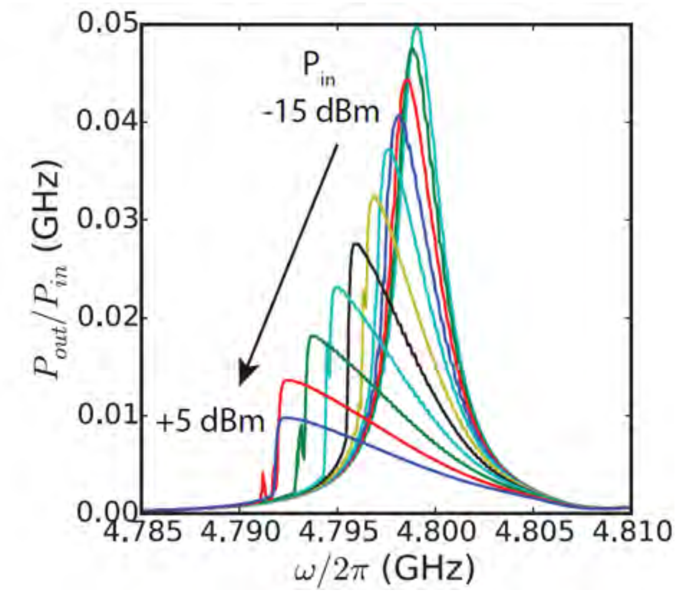

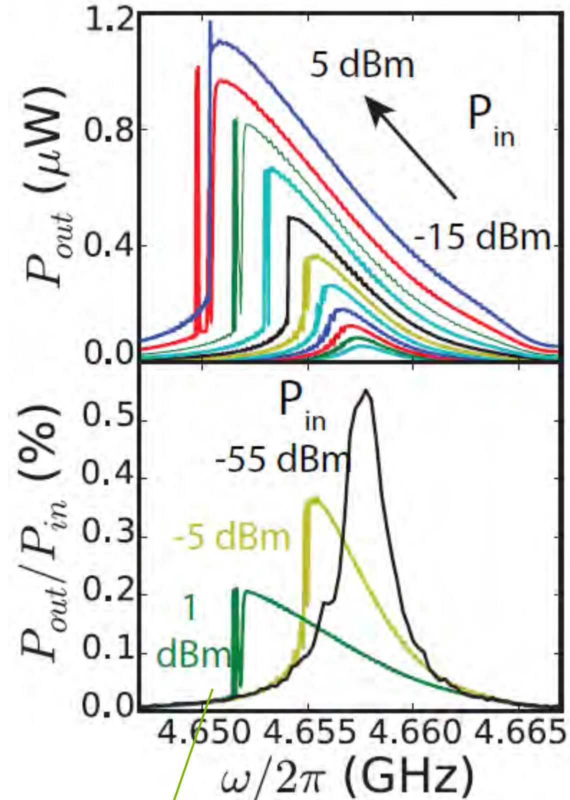

Vortex inductance

$$\frac{\omega}{2\pi} = \frac{1}{\sqrt{LC}}$$

Yi Li, et al. PRL 123, 107701 (2019)

NONLINEARITY FROM SUPERCONDUCTING VORTICES

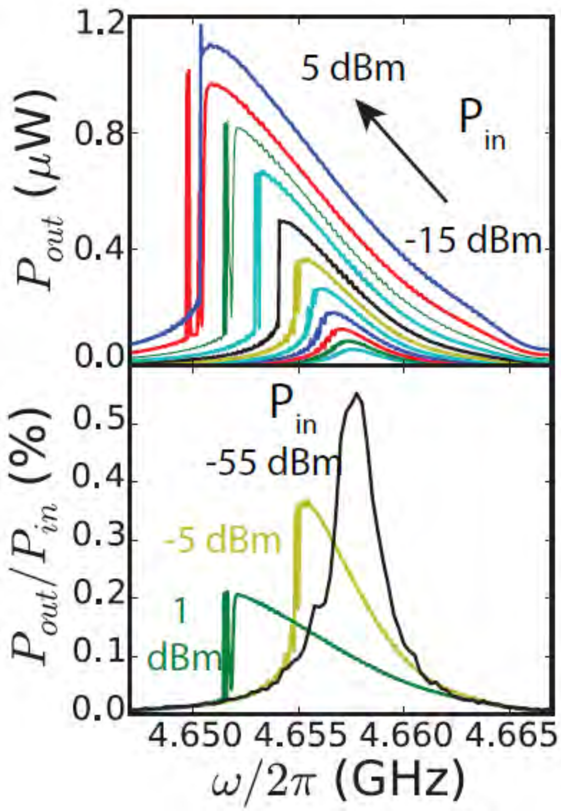

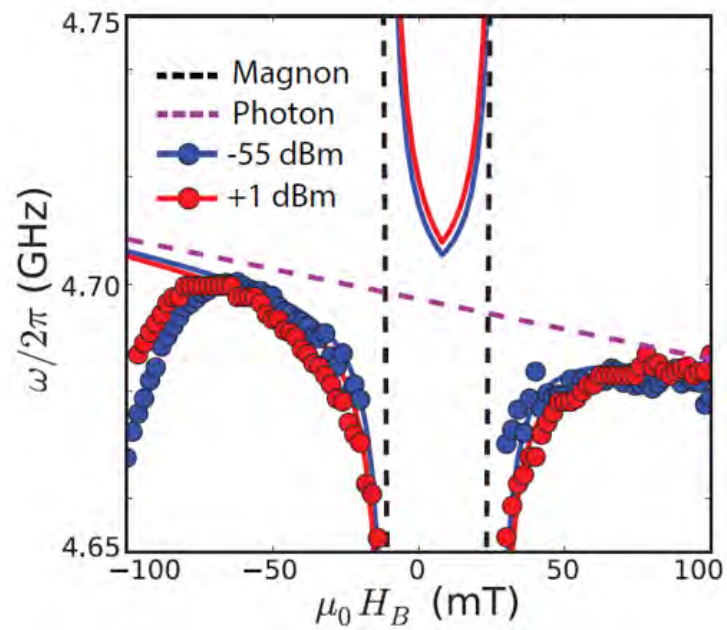

g/2π = 0.139 Ghz (-55 dBm)

+15 %

g/2π = 0.158 GHz(+1 dBm)

Yi Li, et al. PRL 123, 107701 (2019)

OUTLINE

- Introduction
- On-chip magnon-photon coupling with superconducting resonator
- **Magnon-magnon coupling in magnetic bilayer thin film**
- Manipulating phonon transport with magnons
- Conclusions

HYBRID SYSTEMS FROM HETEROSTRUCTURES

y

Microwave quantum circuits

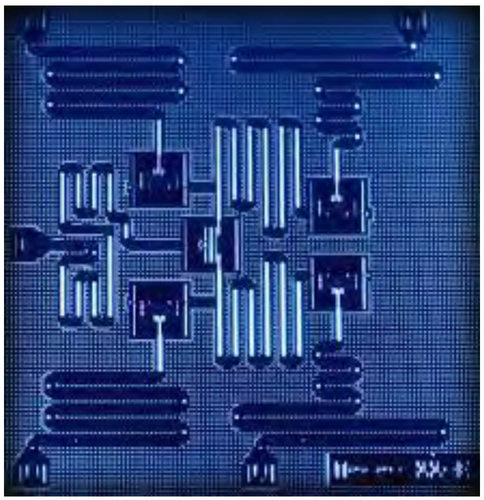

x

HYBRID SYSTEMS FROM HETEROSTRUCTURES

Microwave quantum circuits

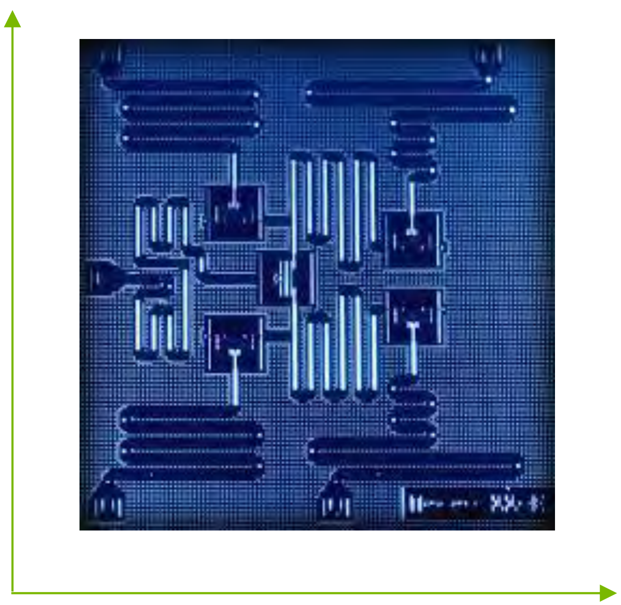

3D hybrid system

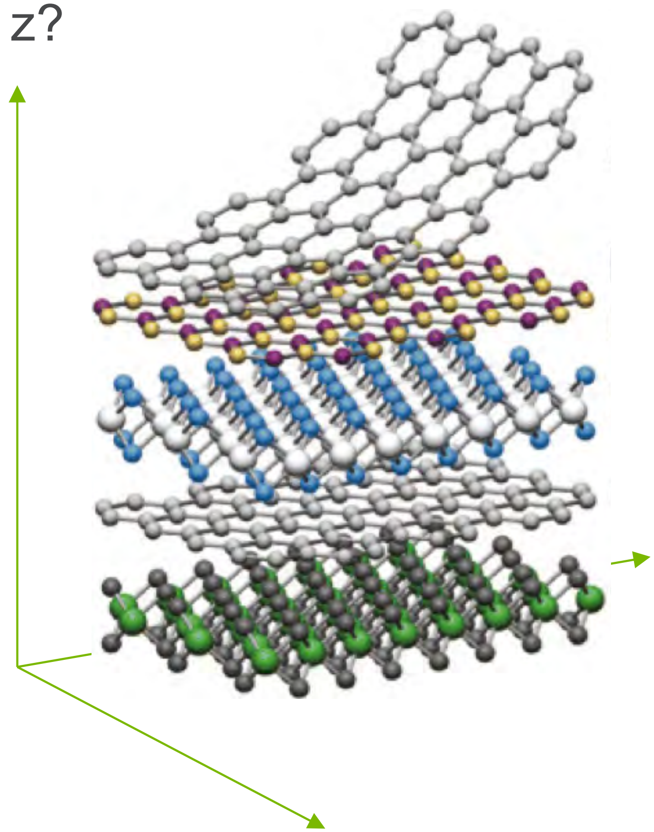

HYBRID SYSTEMS FROM HETEROSTRUCTURES

Microwave quantum circuits

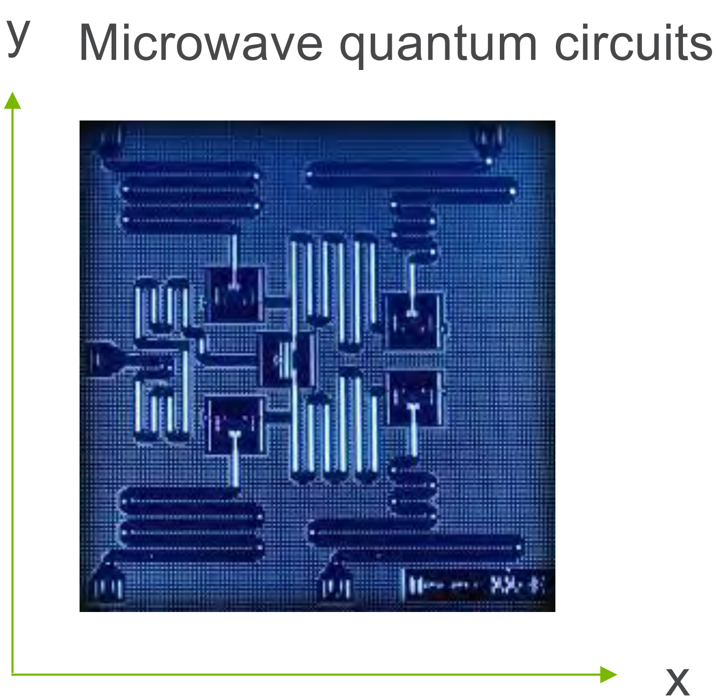

3D hybrid system

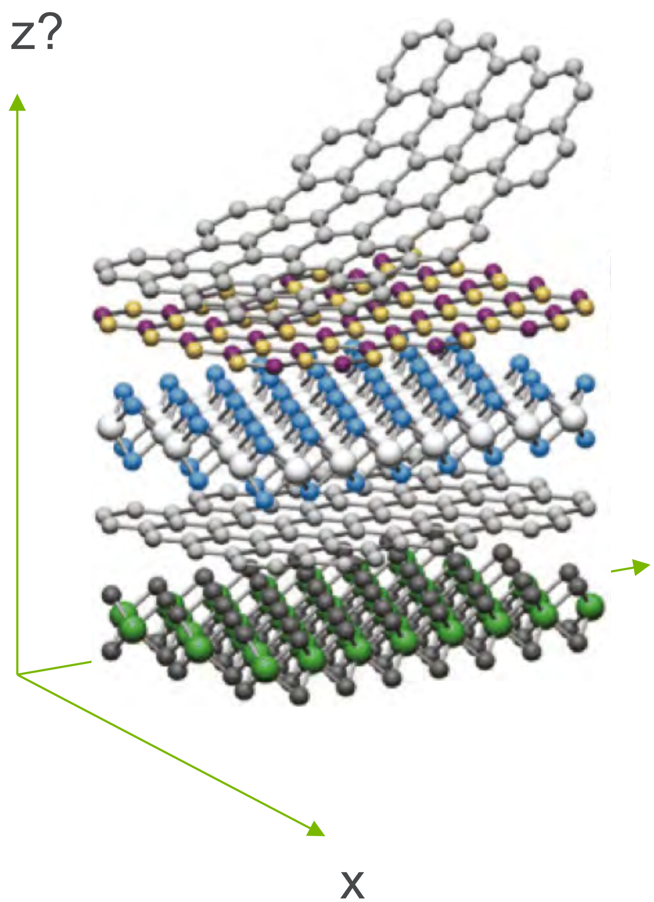

Magnon hybrid system

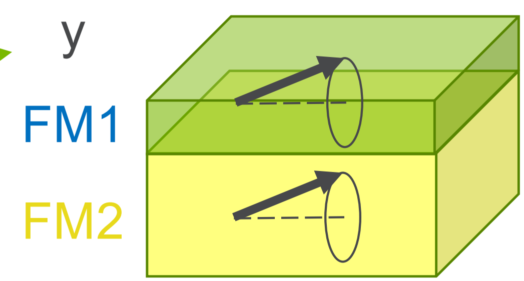

HYBRID SYSTEMS FROM HETEROSTRUCTURES

Microwave quantum circuits

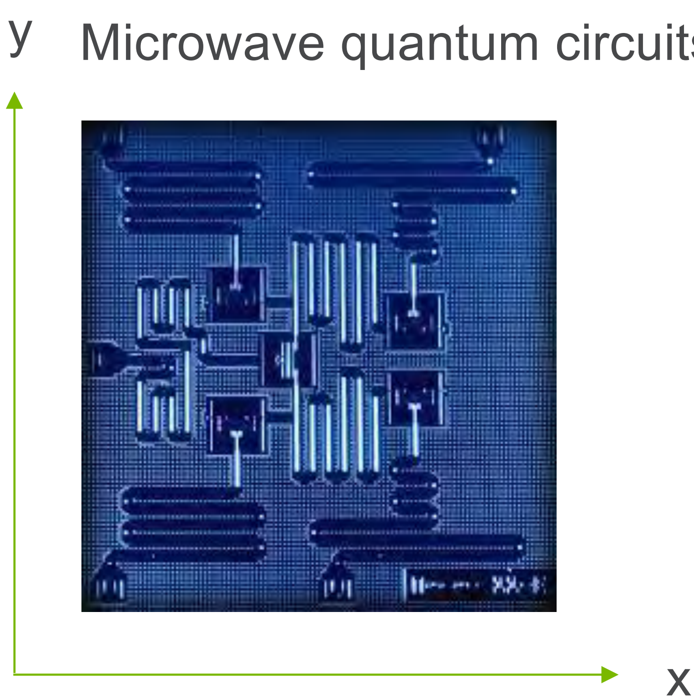

3D hybrid system

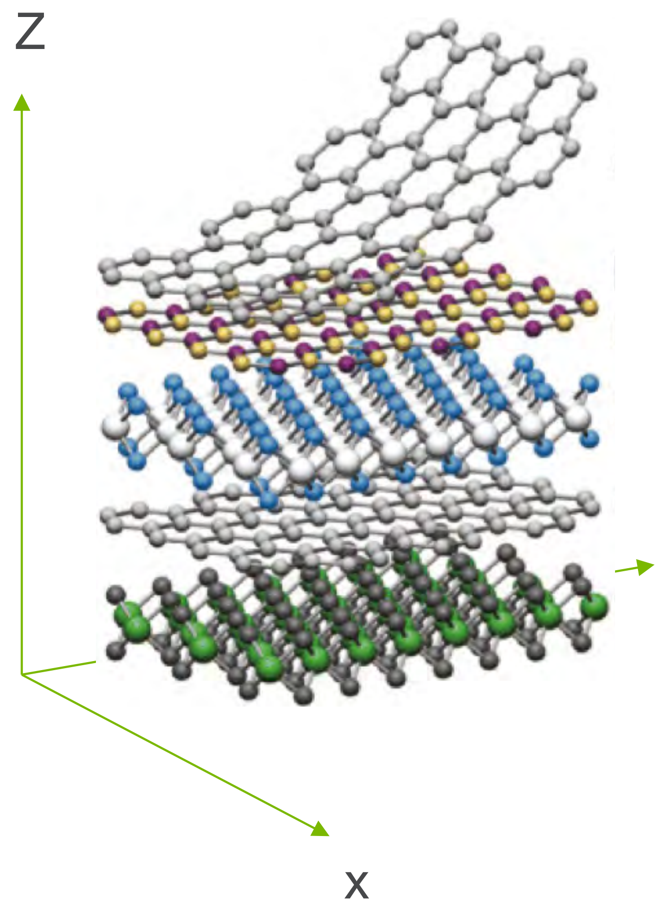

Magnon hybrid system

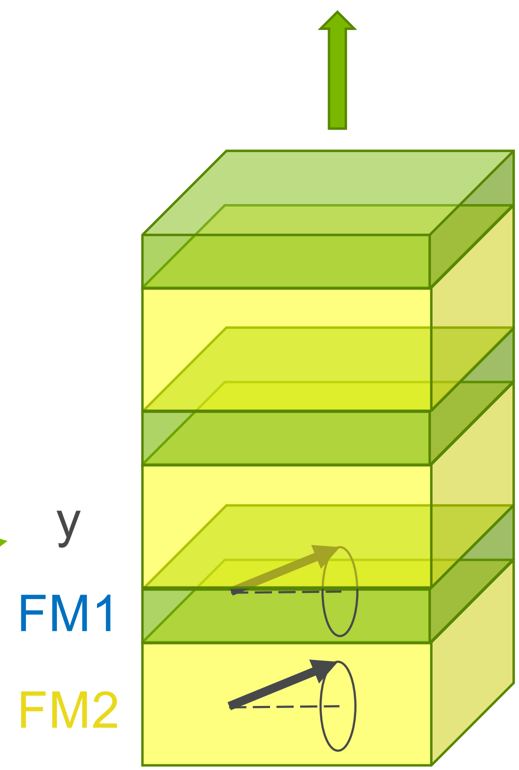

MAGNETIC BILAYER FOR COHERENT INFORMATION PROCESSING

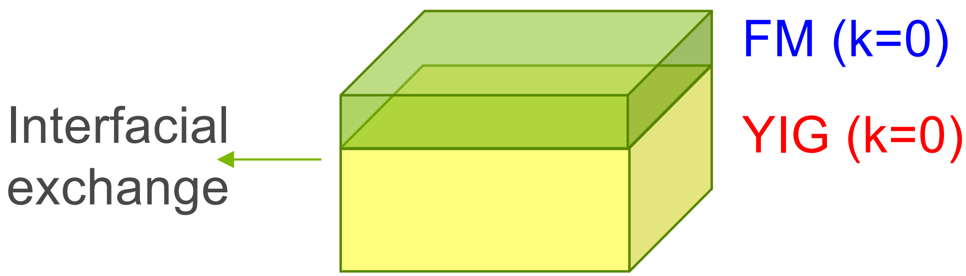

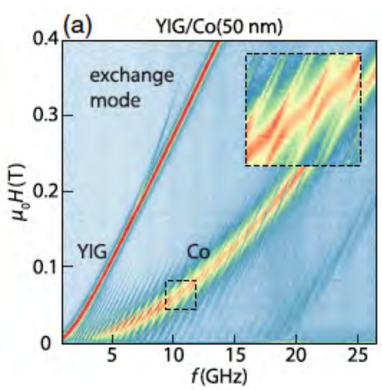

Klingler et al. PRL 120, 127201 (2018)
Chen et al. PRL 120, 217202 (2018)
Qin et al. Sci. Rep. 8, 5755 (2018)

MAGNETIC BILAYER FOR COHERENT INFORMATION PROCESSING

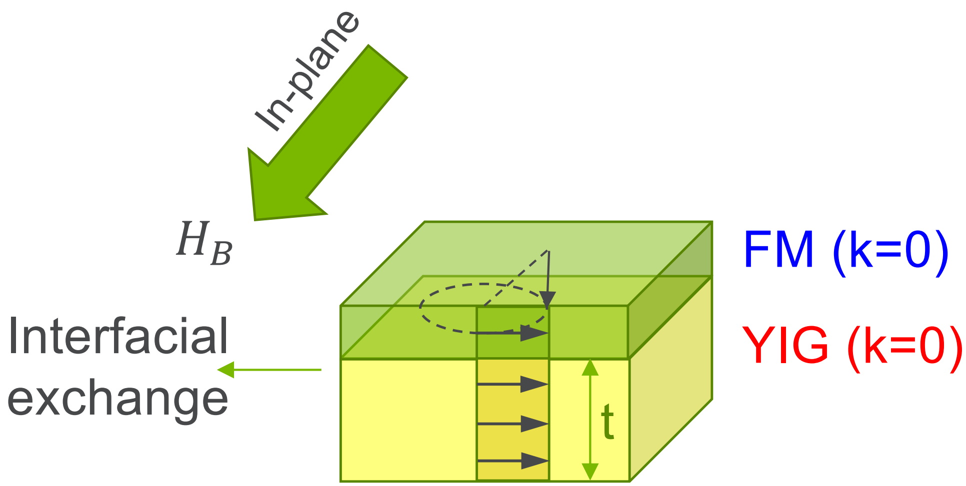

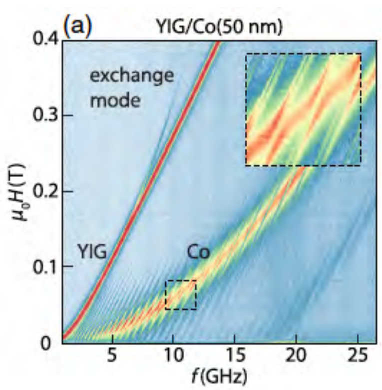

Klingler et al. PRL 120, 127201 (2018)
Chen et al. PRL 120, 217202 (2018)
Qin et al. Sci. Rep. 8, 5755 (2018)

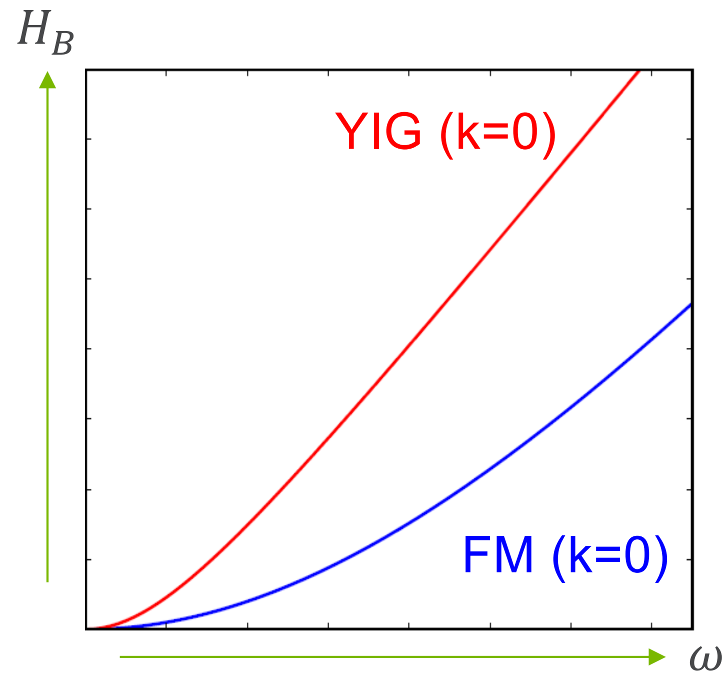

In-plane Kittel equation:

$$\frac{\omega}{\gamma} = \sqrt{H_B(H_B+M_s)}$$

MAGNETIC BILAYER FOR COHERENT INFORMATION PROCESSING

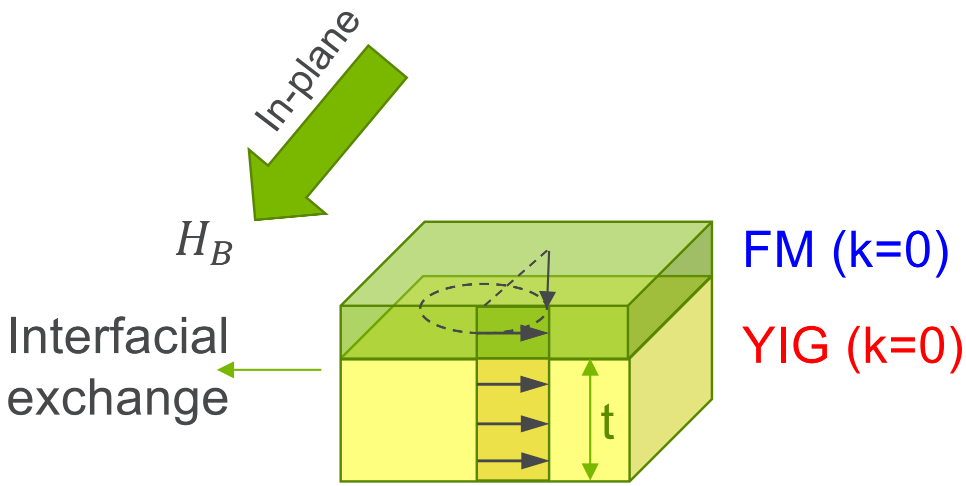

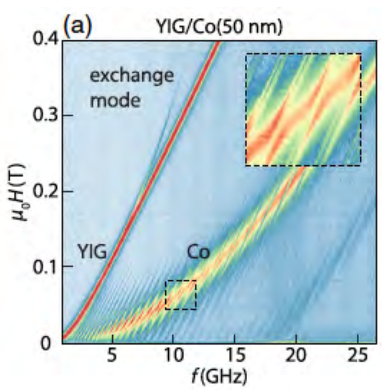

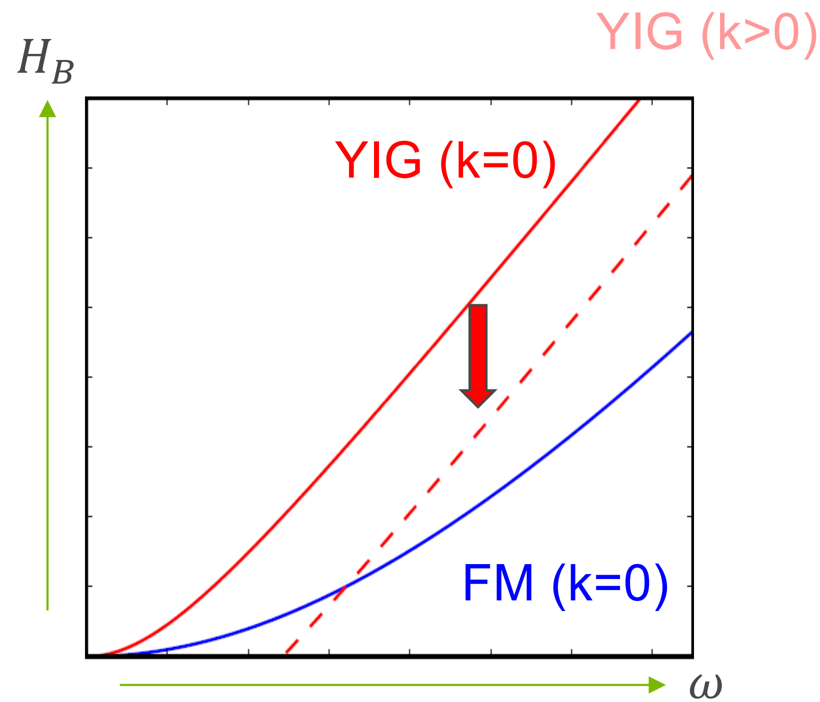

In-plane Kittel equation:

$$\frac{\omega}{\gamma} = \sqrt{H_B(H_B+M_s)}$$

Klingler et al. PRL 120, 127201 (2018)
Chen et al. PRL 120, 217202 (2018)
Qin et al. Sci. Rep. 8, 5755 (2018)

MAGNETIC BILAYER FOR COHERENT INFORMATION PROCESSING

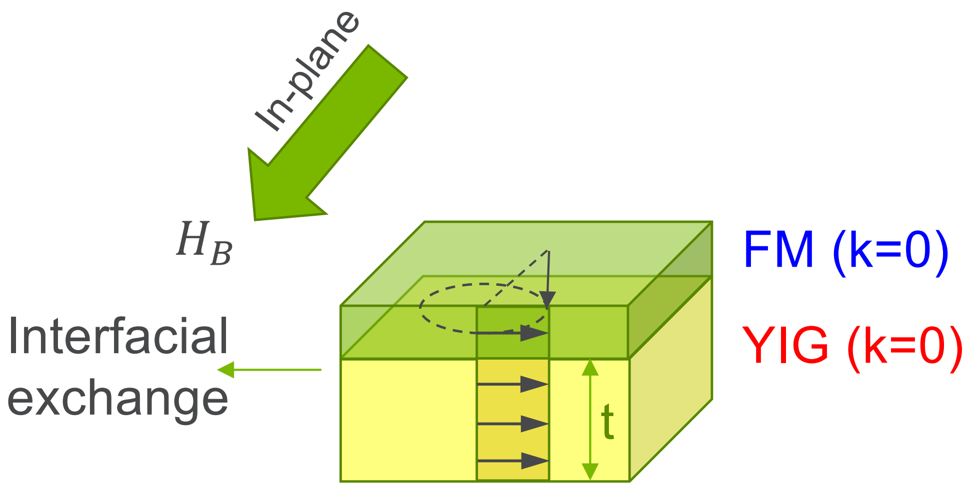

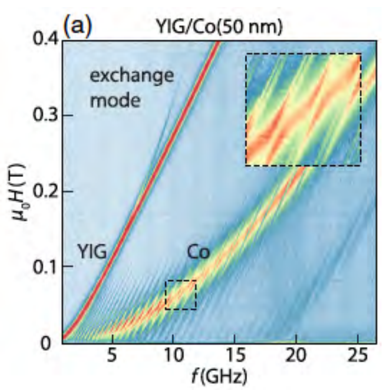

Klingler et al. PRL 120, 127201 (2018)
Chen et al. PRL 120, 217202 (2018)
Qin et al. Sci. Rep. 8, 5755 (2018)

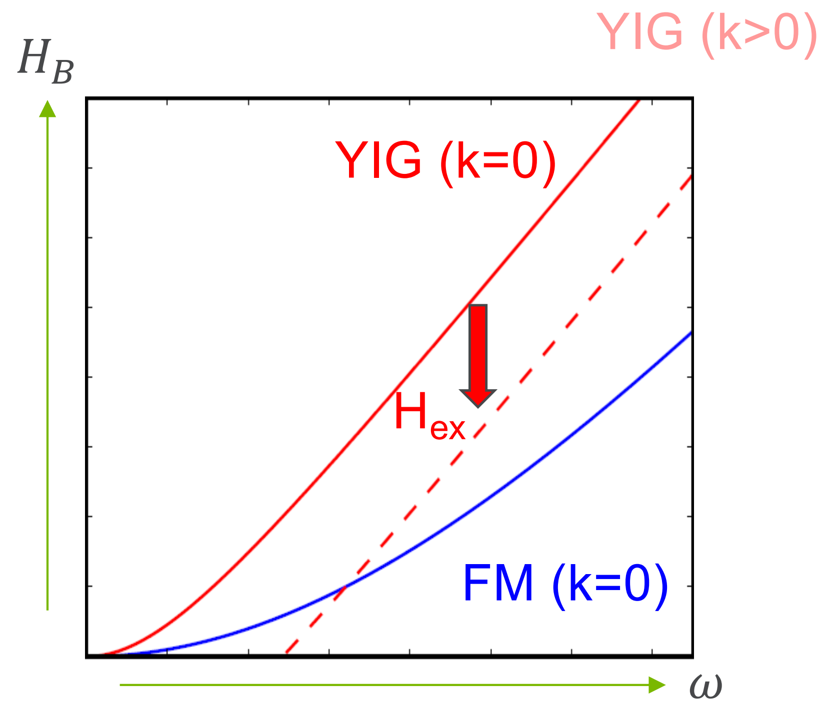

In-plane Kittel equation:

$$\frac{\omega}{\gamma} = \sqrt{(H_B + H_{ex})(H_B + M_s + H_{ex})}$$

$$\mu_0 H_{ex} = D_{ex} k^2$$

MAGNETIC BILAYER FOR COHERENT INFORMATION PROCESSING

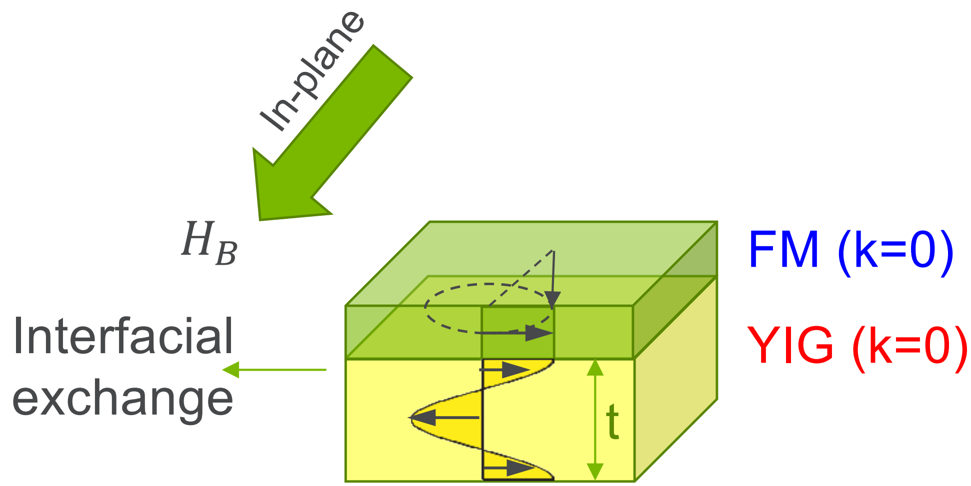

Perpendicular standing spin wave mode

$$k = \frac{n\pi}{t}$$

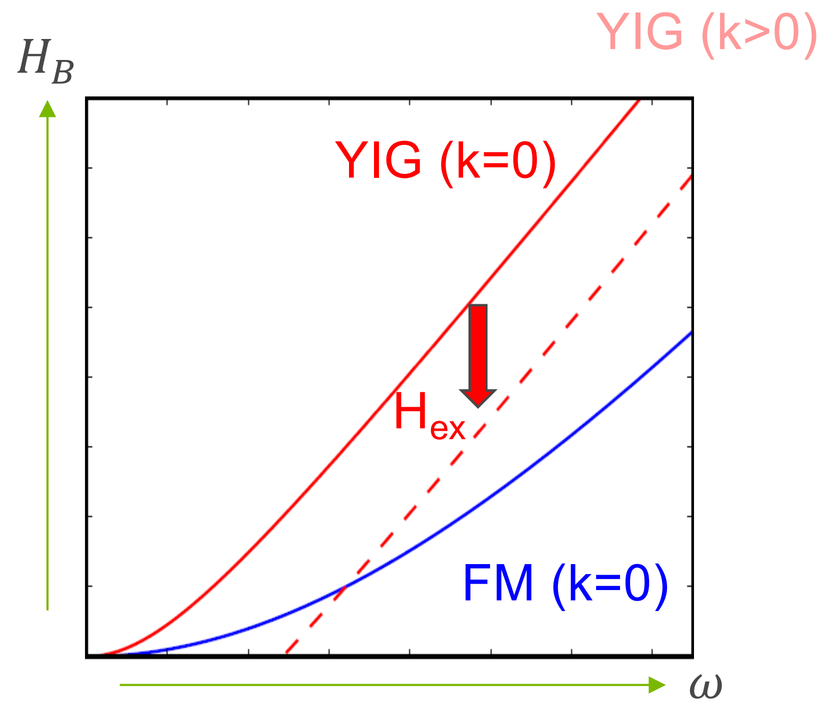

In-plane Kittel equation:

$$\frac{\omega}{\gamma} = \sqrt{(H_B + H_{ex})(H_B + M_s + H_{ex})}$$

$$\mu_0 H_{ex} = D_{ex} k^2$$

Klingler et al. PRL 120, 127201 (2018)
Chen et al. PRL 120, 217202 (2018)
Qin et al. Sci. Rep. 8, 5755 (2018)

MAGNETIC BILAYER FOR COHERENT INFORMATION PROCESSING

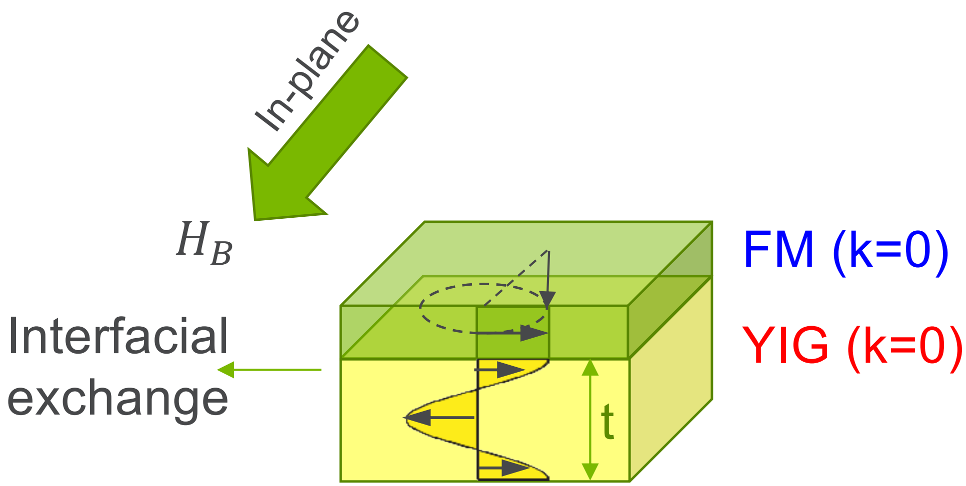

Perpendicular standing spin wave mode

$$k = \frac{n\pi}{t}$$

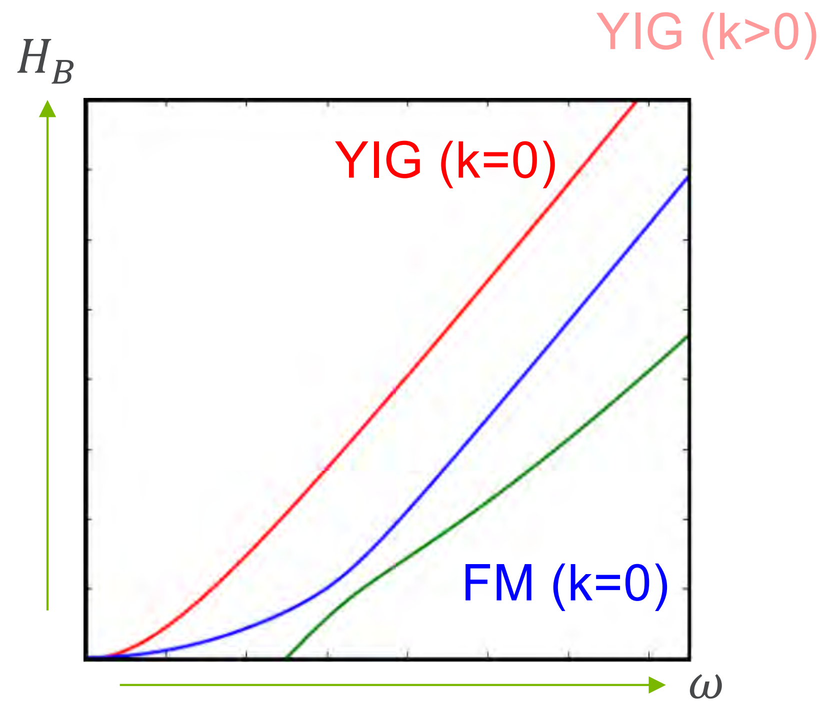

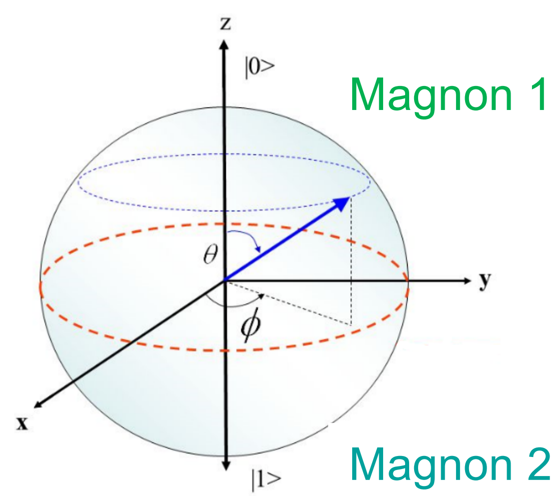

Klingler et al. PRL 120, 127201 (2018)
Chen et al. PRL 120, 217202 (2018)
Qin et al. Sci. Rep. 8, 5755 (2018)

MODE ANTICROSSING

Structure:
YIG(100 nm)/Py(5-60 nm)

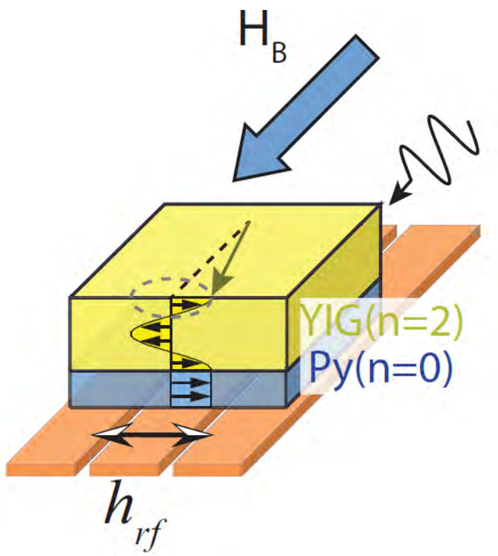

$Y_3Fe_5O_{12}$ (YIG):

- Sputtering on $Gd_3Ga_5O_{12}$ (GGG)
- Post-annealing in air at 850°C

$Ni_{80}Fe_{20}$ (Py):

- Ion milling of YIG surface
- Sputtering of Py on YIG

Yi Li, et al. PRL 124, 117202 (2020)

MODE ANTICROSSING

Structure:
YIG(100 nm)/Py(5-60 nm)

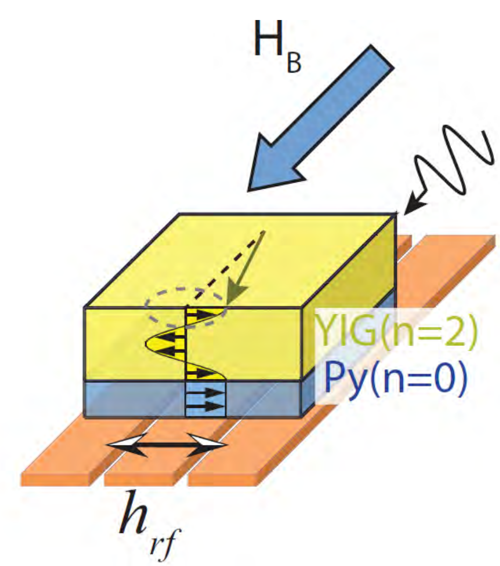

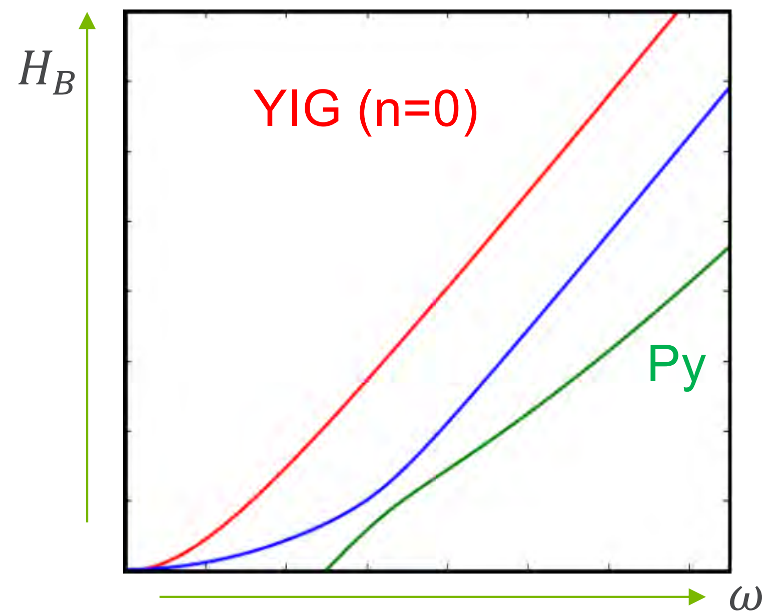

$Y_3Fe_5O_{12}$ (YIG):

- Sputtering on $Gd_3Ga_5O_{12}$ (GGG)
- Post-annealing in air at 850°C

$Ni_{80}Fe_{20}$ (Py):

- Ion milling of YIG surface
- Sputtering of Py on YIG

Yi Li, et al. PRL 124, 117202 (2020)

MODE ANTICROSSING

Structure:
YIG(100 nm)/Py(5-60 nm)

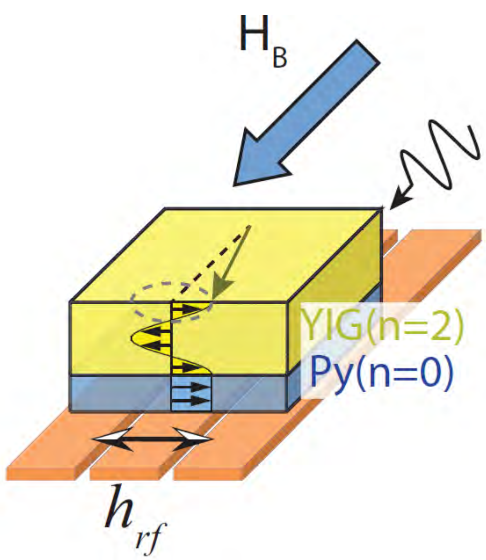

YIG(100 nm)/Py(9 nm)

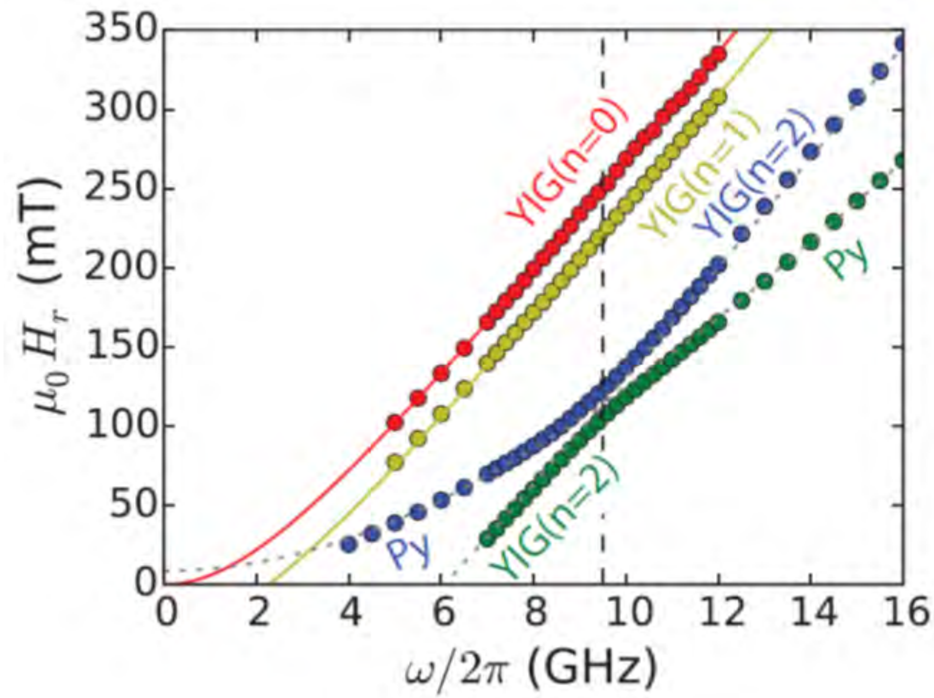

$Y_3Fe_5O_{12}$ (YIG):

- Sputtering on $Gd_3Ga_5O_{12}$ (GGG)
- Post-annealing in air at 850°C

$Ni_{80}Fe_{20}$ (Py):

- Ion milling of YIG surface
- Sputtering of Py on YIG

Yi Li, et al. PRL 124, 117202 (2020)

MODE ANTICROSSING

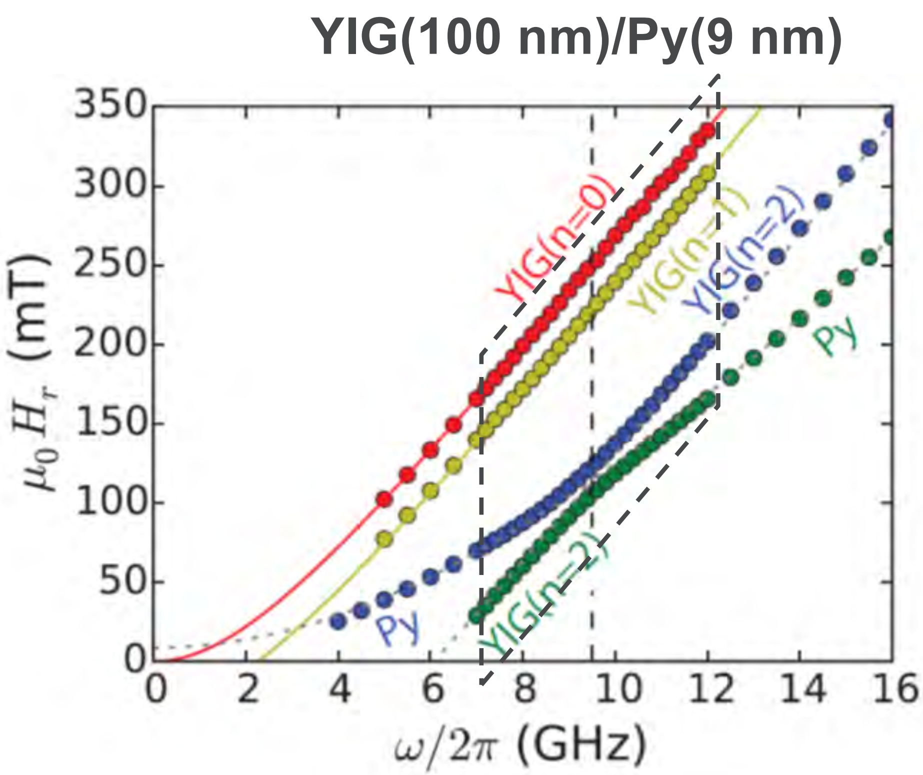

Yi Li, et al. PRL 124, 117202 (2020)

MODE ANTICROSSING

$$\mu_0 H_{ex} = D_{ex}\left(\frac{n\pi}{t_{YIG}}\right)^2$$

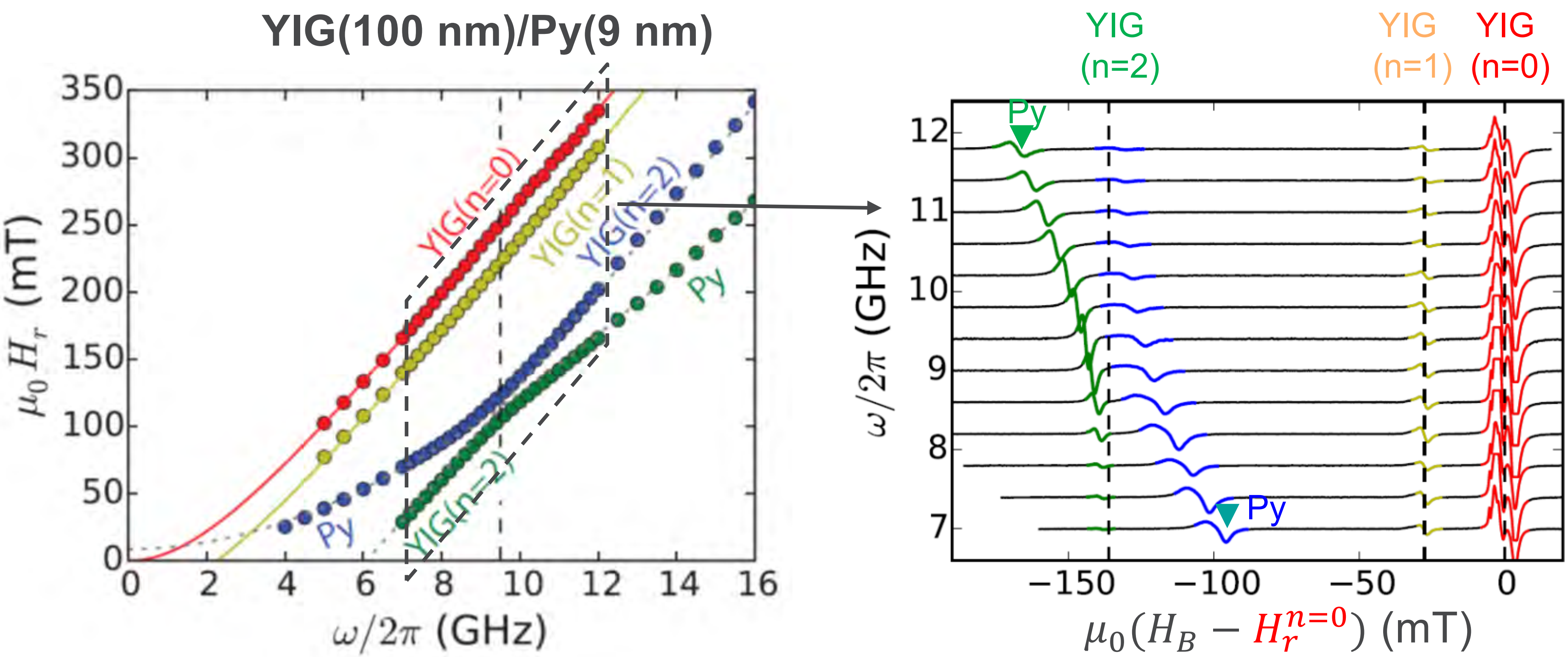

Yi Li, et al. PRL 124, 117202 (2020)

MODE ANTICROSSING

$$\mu_0 H_{ex} = D_{ex}\left(\frac{n\pi}{t_{YIG}}\right)^2$$

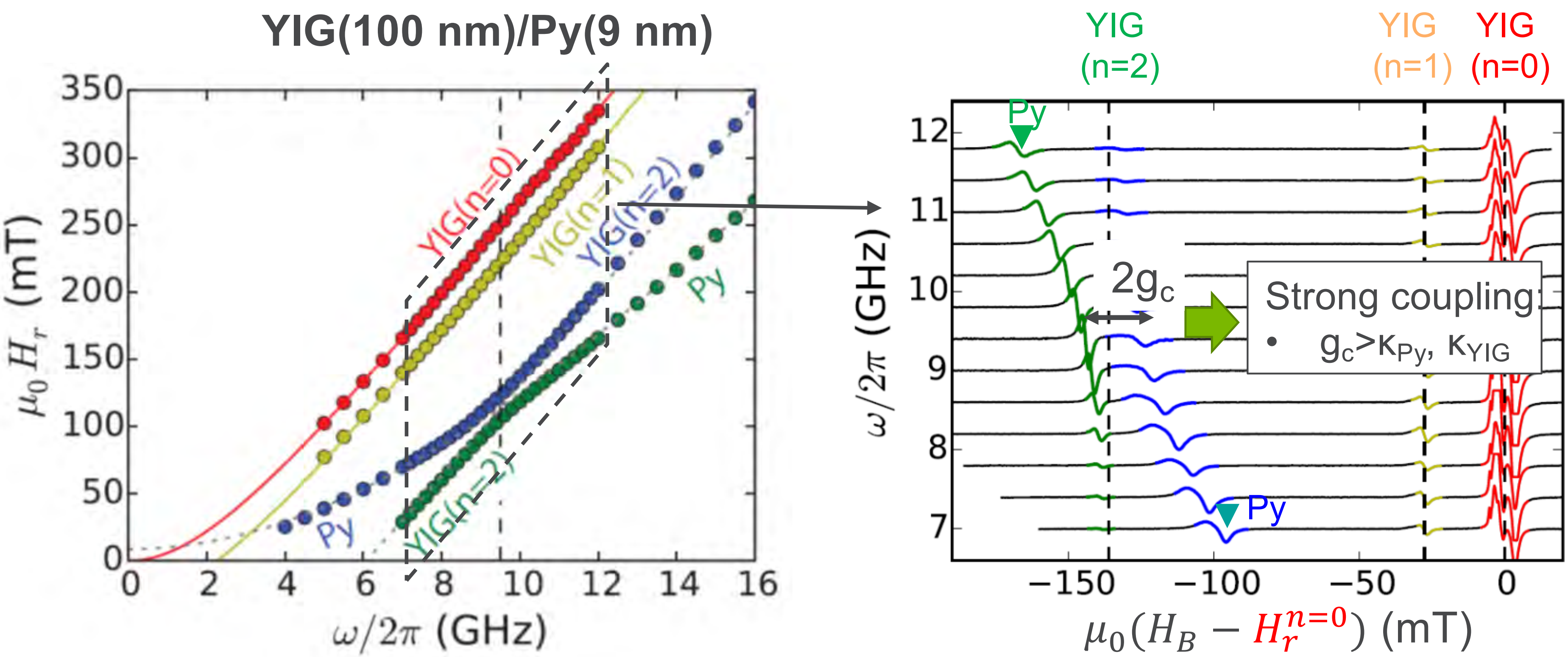

Yi Li, et al. PRL 124, 117202 (2020)

MODE ANTICROSSING

$$\mu_0 H_{ex} = D_{ex}\left(\frac{n\pi}{t_{YIG}}\right)^2$$

YIG(100 nm)/Py(9 nm)

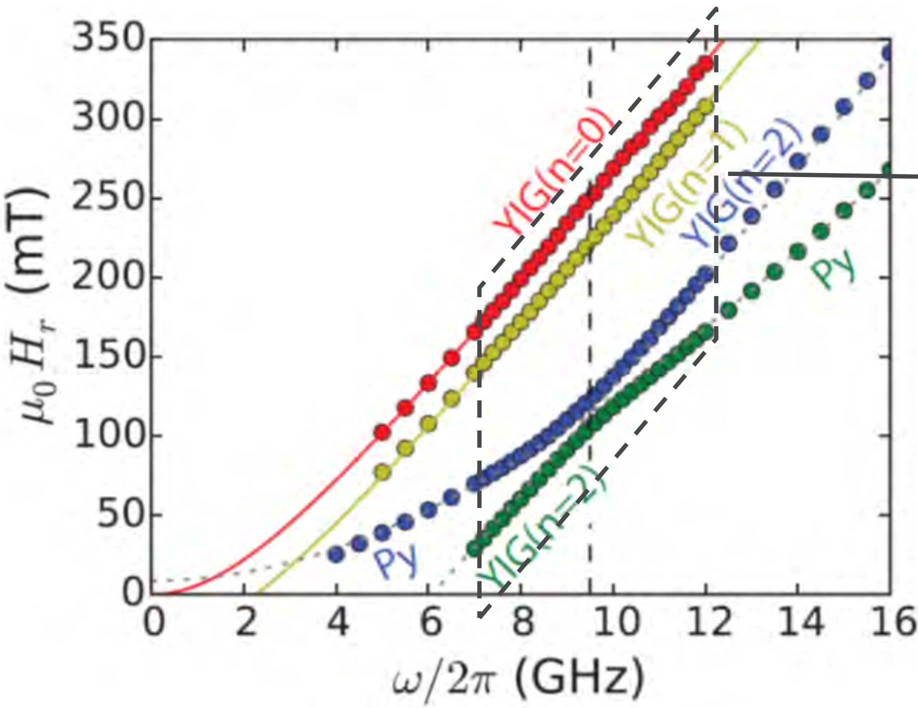

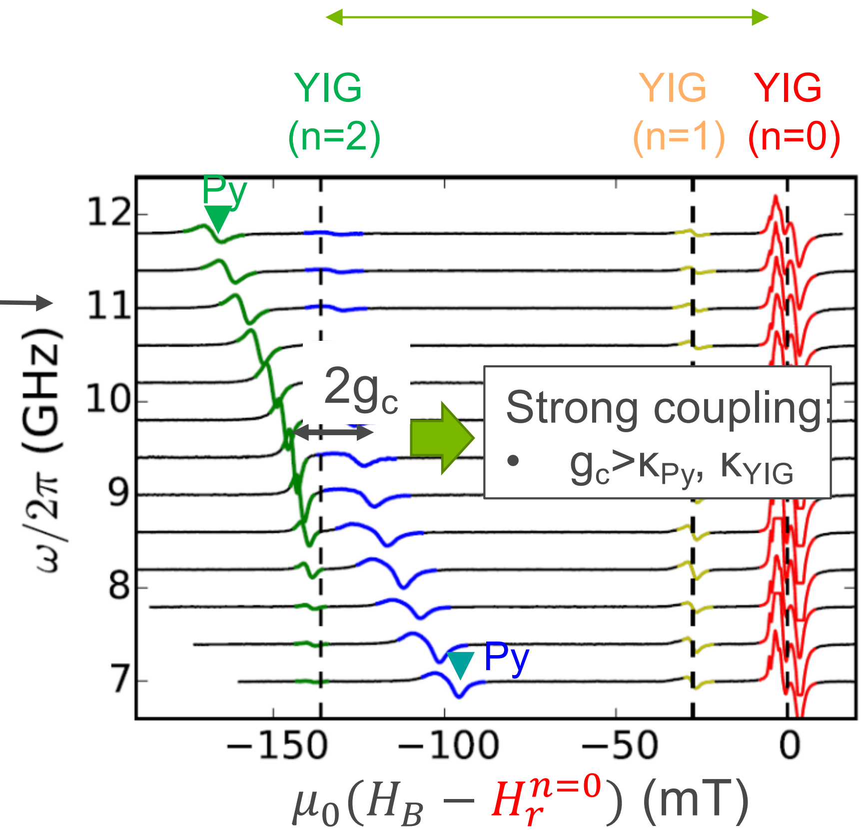

Field domain:

$g_c = 8.4$ mT

Frequency domain:

$g_c/2\pi$ = 0.35 GHz

Cooperativity $g_c^2/\kappa_{Py}\kappa_{YIG}$ = 6

Yi Li, et al. PRL 124, 117202 (2020)

LINEWIDTH: IN-PHASE VS. OUT-OF-PHASE MODES

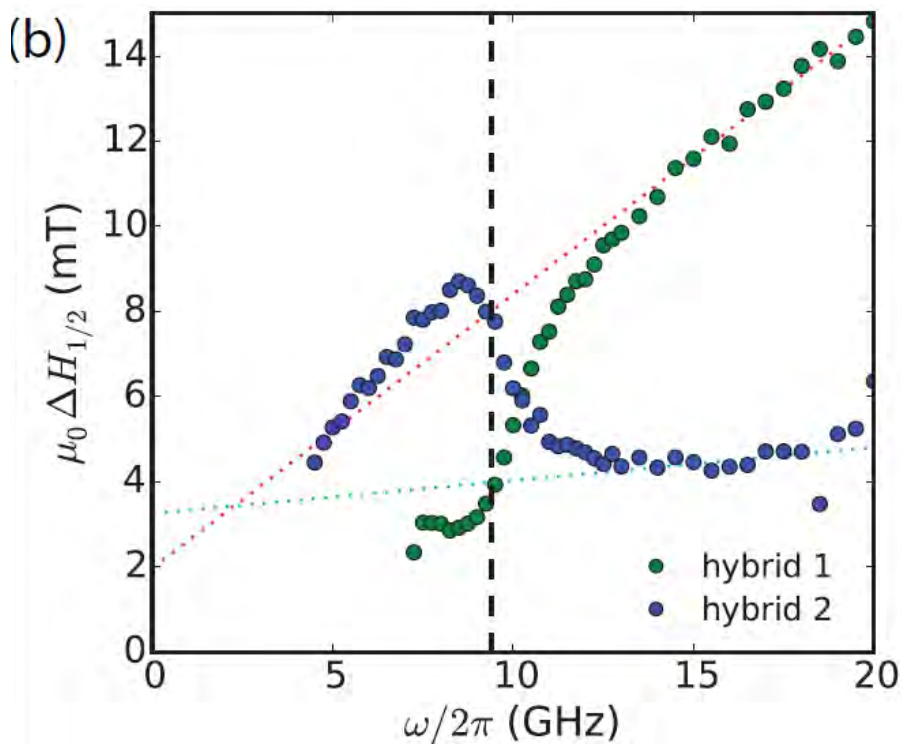

YIG(100 nm)/Py(7.5 nm)

Yi Li, et al. PRL 124, 117202 (2020)

LINEWIDTH: IN-PHASE VS. OUT-OF-PHASE MODES

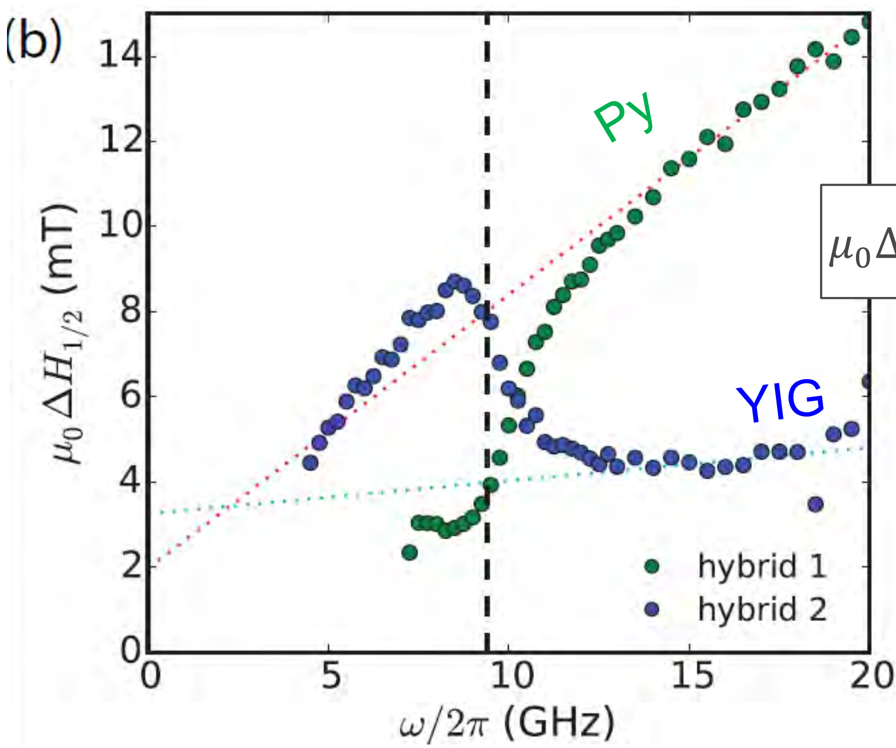

$$\mu_0 \Delta H_{1/2} = \frac{2\alpha\omega}{\gamma} + \mu_0 \Delta H_0$$

YIG(100 nm)/Py(7.5 nm)

Yi Li, et al. PRL 124, 117202 (2020)

LINEWIDTH: IN-PHASE VS. OUT-OF-PHASE MODES

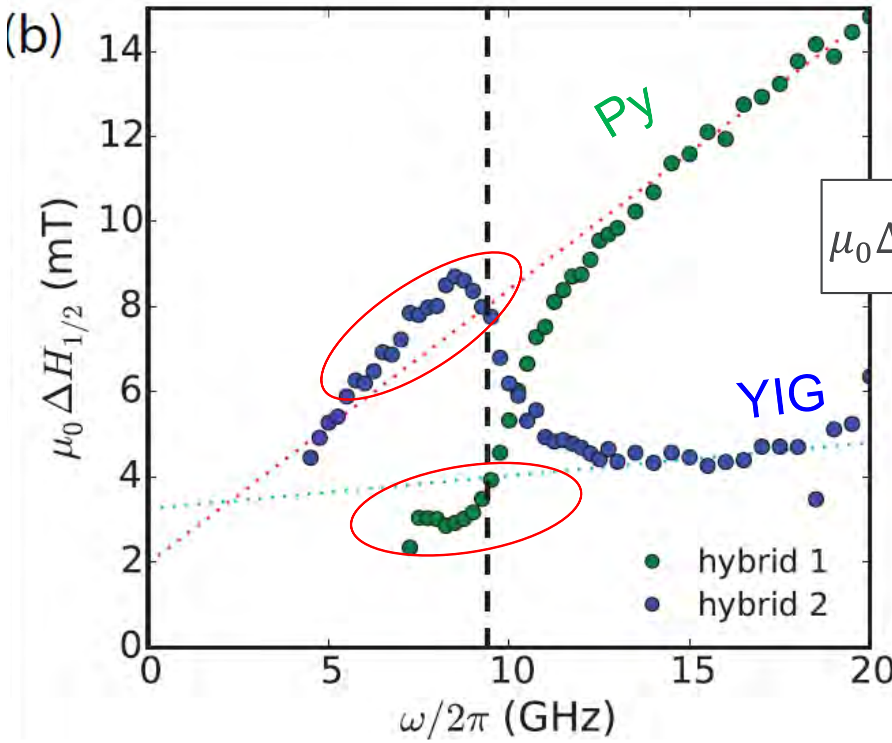

$$\mu_0 \Delta H_{1/2} = \frac{2\alpha\omega}{\gamma} + \mu_0 \Delta H_0$$

YIG(100 nm)/Py(7.5 nm)

Yi Li, et al. PRL 124, 117202 (2020)

LINEWIDTH: IN-PHASE VS. OUT-OF-PHASE MODES

κ_c enhances damping

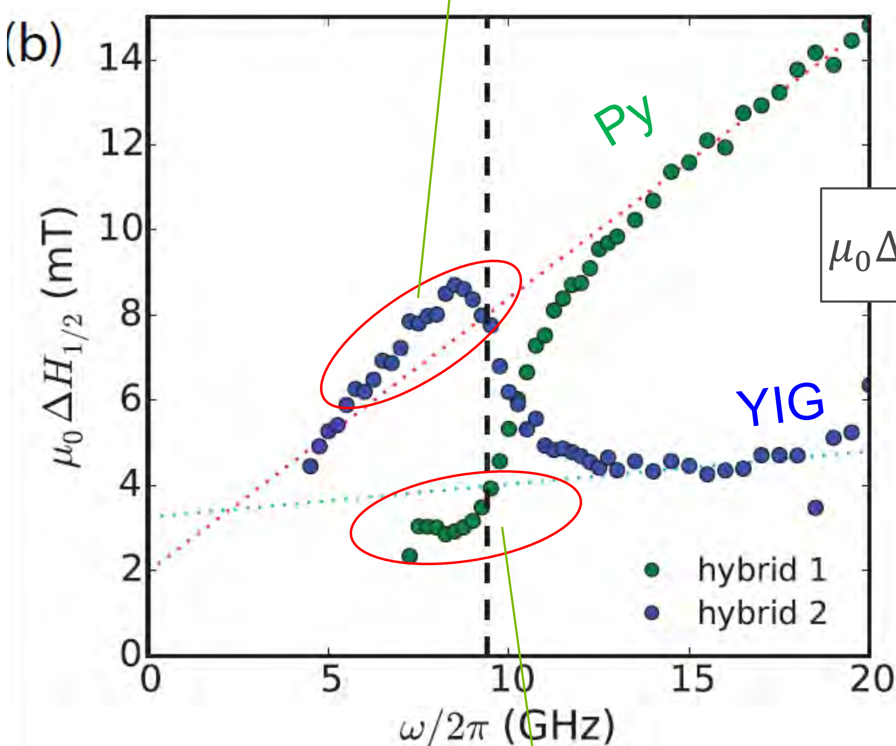

κ_c suppresses damping

$$\mu_0 \Delta H_{1/2} = \frac{2\alpha\omega}{\gamma} + \mu_0 \Delta H_0$$

Coupling: $\tilde{g}_c = g_c + i\kappa_c$

YIG(100 nm)/Py(7.5 nm)

Yi Li, et al. PRL 124, 117202 (2020)

LINEWIDTH: IN-PHASE VS. OUT-OF-PHASE MODES

κ_c enhances damping

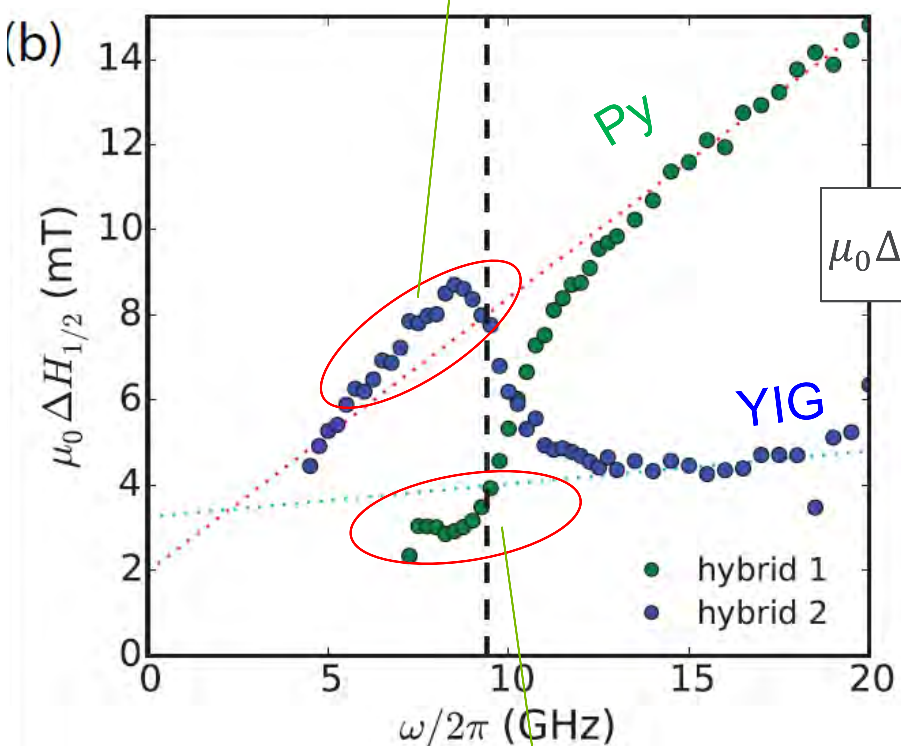

κ_c suppresses damping

$$\mu_0 \Delta H_{1/2} = \frac{2\alpha\omega}{\gamma} + \mu_0 \Delta H_0$$

Coupling: $\tilde{g}_c = g_c + i\kappa_c$

Fieldlike: exchange

Dampinglike: spin pumping

YIG(100 nm)/Py(7.5 nm)

Yi Li, et al. PRL 124, 117202 (2020)

LINEWIDTH: IN-PHASE VS. OUT-OF-PHASE MODES

κ_c enhances damping

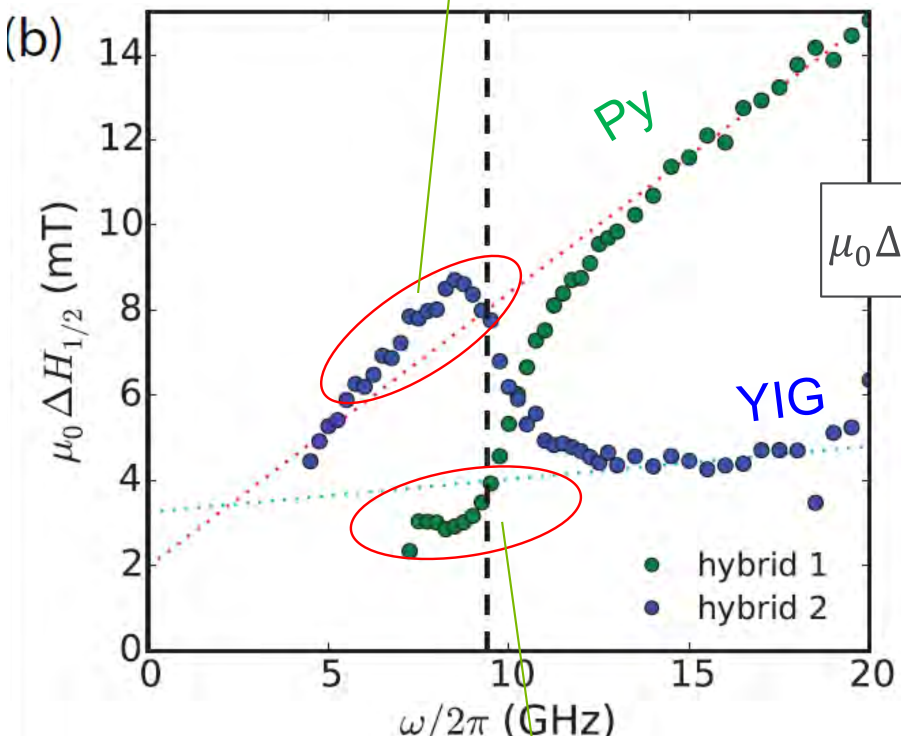

κ_c suppresses damping

YIG(100 nm)/Py(7.5 nm)

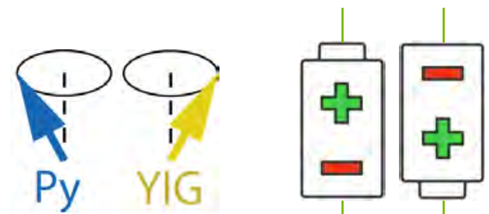

Optic mode

$$\mu_0 \Delta H_{1/2} = \frac{2\alpha\omega}{\gamma} + \mu_0 \Delta H_0$$

Coupling: $\tilde{g}_c = g_c + i\kappa_c$

Fieldlike: exchange

Dampinglike: spin pumping

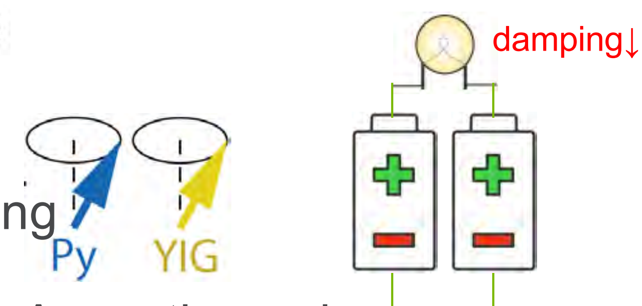

Acoustic mode

Yi Li, et al. PRL 124, 117202 (2020)

LINEWIDTH: IN-PHASE VS. OUT-OF-PHASE MODES

κ_c enhances damping

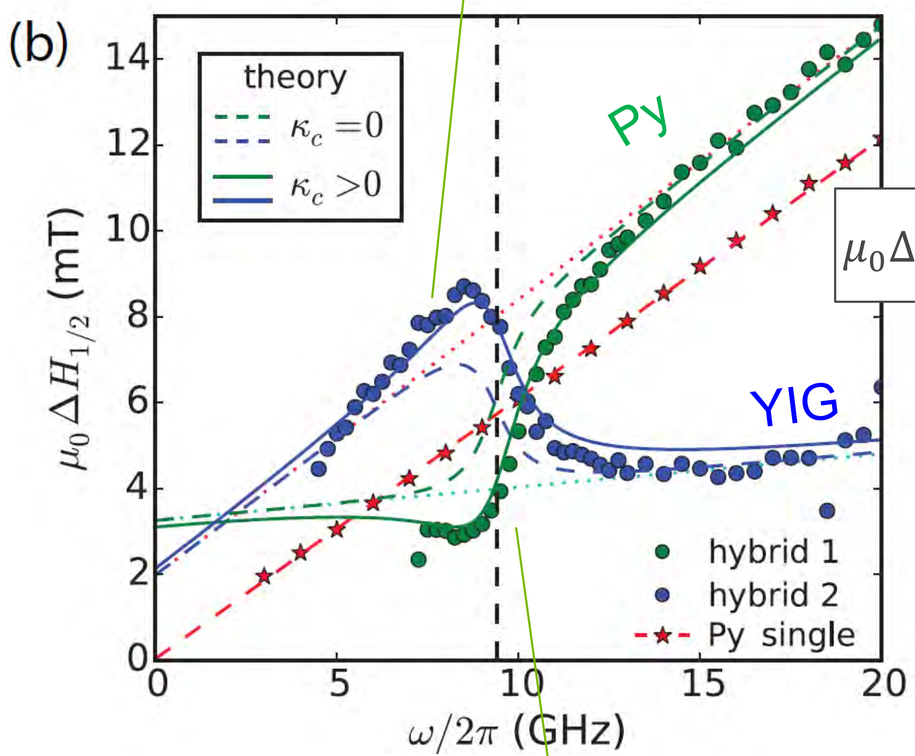

κ_c suppresses damping

YIG(100 nm)/Py(7.5 nm)

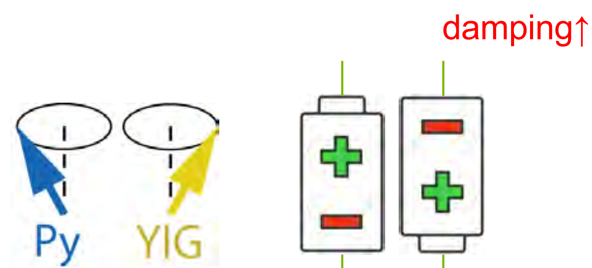

Optic mode

$$\mu_0 \Delta H_{1/2} = \frac{2\alpha\omega}{\gamma} + \mu_0 \Delta H_0$$

Coupling: $\tilde{g}_c = g_c + i\kappa_c$

Fieldlike: exchange	Dampinglike: spin pumping
$g_c/2\pi = 7.2$ mT	$\kappa_c/2\pi = 2.0$ mT

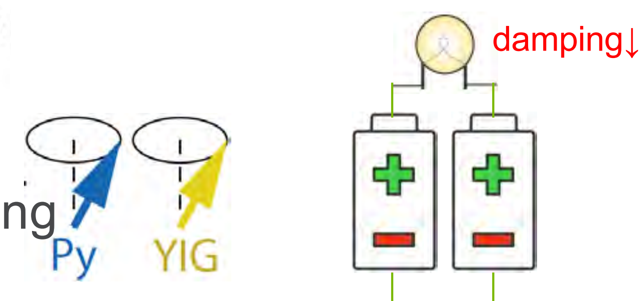

Acoustic mode

Yi Li, et al. PRL 124, 117202 (2020)

MACROSPIN MODEL: COHERENT COUPLING

Macrospin model:

$$\frac{d\mathbf{m}_i}{dt} = -\mu_0\gamma_i\mathbf{m}_i \times \mathbf{H}_{eff} + \alpha_i\mathbf{m}_i \times \frac{d\mathbf{m}_i}{dt}$$

$$\underbrace{-\gamma_i\mathbf{m}_i \times \frac{J}{M_i t_i}\mathbf{m}_j}_{\text{Fieldlike: exchange}} + \underbrace{\Delta\alpha_i\left(\mathbf{m}_i \times \frac{d\mathbf{m}_i}{dt} - \mathbf{m}_j \times \frac{d\mathbf{m}_j}{dt}\right)}_{\text{Dampinglike: spin pumping}}$$

Yi Li, et al. PRL 124, 117202 (2020)

MACROSPIN MODEL: COHERENT COUPLING

Macrospin model:

$$\frac{d\mathbf{m}_i}{dt} = -\mu_0\gamma_i \mathbf{m}_i \times \mathbf{H}_{eff} + \alpha_i \mathbf{m}_i \times \frac{d\mathbf{m}_i}{dt}$$

$$\underbrace{-\gamma_i \mathbf{m}_i \times \frac{J}{M_i t_i}\mathbf{m}_j}_{\text{Fieldlike: exchange}} + \underbrace{\Delta\alpha_i(\mathbf{m}_i \times \frac{d\mathbf{m}_i}{dt} - \mathbf{m}_j \times \frac{d\mathbf{m}_j}{dt})}_{\text{Dampinglike: spin pumping}}$$

Fieldlike: exchange   Dampinglike: spin pumping

Solution:

Fieldlike: $$g_c = \sqrt{\frac{\mathbf{J}}{M_1 t_1} \cdot \frac{\mathbf{J}}{M_2 t_2}}$$

Dampinglike: $$\kappa_c = \sqrt{\frac{\mathbf{J}'}{M_1 t_1} \cdot \frac{\mathbf{J}'}{M_2 t_2}}$$

$$J'(\omega) = \frac{g^{\uparrow\downarrow}}{4\pi}\hbar\omega$$

$g^{\uparrow\downarrow}$: spin mixing conductance, ~ 42 nm^{-2} for YIG/Py

Yi Li, et al. PRL 124, 117202 (2020)

MACROSPIN MODEL: COHERENT COUPLING

$g_c \sim 1/\sqrt{t_{Py}}$ $\beta \sim \sqrt{t_{Py}}$

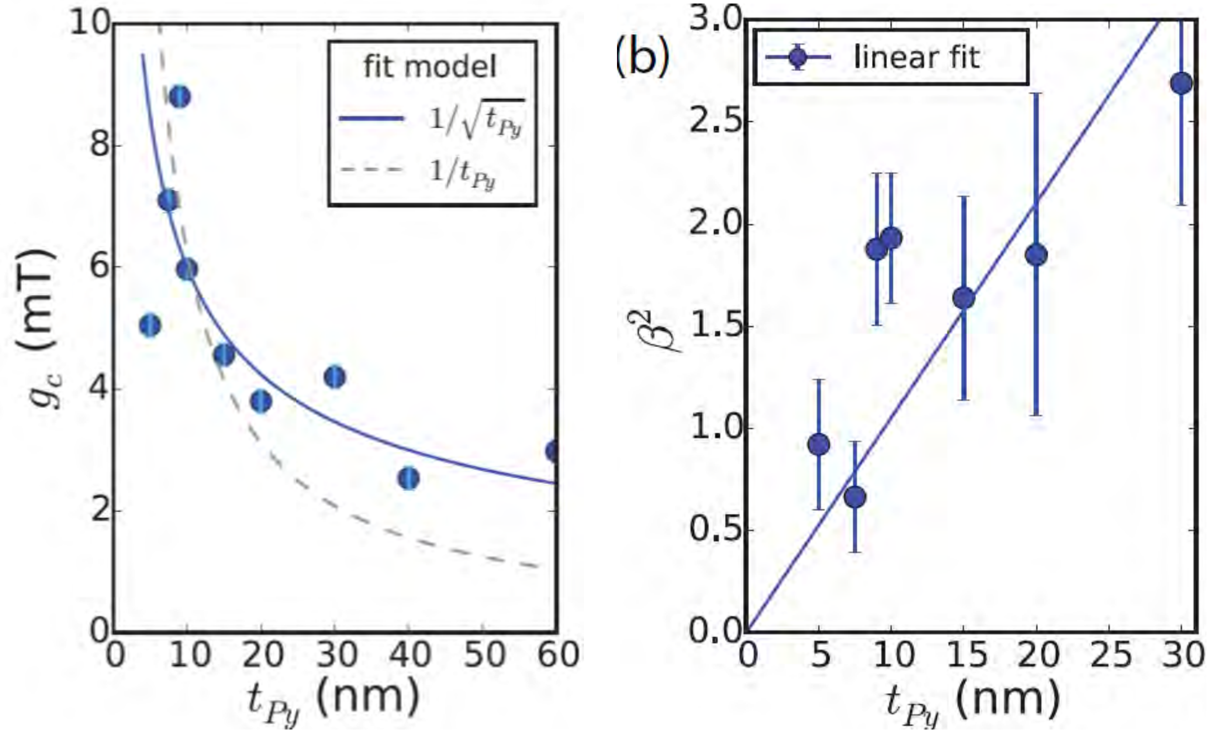

$$\kappa_c(\omega) = \beta\mu_0\Delta H_{sp}^{\mathrm{Py}}(\omega)$$

Solution:

Fieldlike:

$$g_c = \sqrt{\frac{\mathbf{J}}{M_1 t_1} \cdot \frac{\mathbf{J}}{M_2 t_2}}$$

Dampinglike:

$$\kappa_c = \sqrt{\frac{\mathbf{J}'}{M_1 t_1} \cdot \frac{\mathbf{J}'}{M_2 t_2}}$$

Yi Li, et al. PRL 124, 117202 (2020)

ANTIFERROMAGNETIC EXCHANGE COUPLING

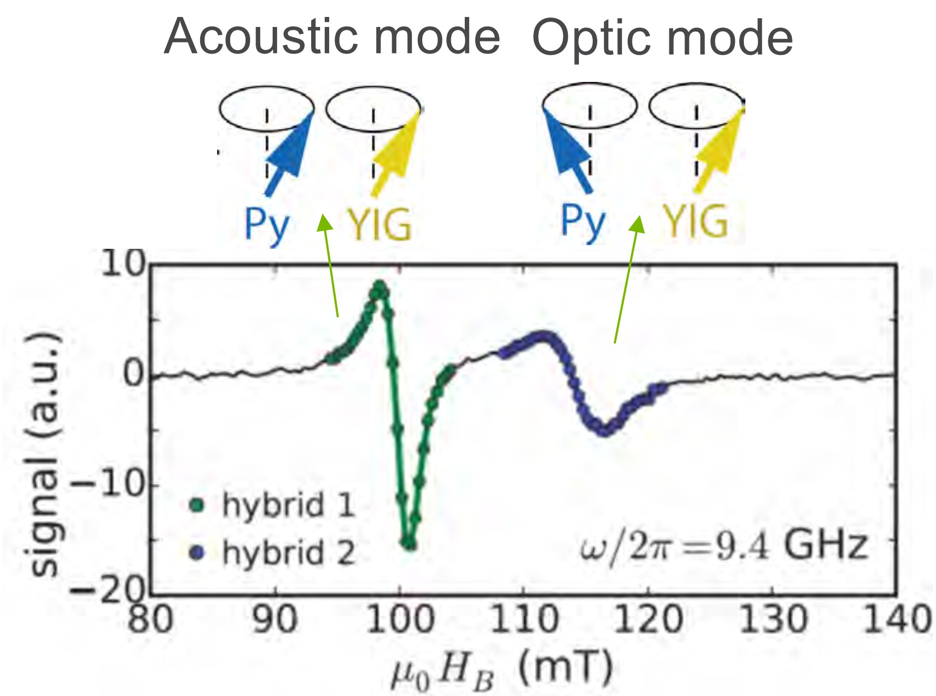

Yi Li, et al. PRL 124, 117202 (2020)

ANTIFERROMAGNETIC EXCHANGE COUPLING

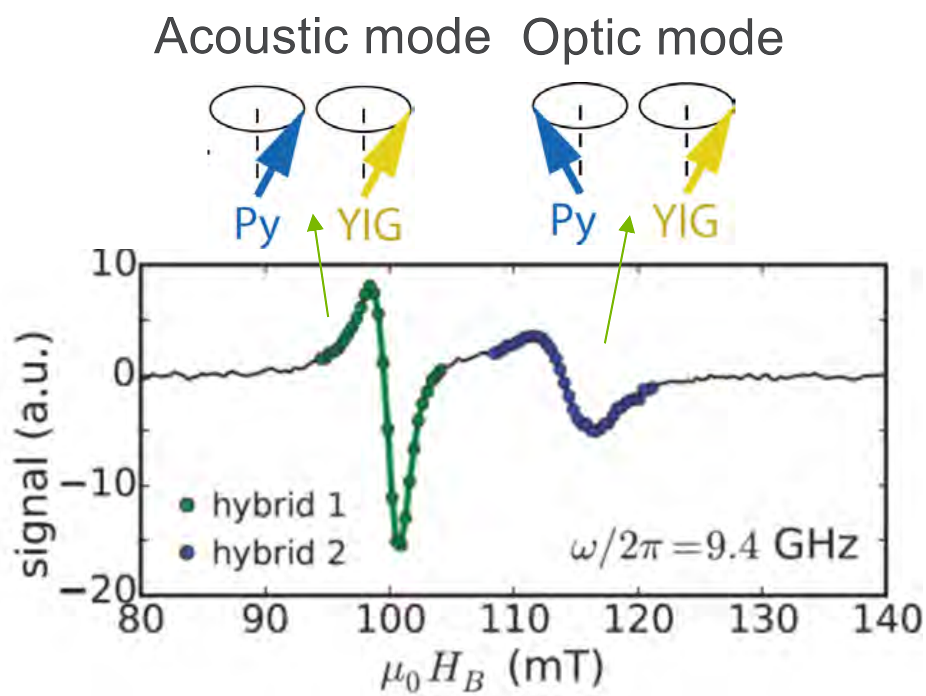

Yi Li, et al. PRL 124, 117202 (2020)

ANTIFERROMAGNETIC EXCHANGE COUPLING

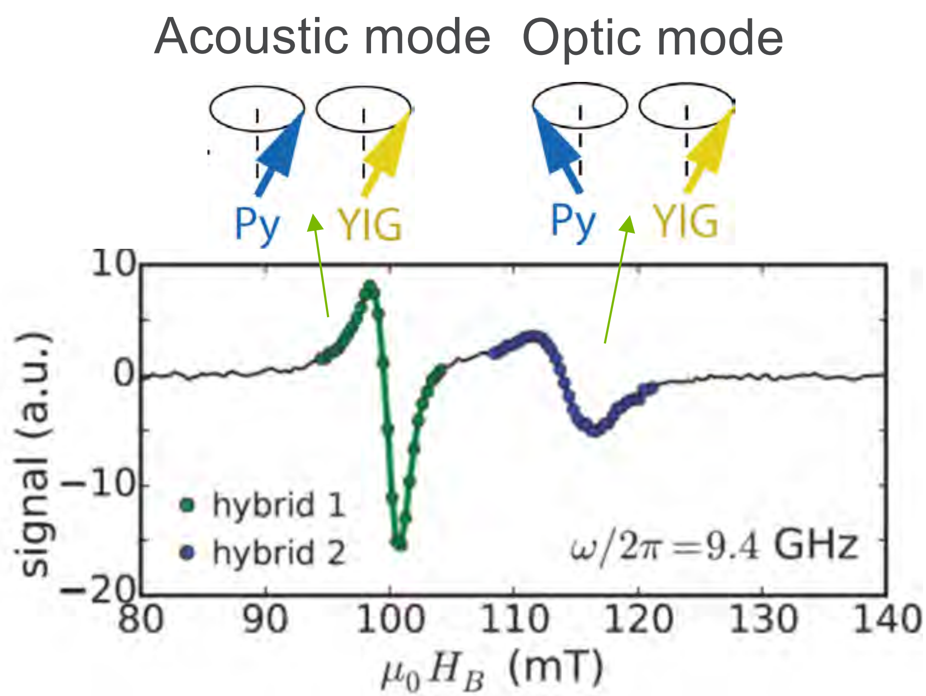

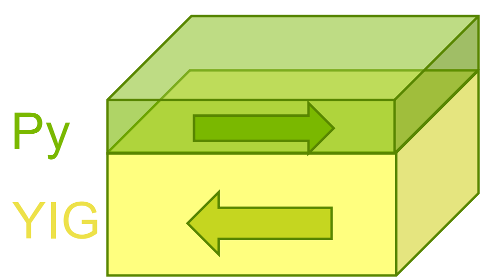

Antiferromagnetic coupling: $g_c < 0$

Yi Li, et al. PRL 124, 117202 (2020)

ANTIFERROMAGNETIC EXCHANGE COUPLING

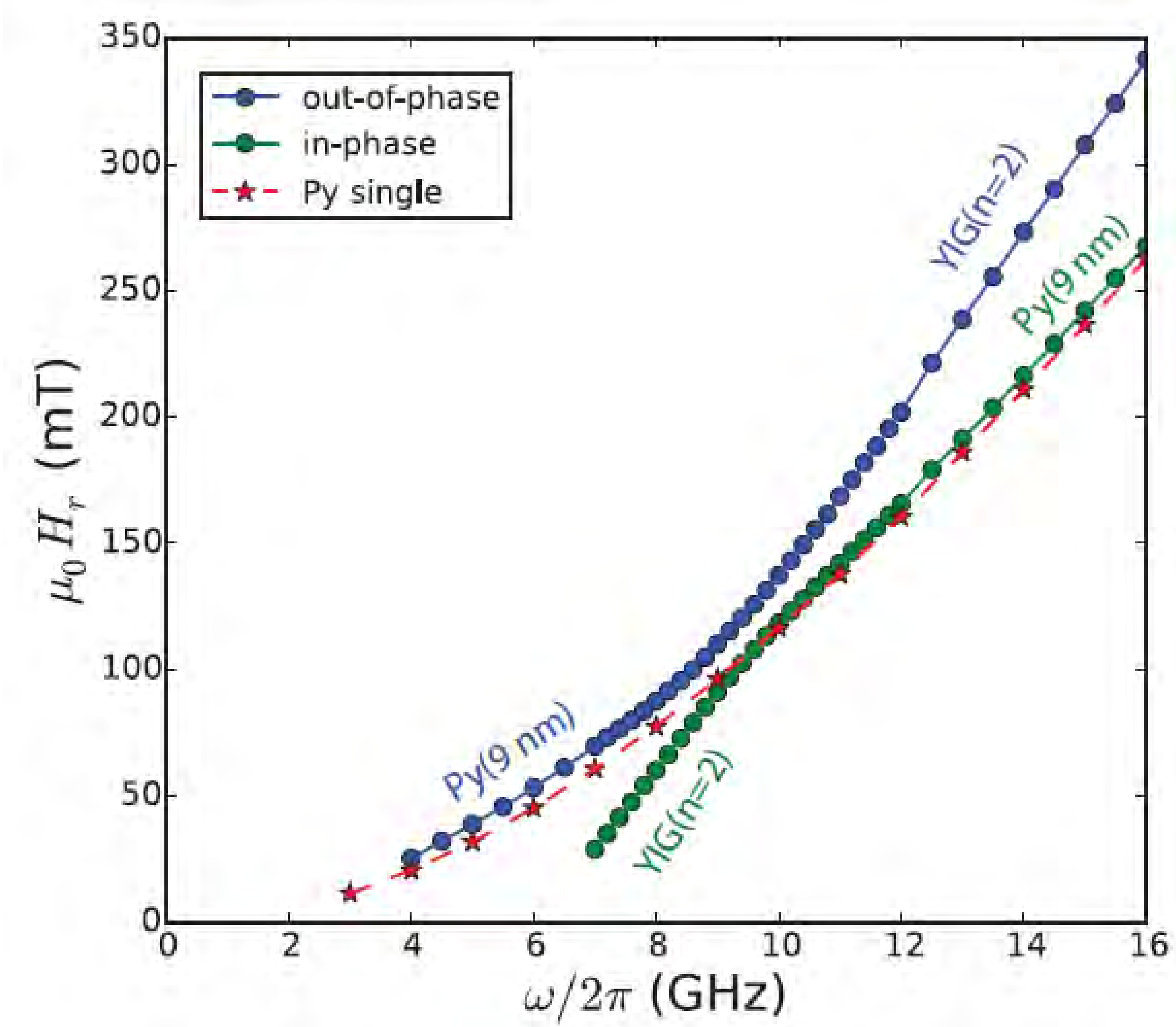

Yi Li, et al. PRL 124, 117202 (2020)

ANTIFERROMAGNETIC EXCHANGE COUPLING

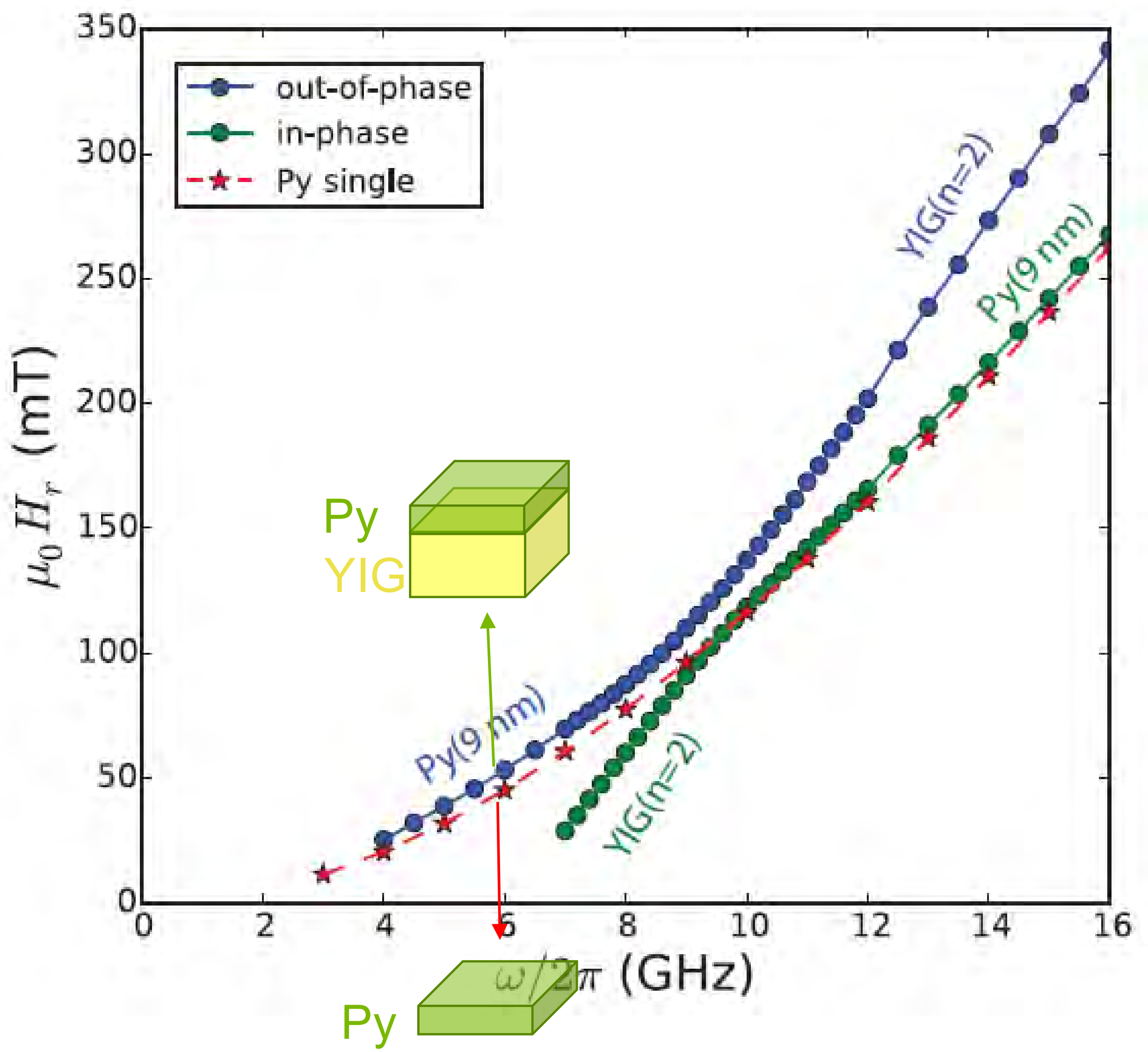

Yi Li, et al. PRL 124, 117202 (2020)

OUTLINE

- Introduction
- On-chip magnon-photon coupling with superconducting resonator
- Magnon-magnon coupling in magnetic bilayer thin film
- **Manipulating phonon transport with magnons**
- Conclusions

ELASTICALLY DRIVEN MAGNETIZATION DYNAMICS

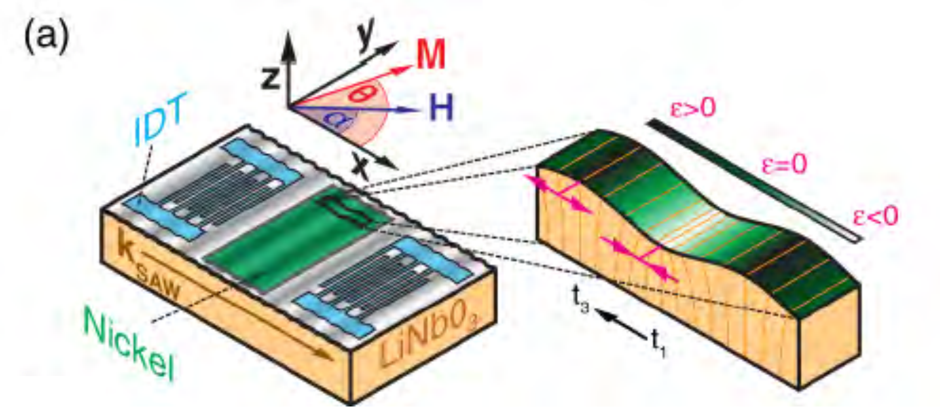

Free Energy for magnetization with Surface Acoustic Wave (SAW):

$$F^0(\mathbf{m}) = -\mu_0 \mathbf{H} \cdot \mathbf{m} + B_d m_z^2 + B_u (\mathbf{u} \cdot \mathbf{m})^2 + B_1 \varepsilon(\mathbf{x}, t) m_x^2$$

Zeeman Demagentizing Anisotropy Magnetoelastic

M. Weiler, et al. PRL **106**, 117601 (2011)

ELASTICALLY DRIVEN MAGNETIZATION DYNAMICS

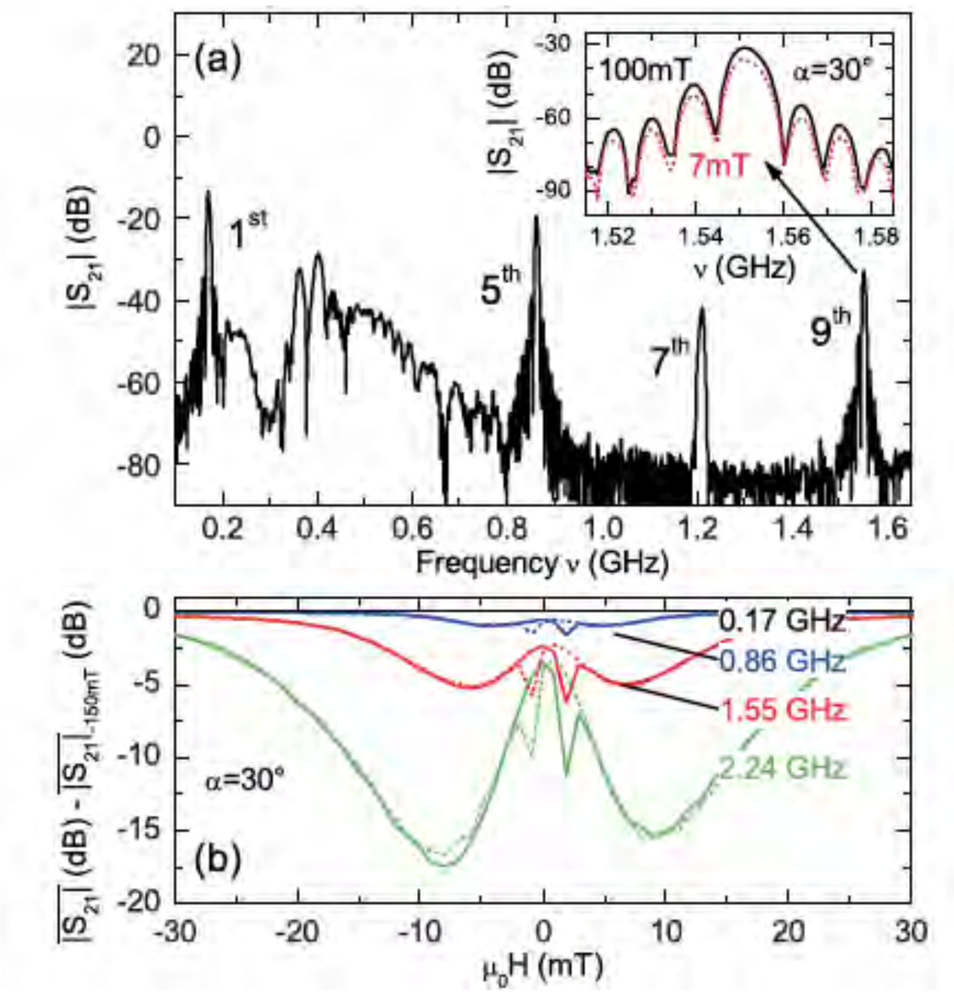

FMR given by broad maxima

Why is the linewidth so large?

M. Weiler, et al. PRL **106**, 117601 (2011)

CAN MAGNONS MODIFY PHONON TRANSPORT?

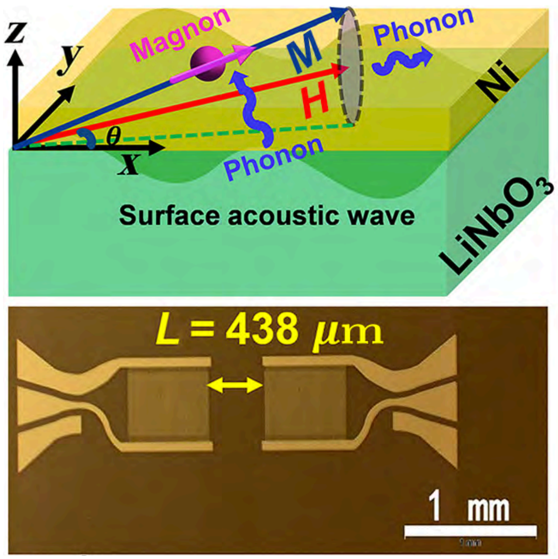

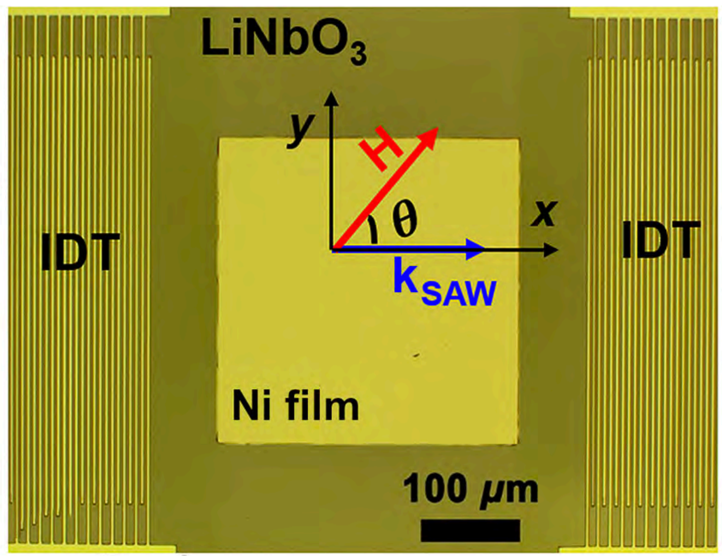

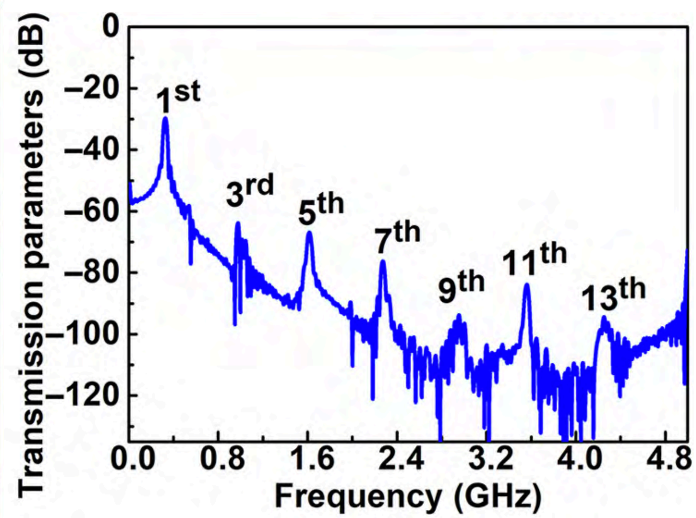

127.86° Y-X-cut $LiNbO_3$ substrate
50-nm thick Ni film

Two types of devices
- As grown
- Annealed in vacuum at 400°C for 30 min.

C. Zhao, et al. PRAppl. **13**, 054032 (2020)

DETECT FERROMAGNETIC RESONANCE

As-Grown

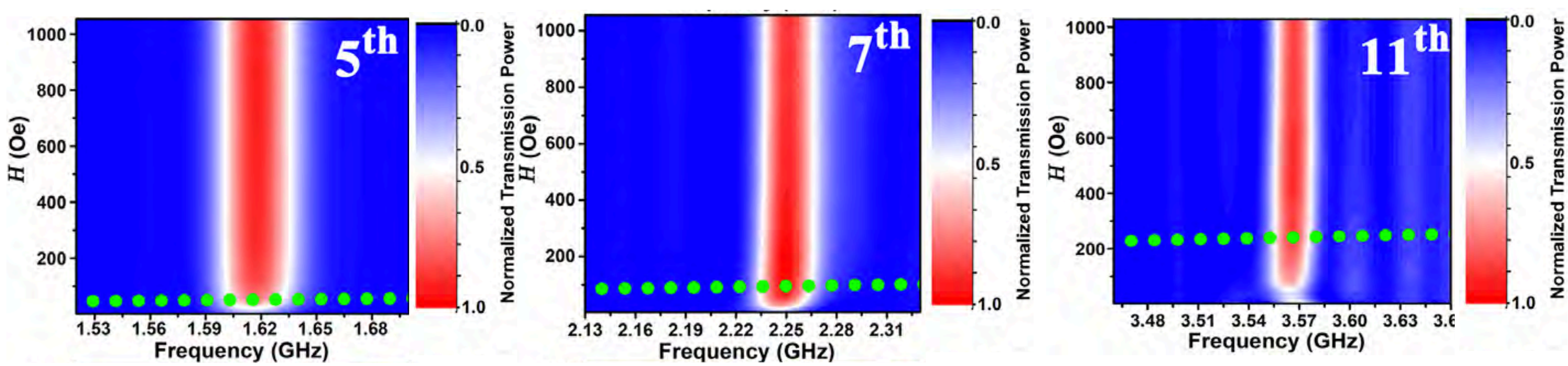

Annealed

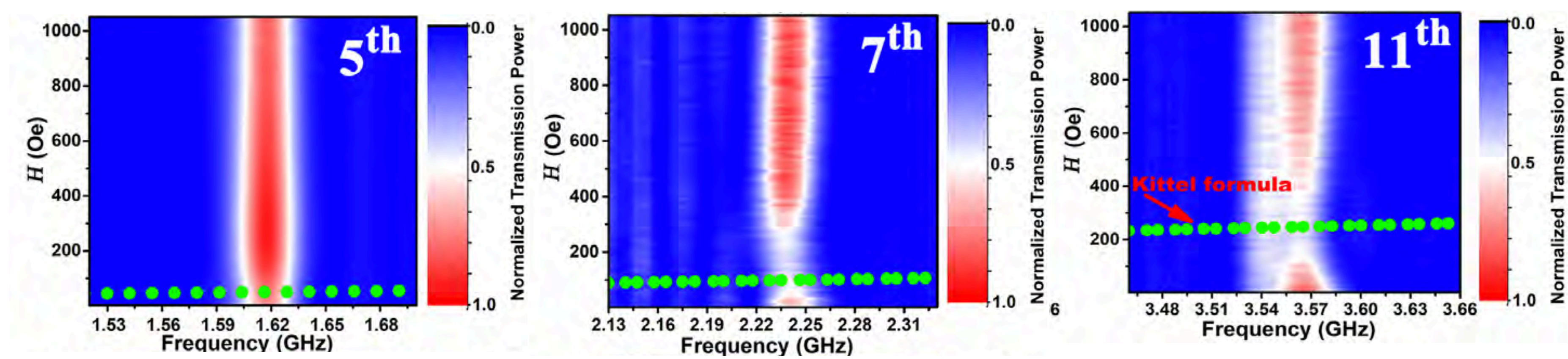

C. Zhao, et al. PRAppl. **13**, 054032 (2020)

PHONON TRANSMISSION

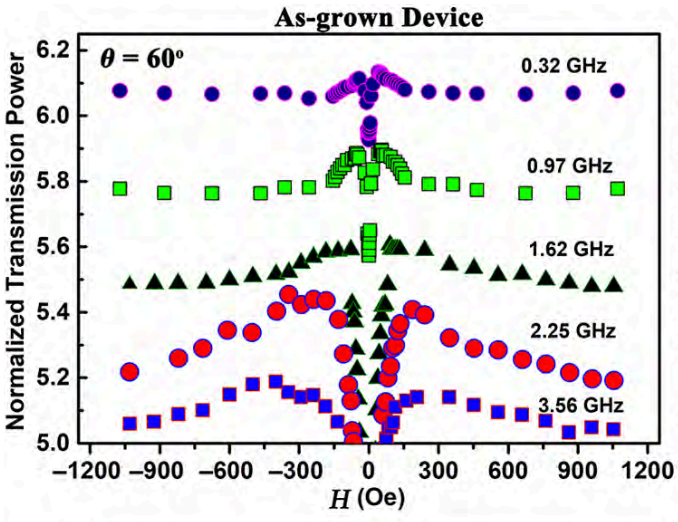

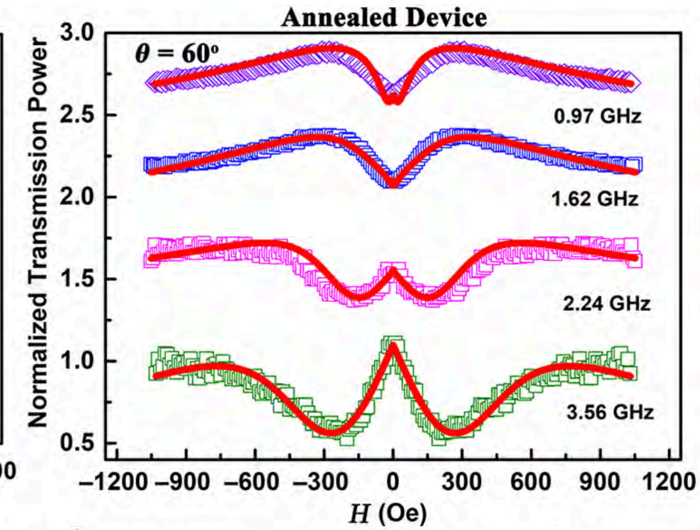

C. Zhao, et al. PRAppl. **13**, 054032 (2020)

PHONON TRANSMISSION

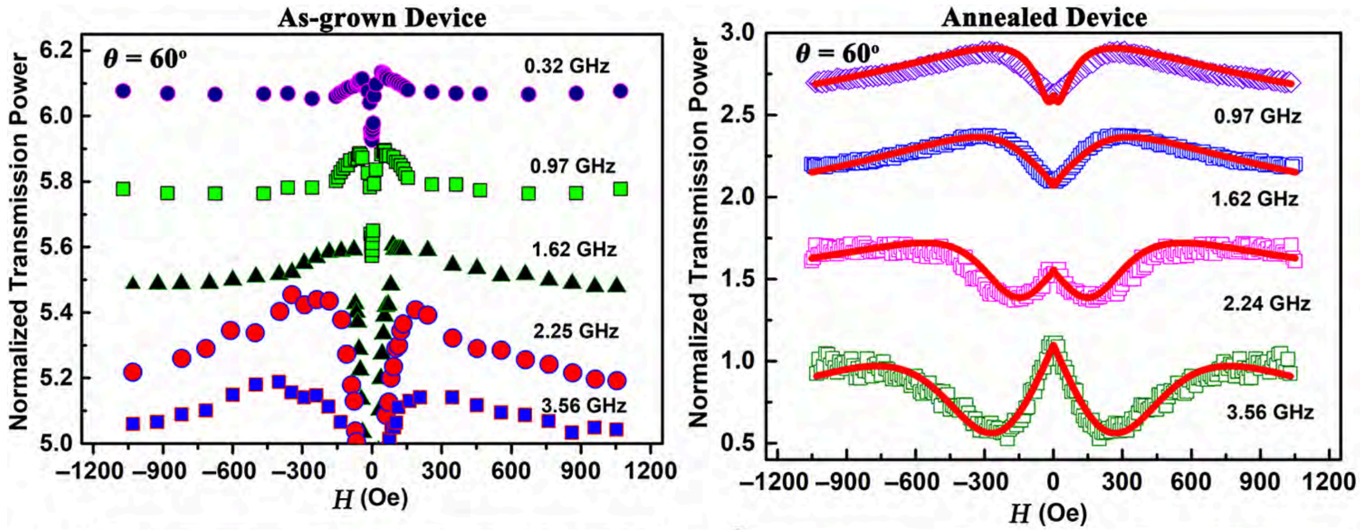

Theoretical Modeling

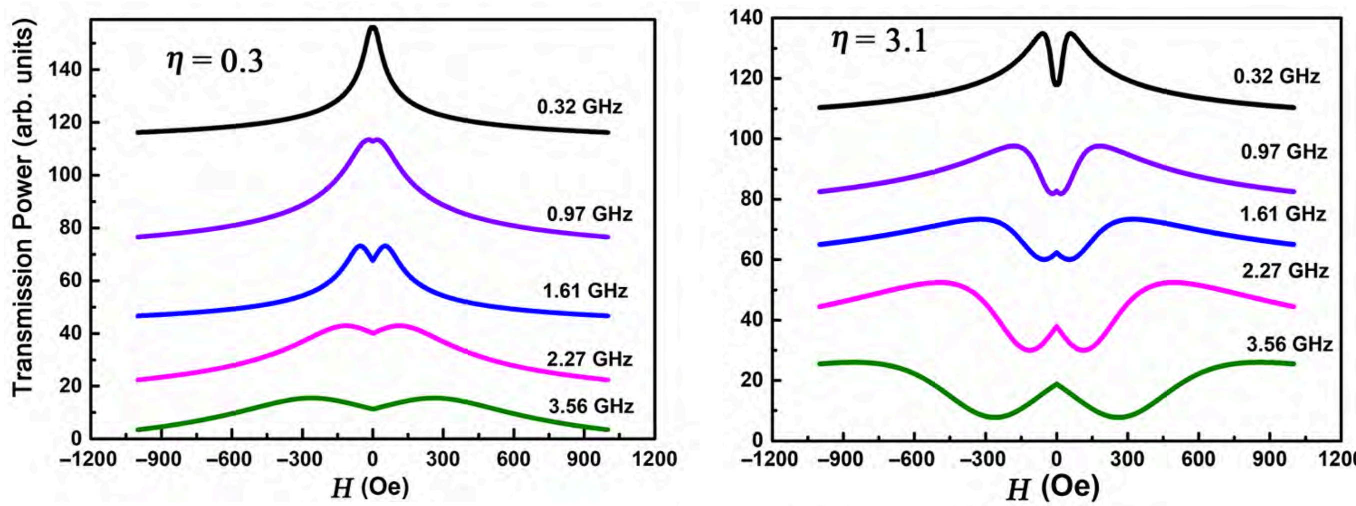

C. Zhao, et al. PRAppl. **13**, 054032 (2020)

PHONON TRANSMISSION

I. A. Privorotskii, IEEE Trans. Mag. **16**, 666 (1980)

$$E = E_0 \frac{v_f}{c} \frac{B_2^2}{C_{44}} \frac{|h_{eff}^{\perp}|}{\Delta H^2} (1+p^2)^{-\frac{1}{2}} [1+(p+\beta)^2]^{-\frac{1}{2}} \exp\left[\frac{-(\eta/2)}{1+(p+\beta)^2}\right] \left[1+\exp\left(\frac{-\eta_0 H}{2}\right)\right]$$

Includes both phonon attenuation and generation

η Is proportional to magnetoelastic coupling

Theoretical Modeling

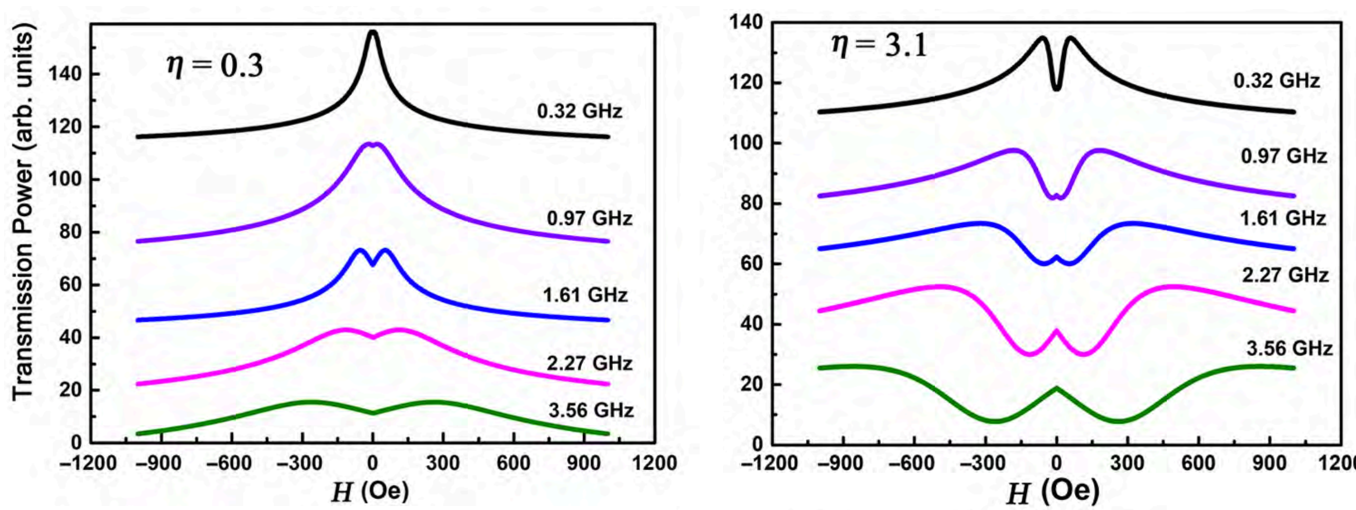

C. Zhao, et al. PRAppl. **13**, 054032 (2020)

LINEWIDTH

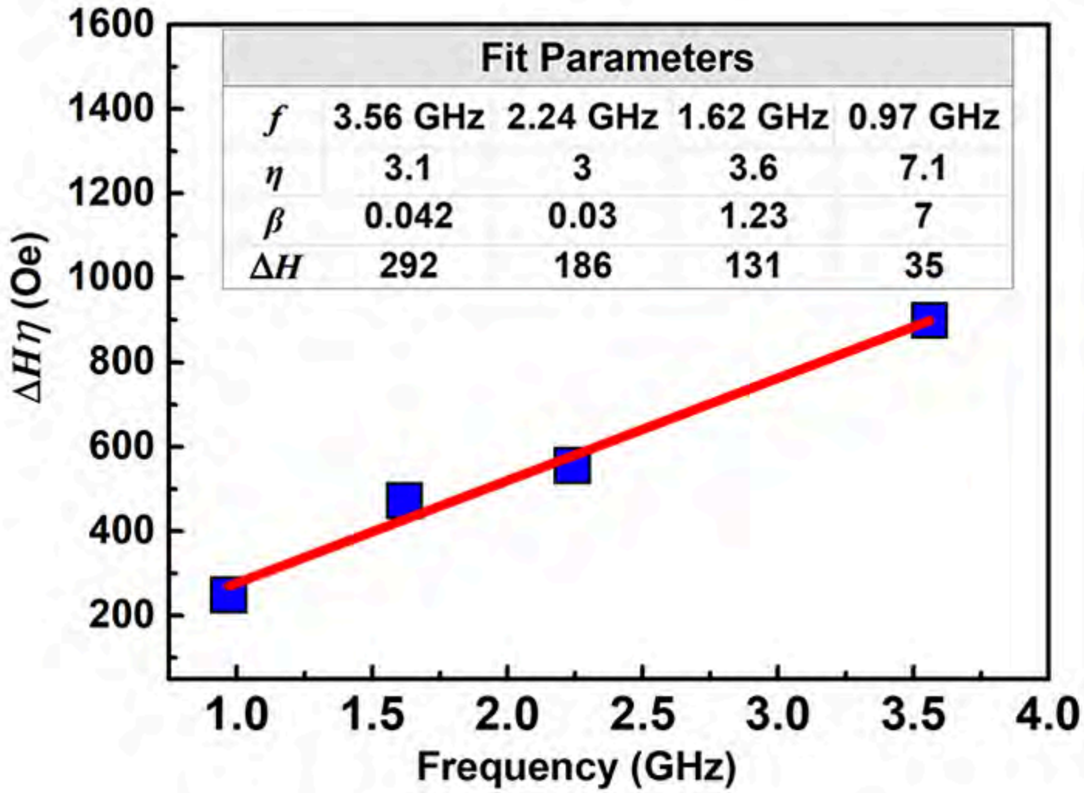

FMR linewidth from fit agrees well with inductively measured FMR of Ni on $LiNbO_3$

Increased apparent linewidth in phonon transmission is due to magnon-phonon interaction and not due to extrinsic inhomogeneities

MAGNETIC FILMS GROUP AT ARGONNE

MAGNETIC FILMS GROUP AT ARGONNE

THANKS TO

Yi Li, Chenbo Zhao, Tomas Polakovic, Yong-Lei Wang, Jing Xu, Sergi Lendinez, Zhizhi Zhang, Junjia Ding, Trupti Kkaire, Hilal Saglam, Jonathan Giobbons, Michael Vogel, Ralu Divan, John E. Pearson, Wai-Kwong Kwok, Zhili Xiao, and Valentine Novosad

Argonne National Laboratory

Wei Zhang

Oakland University

Wei Cao and William E. Bailey

Columbia University

Vivek Amin, Paul M. Haney, and Mark D. Stiles

National; Institute of Standards and Technology

Qingfang Liu

Huazhong University of Science and Technology

Financial Support

DOE-BES Materials Science and Engineering Division

Q-MEEN-C EFRC

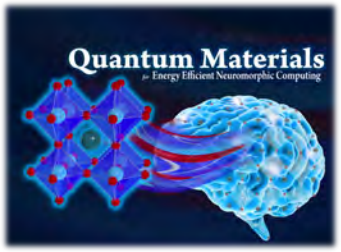

CONCLUSION

Magnon-photon

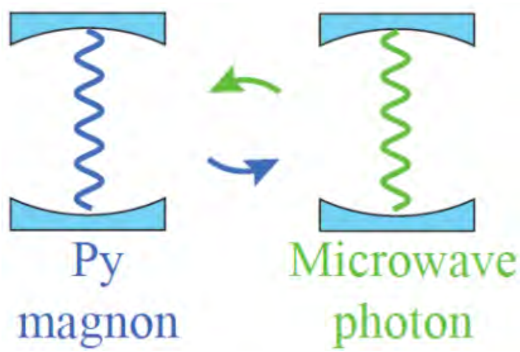

Magnon-magnon

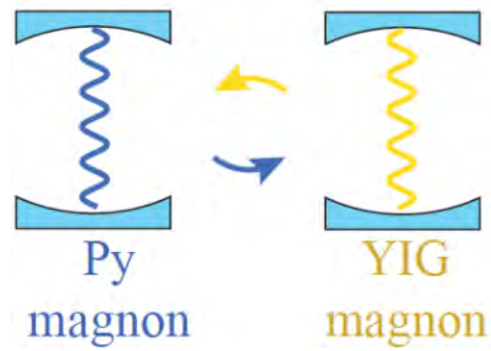

Magnon-phonon

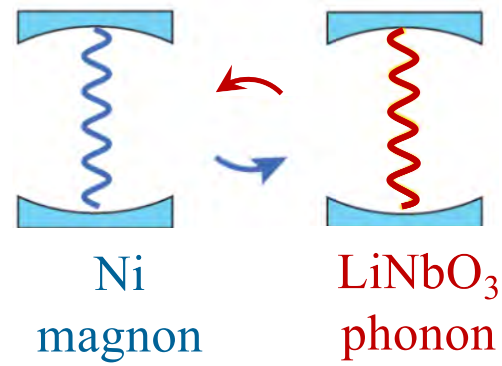

Yi Li, et al.
PRL 123, 107701 (2019)

Yi Li, et al.
PRL 124, 117202 (2020)

Chenbo Zhao, et al.
PRAppl 13, 054032 (2020)

CONCLUSION

Magnon-photon

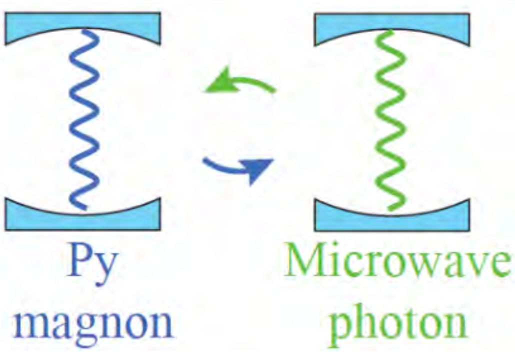

Magnon-magnon

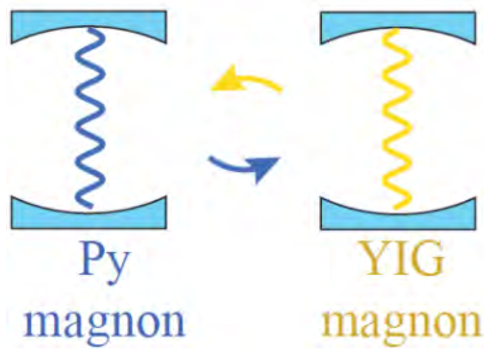

Magnon-phonon

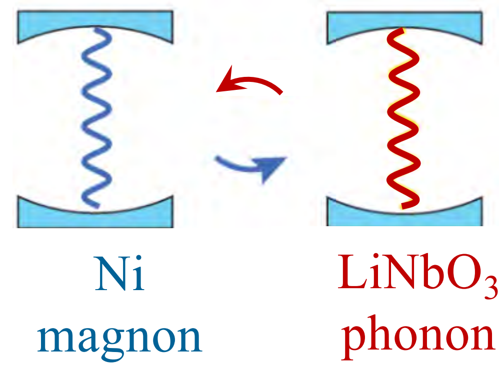

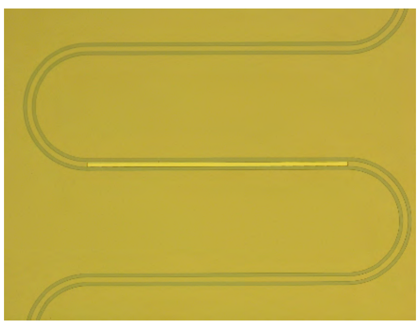

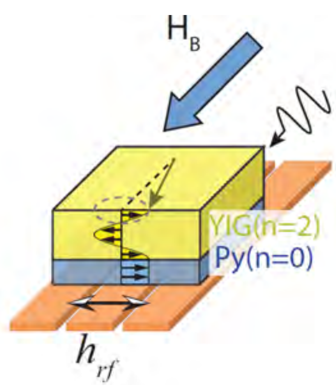

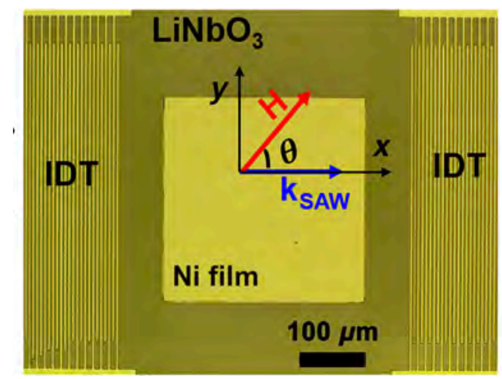

On-chip applications

Yi Li, et al.
PRL 123, 107701 (2019)

Yi Li, et al.
PRL 124, 117202 (2020)

Chenbo Zhao, et al.
PRAppl 13, 054032 (2020)